catena-Phosphorus Cations

by

C. Adam Dyker

Submitted in partial fulfillment of the requirements
for the degree of Doctor of Philosophy

at

Dalhousie University
Halifax, Nova Scotia
December 2006

© Copyright by C. Adam Dyker, 2006

Library and Archives Canada

Published Heritage Branch

395 Wellington Street
Ottawa ON K1A 0N4
Canada

Bibliothèque et Archives Canada

Direction du Patrimoine de l'édition

395, rue Wellington
Ottawa ON K1A 0N4
Canada

Your file Votre référence
ISBN: 978-0-494-27204-6
Our file Notre référence
ISBN: 978-0-494-27204-6

NOTICE:
The author has granted a non-exclusive license allowing Library and Archives Canada to reproduce, publish, archive, preserve, conserve, communicate to the public by telecommunication or on the Internet, loan, distribute and sell theses worldwide, for commercial or non-commercial purposes, in microform, paper, electronic and/or any other formats.

The author retains copyright ownership and moral rights in this thesis. Neither the thesis nor substantial extracts from it may be printed or otherwise reproduced without the author's permission.

AVIS:
L'auteur a accordé une licence non exclusive permettant à la Bibliothèque et Archives Canada de reproduire, publier, archiver, sauvegarder, conserver, transmettre au public par télécommunication ou par l'Internet, prêter, distribuer et vendre des thèses partout dans le monde, à des fins commerciales ou autres, sur support microforme, papier, électronique et/ou autres formats.

L'auteur conserve la propriété du droit d'auteur et des droits moraux qui protège cette thèse. Ni la thèse ni des extraits substantiels de celle-ci ne doivent être imprimés ou autrement reproduits sans son autorisation.

In compliance with the Canadian Privacy Act some supporting forms may have been removed from this thesis.

While these forms may be included in the document page count, their removal does not represent any loss of content from the thesis.

Conformément à la loi canadienne sur la protection de la vie privée, quelques formulaires secondaires ont été enlevés de cette thèse.

Bien que ces formulaires aient inclus dans la pagination, il n'y aura aucun contenu manquant.

Canada

DALHOUSIE UNIVERSITY

To comply with the Canadian Privacy Act the National Library of Canada has requested that the following pages be removed from this copy of the thesis:

Preliminary Pages
- Examiners Signature Page (pii)
- Dalhousie Library Copyright Agreement (piii)

Appendices
- Copyright Releases (if applicable)

Table of Contents

List of Tables

List of Figures

List of Schemes

Abstract

Catenation, or homoatomic bonding, is a principle feature in defining the chemistry of phosphorus. As such, studies directed towards developing new *catena*-phosphorus chemistry are of fundamental value. Although much is known about neutral and anionic *catena*-phosphorus compounds, only a limited number of cationic species have been prepared to date.

New synthetic methods have now been developed for the preparation of triflate salts of a number of new *catena*-phosphorus cations consisting of phosphine and phosphonium units. The isolation and characterization of the first monocyclic tri-, tetra- and pentaphosphorus monocations has been achieved. Some examples of acyclic tri- and tetraphosphorus monocations have also been characterized, and the first cyclic tetraphosphorus 1,2-dication and acyclic tetraphosphorus 1,4-dications are reported. Compounds have been characterized by use of multinuclear NMR, including simulations of their often complex $^{31}P\{^{1}H\}$ NMR spectra, and X-ray structures have been obtained in most cases. These findings contribute to a systematic development of this emerging area of fundamental phosphorus chemistry.

List of Abbreviations and Symbols Used

^{1}H	Proton
^{31}P	Phosphorus-31
^{13}C	Carbon-13
$\{^{1}H\}$	Proton decoupled
$\{^{31}P\}$	Phosphorus-31 decoupled
Å	Angstrom (10^{-10} m)
^{t}Bu	Tertiary butyl
Calcd	Calculated
Cy	Cyclohexyl
d	Doublet (NMR)
d.e.	Diastereomeric excess
D.p.	Decomposition point
E	Envelope conformation
FT	Fourier transform
Hz	Hertz
IR	Infrared
m	Multiplet
M^{I}	Alkali metal
Me	Methyl
Mes	2,4,6-Trimethylphenyl
Mes*	2,4,6-Tri-tertbutylphenyl
M.p.	Melting point
$^{n}J_{AB}$	n-bond coupling constant between nuclei A and B
NMR	Nuclear magnetic resonance
OTf	Trifluoromethylsulfonate (Triflate)
Ph	Phenyl
ppm	Parts per million

^{i}Pr	Isopropyl
R	Organic substituent
RA	Reducing Agent
s	Singlet
t	Triplet
T	Twist conformation
THF	Tetrahydrofuran
TMS	Trimethylsilyl
X	Halogen or general anion
δ	Chemical shift
τ	Torsional angle

Acknowledgements

I must first sincerely thank my supervisor, Dr. Neil Burford, who provided me with an exceptional working environment, including an excellent mix of guidance and freedom, in which I could increase my knowledge, interest and synthetic abilities in chemistry. Neil also taught me the value of the low-percentage shots in squash. Thanks to all the past and present members of the Burford lab, especially Yuen-ying Carpenter, Eamonn Conrad, Reagen Davidson, Mark D'eon, Dr. Melanie Eelman, Katie Groom, David Herbert, Ian Mallov, Gabriel Menard, Robyn Ovans, Heather Phillips, Dr. Paul Ragogna, Susie Riegel, Cheryl Saunders, Kenny Sharp, and Dr. Jan Weigand who made my PhD studies a great deal of fun. Special thanks to my very good friend, and former lab-mate Dr. Jeff Landry for the great discussions about life, chemistry, and anything else. Among other important things, like standing up with me in my wedding, it was great to have a friend to play squash with on a moment's notice.

Thanks to Dr. Mike Lumsden for his amazing enthusiasm and abilities in simulating the complex NMR spectra presented in this thesis and to Dr. Ulli Werner-Zwanziger for her assistance with solid state NMR. Thanks to Dr. Andreas Decken, not only for his collaborations involving the X-ray crystallography in this thesis, but also for sparking my interest in research. More importantly, his lab in UNB was the place where I met my wife, Erin.

Things would not have run so smoothly if it were not for the help of the office staff (Giselle Andrews, Cheryl Stanton, Shelley Dorey, Deana Wentzell) and technical staff (Jürgen Müller, Rick Conrad, Mike Boutilier, Brian Millier); thanks.

I would also like to thank family. Many heartfelt thanks to my wife Erin for her love, patience, understanding and hard work; especially for her ability to look after me and our newborn son Samuel. Thanks to Samuel for his smiles which were a great break from writing this thesis, and to my parents for always supporting me even though I have been going to school for most of my life.

Chapter 1.0: Introduction

1.1 Catenation

Derived from the Latin word *catena*, for chain, the Encyclopædia Britannica describes catenation as the chemical linkage into chains of atoms of the same element.[1] In this thesis, rings shall be considered as simple chains that are joined end-to-end, and the term catenation will be used to refer to homoatomic bonding within both acyclic and cyclic compounds.

Of all the elements, carbon has shown the most pronounced ability to catenate. This is illustrated by the diversity within its allotropes, such as diamond, graphite, and the fullerenes. The carbon-carbon bond also plays a pivotal role in the well developed field of organic chemistry, in that most organic molecules are built around carbon-based frameworks. The field is at a point now where highly complex natural products can be rationally synthesized in the laboratory. High molecular weight carbon-based polymers, such as industrially relevant polyethylene, also consist of huge numbers of directly bonded carbon atoms.

Though much less developed, many other elements (for example Si, Ge, P, S) have significant tendencies towards homoatomic bonding. Of these, phosphorus, not silicon, displays a more analogous chemistry to carbon.[2-4] This results from the similar electronegativities of phosphorus and carbon, and follows the trend for elements with a diagonal relationship on the periodic table. In this context, the *catena* chemistry of phosphorus is expected to consitute a significant portion of the fundamental chemistry of the element, as is the case for carbon.

1.2 Allotropes of Phosphorus

Perhaps the most fundamental *catena*-phosphorus compounds are the elemental forms, or allotropes, of phosphorus. These allotropes are a special class of *catena*-phosphines in which each phosphorus atom is involved in three bonds only to other phosphorus atoms. Though there have been more than eleven different allotropes reported, including a recent report on phosphorus nanorods,[5] the most common are the white (yellow), red and black forms.[6] White phosphorus (P_4, **1.1**), the least stable of the three common forms, is defined as the standard state of the element and consists of four

atoms arranged in a tetrahedron (P-P = 2.21 Å). Above 1070 K, this form is in equilibrium with the diatomic nitrogen analogue P_2 (**1.2**, P-P = 1.87 Å).[6] Hittorf's phosphorus (**1.3**, P-P = ~ 2.22 Å) is a well known derivative of red phosphorus which consists of infinite arrays of interlocking chains. Black phosphorus (**1.4**, P-P = 2.20 Å) consists of layers of arrays of six-membered phosphorus rings with chair conformations, and is the most stable of the allotropes.[6]

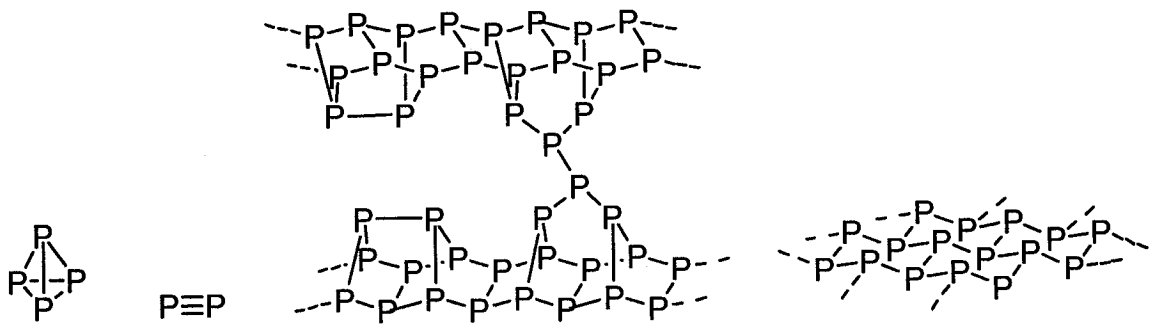

1.1 **1.2** **1.3** **1.4**

1.3 Substituted *catena*-Phosphines

Marianne Baudler's group has produced over 200 publications entitled "Contibutions to the Chemistry of Phosphorus" which deal principally with neutral or anionic compounds involving phosphorus-phosphorus bonds. Many others have also contributed to these areas of phosphorus chemistry, which have been the subject of a number of reviews.[3;7-11] This section, and the following, will not be a comprehensive review of the chemistry of *catena*-phosphines or phosphorus anions, respectively, but will focus on reports that are directly related to compounds described in this thesis, or compounds that exemplify some aspect of *catena*-phosphorus chemistry.

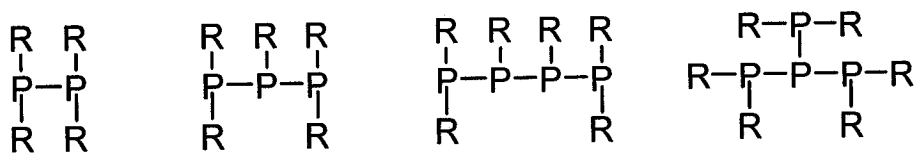

1.5 **1.6** **1.7** **1.8**

Substituted *catena*-phosphines can be divided into two broad classes: acyclic and cyclic. The simplest acyclic *catena*-phosphines are the diphosphine **1.5**, triphosphine **1.6**, and tetraphosphine **1.7**, which consist of two, three or four directly bonded phosphorus atoms, respectively.[11] Iso-tetraphosphines **1.8** have also been isolated in the presence of bulky organo-substituents (^{t}Bu, Cy, Ph).[12;13] One of the major problems associated with acyclic *catena*-phosphines **1.6** and **1.7** is the disproportionation into diphosphines and cyclopolyphosphines $(RP)_n$, as illustrated in **Scheme 1.1**, and these compounds often require particular conditions, such as low temperature, for their synthesis and isolation.[11]

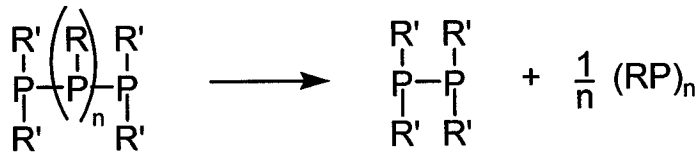

Scheme 1.1 Disproportionation of longer-chain *catena*-phosphines into diphosphines and cyclopolyphosphines.

Cyclopoyphosphines $[(RP)_n]$ are much more robust and diverse than acyclic *catena*-phospines, and are generally prepared by the reduction of the corresponding dichlorophosphines ($RPCl_2$). The general reactions outlined in **Scheme 1.2**[8;10;11] are not ring-size specific, but one $(RP)_n$ oligomer is usually formed preferentially for a given substituent (R). Increasing the steric bulk of the substituent favors a smaller ring size. In fact, using extremely bulky groups such as Mes* (2,4,6-tri-tert-butlyphenyl)[14] or terphenyls,[15;16] allows for the formation of diphosphenes (R-P=P-R). The cyclic compounds shown in **Scheme 1.2** can be isolated in good yields by the indicated method.

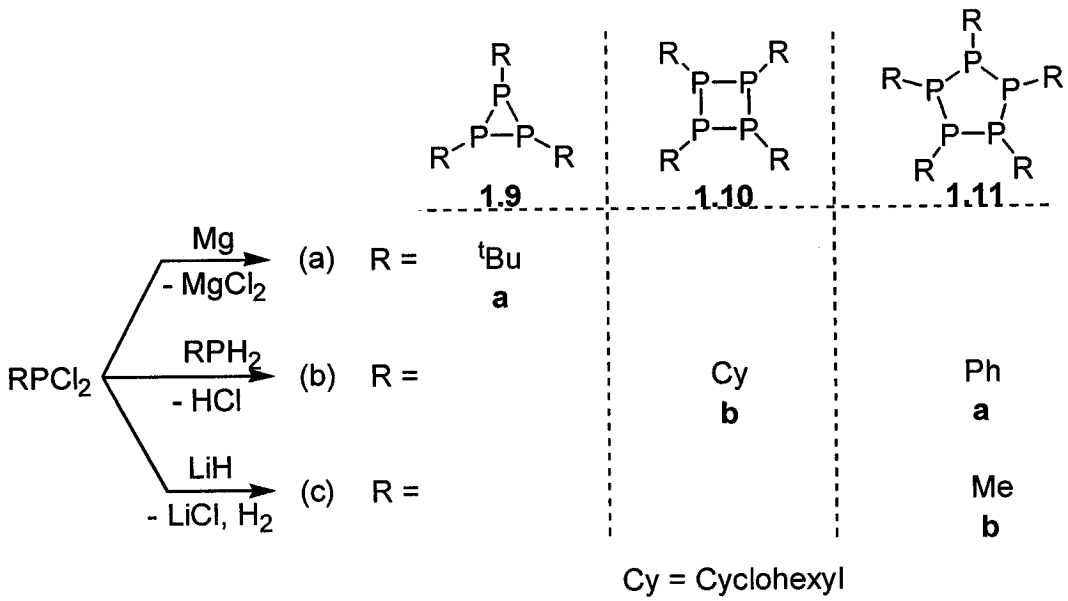

Scheme 1.2 Commonly used routes for the synthesis of cyclopolyphosphines **1.9a**,[17] **1.10b**,[18] **1.11a**,[18] **1.11b**.[17]

Some substituents (^{t}Bu, Cy, Ph as examples) can allow for the isolation of cyclic *catena*-phospines of multiple ring sizes (**Figure 1.1**). For example, cyclotriphosphine (^{t}BuP)$_3$[17] **1.9a** and cyclotetraphosphine (^{t}BuP)$_4$[19] **1.10c** are both isolable, with the latter being isolated as the minor product in the formation **1.9a**, according to **Scheme 1.2a**. Using cyclohexyl substituents, Baudler *et al.* were able to isolate cyclotriphosphine **1.9c** and cyclopentaphosphine **1.11c** from KCyP-PCy-PCy-PCyK, and $CyPCl_2$ with sodium respectively.[20] Though the pentamer **1.11a** is thermodynamically preferred, phenyl substituted cyclotetraphosphine **1.10d** can be isolated from $Cp_2Zr(PPh)_3$ (**1.17**) or $(Me_3Si)PhP$-PPh-$PPh(SiMe_3)$ and $PhPCl_2$.[21;22] A rare example of a cyclohexaphosphine $(PhP)_6$ **1.18a** has also been isolated with phenyl substituents.[23]

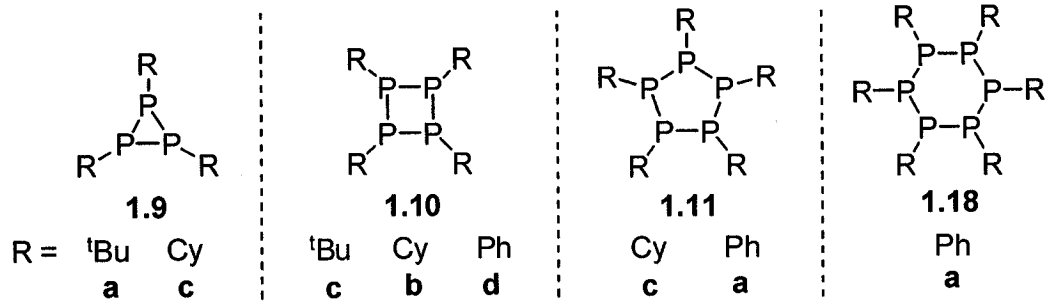

Figure 1.1 Cyclopolyphosphines that have been isolated in multiple oligomeric forms for a given substituent at phosphorus.

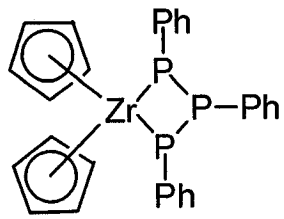

1.17

A large percentage of these and related cyclopolyphosphines were first prepared before advanced multinuclear NMR and X-ray diffraction experiments were readily available, and as a result, some of these *catena*-phosphines have been reported as the incorrect $(RP)_n$ oligomer. Caution is therefore needed when reading these earliest reports, where characterization relies heavily on inaccurate (for these systems) molecular weight determination experiments.[10] Perhaps the most telling example of this is the $(PhP)_n$ system, which was originally reported in 1877 as the diphosphene Ph-P=P-Ph,[24] being isovalent to the well known azobenzene Ph-N=N-Ph. Later, much debate arose as to the degree of oligomerization, and a tetrameric formula was proposed.[18;25] Finally, X-ray crystallography[26;27] and solution ^{31}P NMR studies[28] demonstrated that this compound was the pentamer $(PhP)_5$ **1.11a** in solution and solid phases (Mp. 151 °C). Interestingly, a commonly cited preparation of $(PhP)_5$ is a report in which the product is erroneously assigned to $(PhP)_4$ (refered to as "tetraphenyltetraphosphine A").[18]

The use of both transition metal catalysis and skeletal stabilization (where phosphorus atoms are bridged by a common substituent), has allowed for the isolation of a 16-membered ring of catenated phosphorus atoms.[29] Though mechanistic details remain uncertain, the macrocycle $(C_6H_4P_2)_8$ **1.19** has been isolated in 58% yield from 1,2-

$C_6H_4(PH_2)_2$ **1.20** and 0.05 equivalents of the anionic zirconium complex $[Cp^*_2ZrH_3][K(THF)_2]$. This marks the largest array of phosphorus atoms in a single ring, and is a substantial jump from the three-, four-, five-, and six membered rings more typical for cyclopolyphosphines.

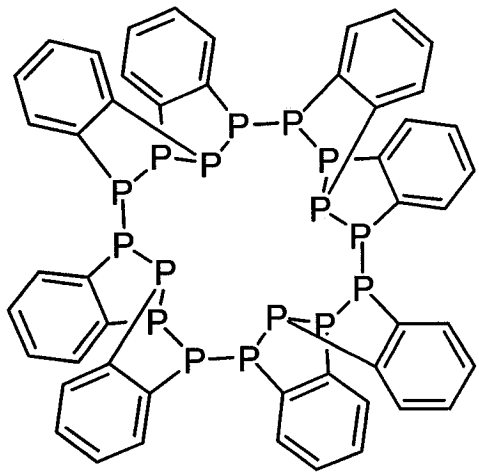

1.19

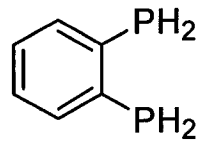

1.20

Besides the polymeric allotropes of phosphorus, the neutral compounds that best illustrate the propensity for phosphorus to form homoatomic bonds are the polycyclic *catena*-phosphines, for which even octacyclic derivatives have been characterized.[3;8;9] Such polycyclic species can be formed from alkylation of the corresponding polycyclic *catena*-phophorus anions, but more general methods come from the reactions outlined in **Scheme 1.3**.[3;8;9]

a) $x\ RPCl_2 + y\ PCl_3 + [2x+3y]/2\ Mg \longrightarrow R_xP_{x+y} + [2x+3y]/2\ MgCl_2$

b) $x/n\ (RP)_n + y\ PCl_3 + 3y/2\ Mg \longrightarrow R_xP_{x+y} + 3y/2\ MgCl_2$

c) $x\ RPCl_2 + y/4\ P_4 + x\ Mg \longrightarrow R_xP_{x+y} + x\ MgCl_2$

d) $[(2x+3y)/2n]\ (RP)_n + y\ PCl_3 \longrightarrow R_xP_{x+y} + 3y/2\ RPCl_2$

Scheme 1.3 General reactions for the formation of polycyclic *catena*-phosphines.

For each of these reactions the phosphorus containing products will contain *x* "RP" groups [from $RPCl_2$ or $(RP)_n$], and *y* "P" atoms bonded to another three phosphorus atoms (from PCl_3 or P_4). There are multiple polycyclic *catena*-phosphines produced in these reactions, and products depend on the organic substituent (R) and the method used. Although only a limited number of these have been isolated as analytically pure oils or crystallographically characterized (some highly catenated examples include **1.21**,[30] **1.22**,[31] and **1.23**[32]), about two dozen different structural arrangements of general formula P_nR_m (n > m) have been identified by a detailed analysis of their often complex phosphorus-31 NMR spectra in solution.[8]

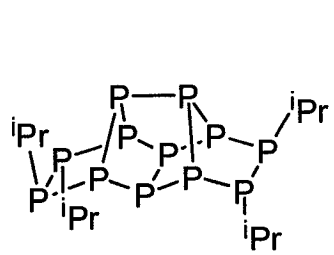

$P_{12}{}^iPr_4$

1.21

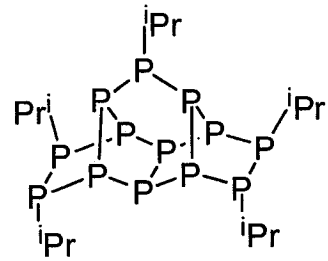

$P_{13}{}^iPr_5$

1.22

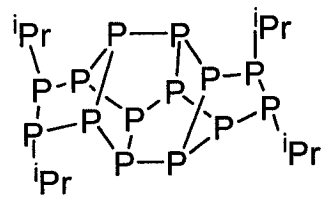

$P_{14}{}^iPr_4$

1.23

The favorability of five- and six-membered rings in *catena*-phosphorus systems is clear from their dominant presence in the structures of these polycyclic molecules.[8] Importantly, if lone-pairs and P-R bonds are each considered as C-H bonds, these polyphosphines can be seen as analogous to known hydrocarbon polyhedrons. These observations formed the basis for developing the carbon-phosphorus analogy in terms of the tendancy within each element for catenation. Other important parallels between phosphorus and carbon are prevelant in low-coordinate compounds of each element.[4;33]

1.4 *catena*-Phosphorus Anions

Like their neutral counterparts, *catena*-phosphorus anions (commonly referred to as polyphosphides) are found both in cyclic and acyclic arrangements. Acyclic derivatives of diphosphides **1.24** – **1.26**, involving various organic substituents, were first identified as products from the reactions of cyclopolyphosphines and different

stoichiometric ratios of alkali metals.[34-37] More recently, phenyl substituted dianions **1.24a**, **1.25a**, **1.26a** have been isolated directly from reduction of $PhPCl_2$ with the appropriate stoichiometric amount of sodium metal.[38] Derivatives **1.26b** (Mes = 2,4,6-trimethylphenyl) and **1.26c** have also been isolated by a similar procedure.[39]

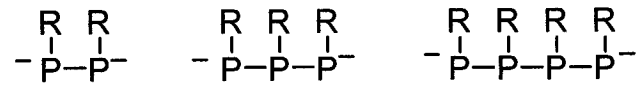

1.24 **a**: R = Ph

1.25 **a**: R = Ph

1.26 **a**: R = Ph **b**: R = Mes **c**: R = ^{t}Bu

Although double bonds between phosphorus atoms in neutral *catena*-phosphorus systems are generally less thermodynamically stable than single bonds, following the double-bond rule,[40] the anionic charge associated with phosphides increases the tendancy for P-P π-systems.[41] The nucleophilic degradation of P_4 by alkali silanides (R_3SiM^I) has allowed for the isolation of unsaturated anions **1.27** and **1.28** (produced along with other saturated species).[41-43] Potassium,[44] rubidium,[45;46] and cesium[46] salts of cyclo-P_6^{4-} (**1.29**) have been isolated in the solid state, but are unstable in solution.[47] Other noteworthy anions involving P-P π-bonding are the cyclic species P_5^- (**1.30**)[48-51] and P_4^{2-} (**1.31**),[47;52] both of which are 6π aromatic systems.[52]

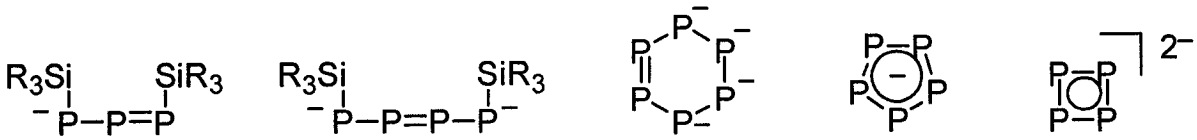

1.27 **1.28** **1.29** **1.30** **1.31**

Although cyclopolyphosphines $(RP)_n$ are well known, reports on the isolation of cyclic monophosphides, cyclo-$(RP)_nP^-$, are few. The alkali metal reduction of $(RP)_n$ occurs preferentially at P-P (giving anions **1.24** - **1.26**), rather than P-C bonds; therefore, aternative synthetic methods to these anions are needed. Recently, the syntheses of cyclic pentaphosphorus monoanions **1.32a-c** have been achieved according to **Scheme 1.4**.[39;53]

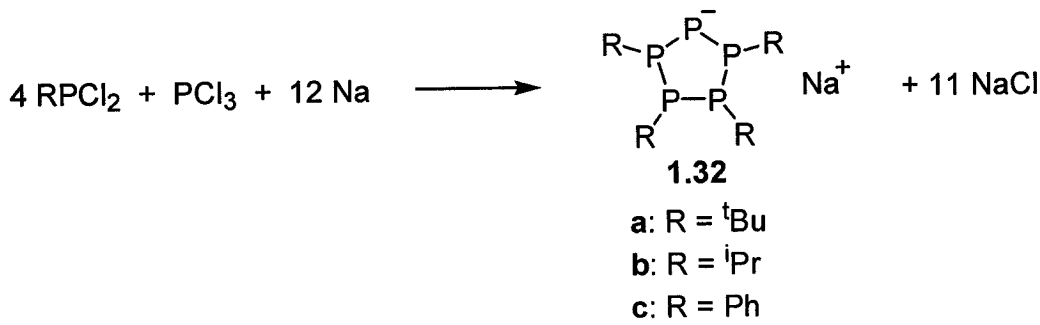

1.32

a: R = ^{t}Bu
b: R = ^{i}Pr
c: R = Ph

Scheme 1.4 Synthesis of isolable cyclic pentaphosphorus monophosphides.

In analogy to neutral polyphosphines, catenated polyphosphorus anions have also been observed as polycyclic species.[3;8;9;54] Crystallographically characterized examples of such anions include **1.33**,[55] **1.34**,[56] **1.35**,[57] **1.36**.[58;59] These compounds and others, such as P_{16}^{2-} (**1.37**) and P_{19}^{3-} (**1.38**), have also been identified in solution from the NMR parameters derived by simulating the complex phosphorus-31 spectra they exhibit in solution.[8] Again, these studies demonstrate the preference for catenated five- and six-membered rings of phosphorus atoms. These compounds are not only remarkable for their high degree of catenation, but also for their ability to accommodate up to four negative charges within a single molecule. These compounds are principally made by the reduction of white phosphorus with the proper stoichiometry of an alkali metal or an alkali metal phosphide ($M^{I}PH_2^{-}$).[3;8;9]

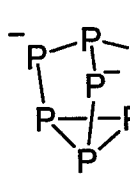

P_7^{3-}

1.33

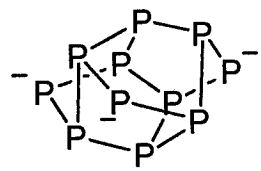

P_{11}^{3-}

1.34

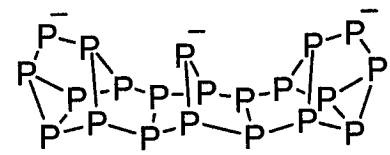

P_{21}^{3-}

1.35

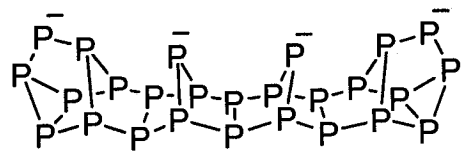

P_{26}^{4-}

1.36

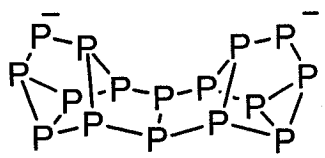

P_{16}^{2-}

1.37

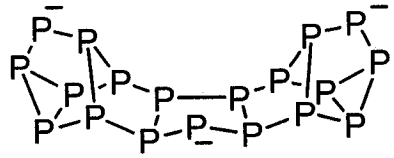

P_{19}^{3-}

1.38

1.5 *catena*-Phosphorus Cations

Much in the same way that the catenated phosphorus anions are principally comprised of phosphine (**I**) and phosphide (**II**) units of full octets, *catena*-phosphorus cations can be envisaged from a combination of phosphine (**I**) and phosphonium (**III**) units. The phosphenium ion (**IV**)[60] is another potential cationic building unit, but the inherent electron deficiency of these species make them less robust than phosphonium centers.

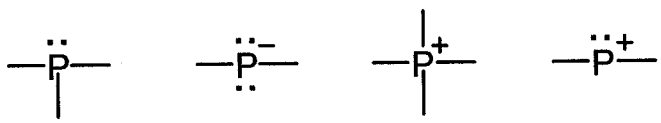

I **II** **III** **IV**

The simplest catenated phosphorus cation is the phosphinophosphonium ion (**A**), which can also be described as a phosphine complex of a phosphenium ion (**A'**).[61;62]

A **A'**

These cations were first proposed as products in the reaction of a diphosphine with alkyl or aryl halides.[63] Derivatives of **1.39** involving amino, aryl, or alkyl groups are easily prepared from a chlorophosphine and half an equivalent of an appropriate halide abstracting agent ($AlCl_3$, $GaCl_3$ or TMSOTf = $Me_3SiOSO_2CF_3$).[61;62;64-68] Other derivatives such as **1.40** can be prepared by ligand exchange with **1.39**[61;62] (consistent

with description **A'**) or directly from combinations of a chlorophosphine, a phosphine, and a halide abstractor.[61;62] These reactions are highlighted in **Scheme 1.5a-c**, respectively, using gallium trichloride as the halide abstracting agent.

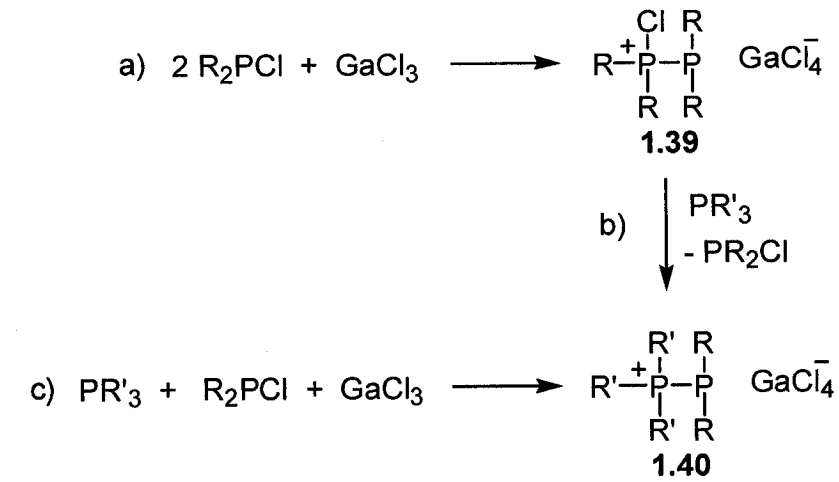

Scheme 1.5 General synthetic pathways to phosphinophosphonium salts.

Discounting the work detailed in the following chapters of this thesis, the only known 1,3-diphosphino-2-phosphonium ions (**B**) are acyclic **1.41a**,[69] cyclic **1.41b**,[62] and polycyclic **1.42**,[70] the latter being a complex situation involving a square-based pyramidal geometry at phosphorus.

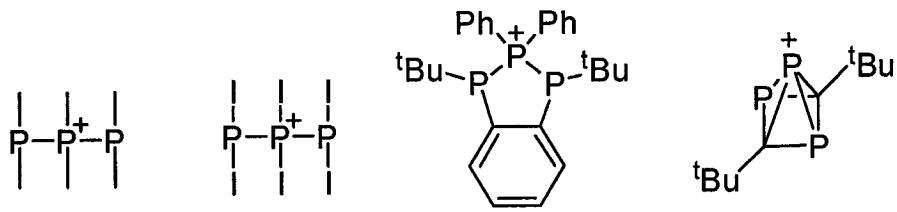

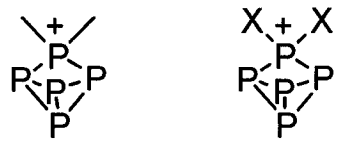

C

1.43
a: X = Br
b: X = I

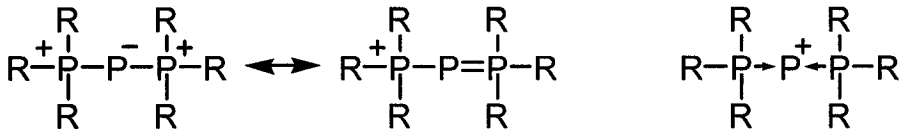

1.44 **1.44'** **1.44''**

R = alkyl, aryl, amino

Other examples of *catena*-phosphorus monocations involve four phosphine centers, such as polycyclic tetraphosphinophosphonium ion (**C**), represented by **1.43**.[69;71;72] Formally, a combination of phosphide and phosphonium environments is found in monocationic derivatives of **1.44**.[73-78] Despite the relatively short bonds (P-P = ~2.13 Å) which indicate partial double bond character (**1.44'** is one resonance contributor),[78] these cations, commonly referred to as triphosphenium cations, can also be regarded as diphosphine complexes of a P(I) center (**1.44''**).[78] Accordingly, the PR_3 groups are easily exchanged in the presence of stronger phosphine donors.[76] Some sample synthetic methods for the preparation of derivatives of **1.44**, involving the reduction of a phosphorus trihalide in the presence of phosphine (PR_3) ligands, are illustrated in **Scheme 1.6**.

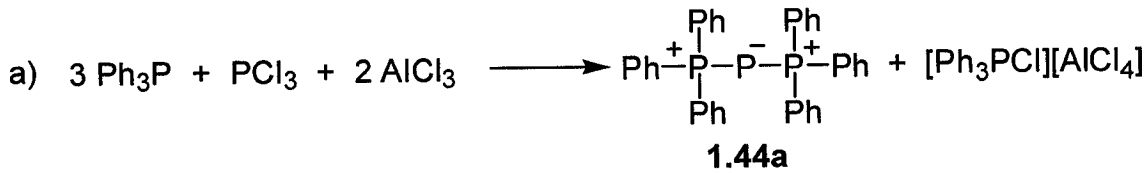

1.44a

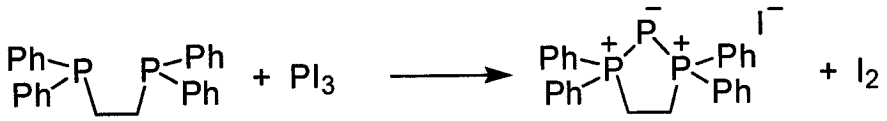

1.44b

Scheme 1.6 Synthesis of some acyclic (**1.44a**)[76;79] and cyclic (**1.44b**)[75] derivatives of triphosphenium cations.

Unique crystallographically characterized examples **1.45**[80] and the phosphonio-substituted phosphene **1.46**[81;82] involve multiple bonding between phosphorus atoms. Cation **1.45** has been prepared by methylation of the corresponding diphosphene, and is best represented as drawn, rather than the potential phosphinophosphenium resonance isomer (**1.45'**), as it has a planar geometry about a short (2.02 Å) P-P bond.[80]

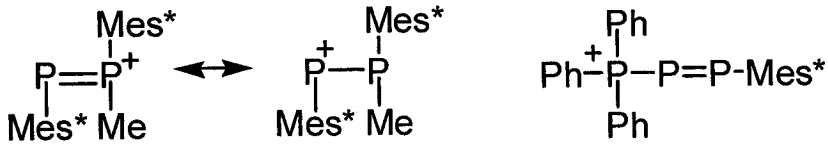

1.45 **1.45'** **1.46**

Although no monocationic analogue $[(RP)_nPR_2^+$; such as **1.47** - **1.49** (n = 2 – 4)] of the catenated cyclopolyphosphines [$(RP)_n$; **1.9** – **1.11**, **1.18** (n = 3 – 6)] or cyclopolyphosphorus anions [$(RP)_nP^-$; **1.32**, n = 4] have been definitively characterized prior to this thesis (**Chapter 2 - 4**), a single monocyclic dication **1.50** $[(RP)_n(PR_2)_2^{2+}$, n = 2] has been crystallographically characterized. This example of a cyclic 2,4-diphosphino-1,3-diphosphonium ion (**D**) was formed serendipitously from $RSnMe_3$ (R = 2,6-dimethoxyphenyl) and $PClF_2$ in an attempt to make RPF_2.[83] Disregarding substituents, it can be seen that dication **1.50** is formally the dimer of monocation **1.45**, via a head-to-tail, [2 + 2] cycloaddition (**Scheme 1.6**). This suggests that analogues of **1.45** may be unstable with respect to oligomerization in the absence of bulky ligands.

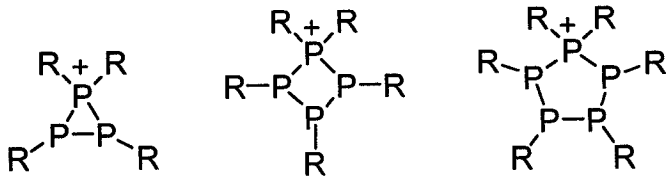

1.47 **1.48** **1.49**

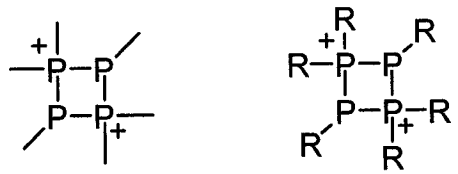

D **1.50**

R = 2,6-dimethoxyphenyl

Other *catena*-phosphorus dications include diphosphonium (**E**) and 2-phosphino-1,3-diphosphonium (**F**). These are represented by crystallographically characterized derivatives **1.51a-c**, with amino[84-86] or bridging alkane ligands,[87-89] and the P-H derivative **1.52a**,[90] respectively.

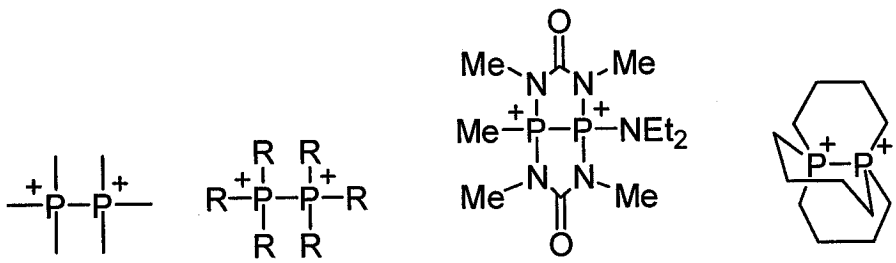

E **1.51** **1.51b** **1.51c**

a: R = NEt_2

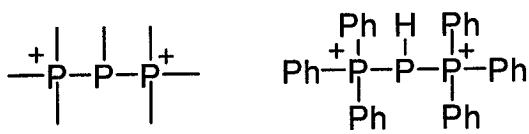

F **1.52a**

Other derivatives of **1.52**, have been prepared as tetrachloroaluminate salts from PCl_3, R_3P (R = alkyl, Ph) and $AlCl_3$ (**Scheme 1.7a**), or by akylation of cations of type **1.44** with R'Cl (R' = H, alkyl) in the presence of $AlCl_3$, according to **Scheme 1.7b**.[90]

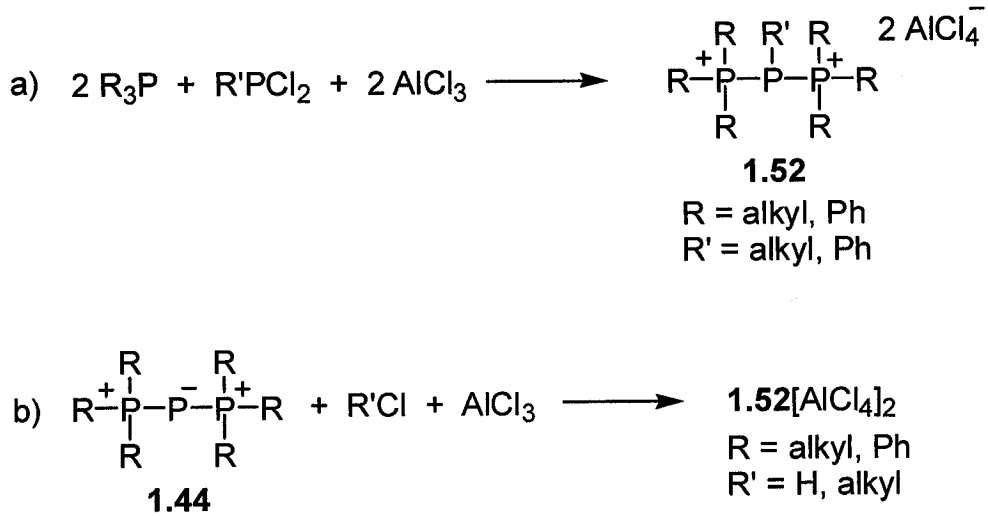

Scheme 1.7 Synthesis of tetrachloroaluminate salts of **1.52**.

There have also been two reports on acyclic tetraphosphorus dications. In 1986, Schmidpeter's group reported the synthesis of a number of 1,2-diphosphonio-diphosphirane drivatives, one of which was crystallographically characterized as **1.53**.[91] These cations are specific examples of 2,3-diphosphino-1,4-diphosphonium cations (**G**), where the phosphine centers are part of a three-membered ring involving two phosphorus atoms and one carbon center (a diphosphirane). These compounds were synthesized from a complex reaction involving derivatives of **1.44** where the diphosphirane unit was formed by dichloromethane activation.

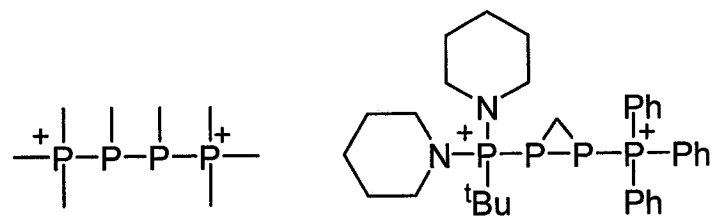

More recently, the group of Woollins has prepared another derivative of this dicationic framework (**G**). In crystallographically characterized **1.54**, the phosphine centers are joined to the adjacent phosphonium center by a bridging naphthalene unit. Though the reaction pathway is not completely understood, the iodide salt of this dication was prepared from **1.55** and tetraiododiphosphine (I_2P-PI_2).[92]

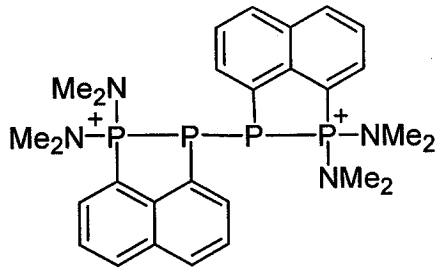

1.54

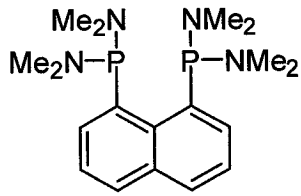

1.55

Phosphorus is capable of hypervalency and this opens up many other potential bonding possibilities for catenated phosphorus cations. There have been only a few examples of *catena*-phosphorus cations involving a hypervalent phosphorus atom. A disphenoidal geometry is observed in spirocyclic **1.56**,[93] as it involves a tetracoordinate phosphorus with a stereochemically active lone-pair. Cation **1.57**[94] contains an octahedral environment at the central phosphorus, and can be considered as a bisphosphine complex of planar phosphonium ion (**1.57'**). Our group has recently been able to isolate a hypervalent triphosphorus monocation (**1.58**, **1.58'**; Mes* = 2,4,6-tri-tertbutylphenyl), where the central phosphorus atom formally has 12 valence electrons, despite its low coordination number of three.[95] Recent examples of phosphoranophosphonium ions (**1.59**, **1.59'**) featuring two phosphorus atoms have also been reported.[96]

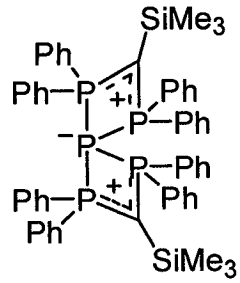

1.56

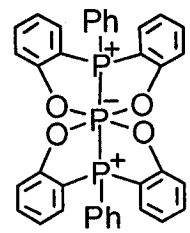

1.57

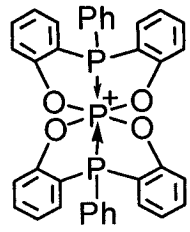

1.57'

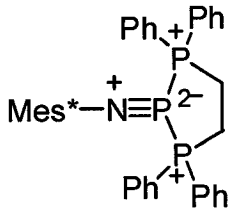

1.58

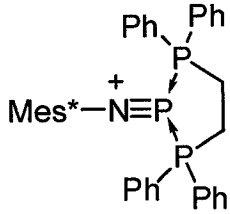

1.58'

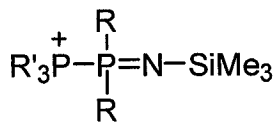

1.59

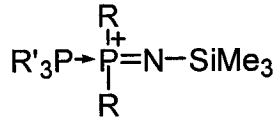

1.59'

a: R = Me, R' = ^{n}Bu

b: R = R' = Me

c: R = OCH_2CF_3, R' = ^{n}Bu

d: R = OCH_2CF_3, R' = Me

1.6 Summary

As for carbon, catenation is an important feature in the chemistry of phosphorus. Although many studies have been reported on *catena*-phosphines and *catena*-phosphorus anions,[3;7-9;54] there have been relatively few reports on *catena*-phosphorus cations. **Figure 1.2** shows representations (general topologies only) for all known catenated phosphorus monocations (**A** - **C**), or dications (**D** - **G**) involving phosphine and phosphonium units.

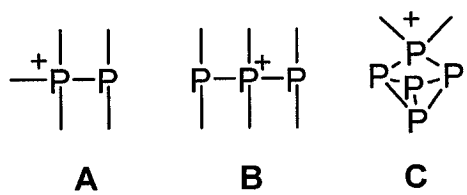

A **B** **C**

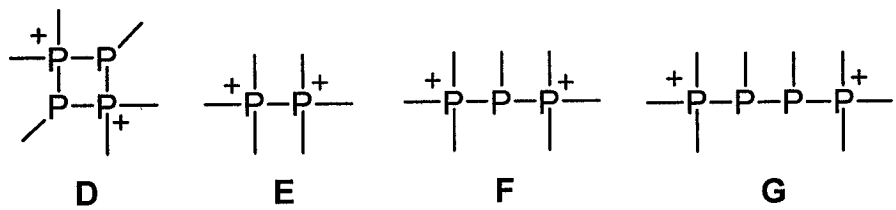

D **E** **F** **G**

Figure 1.2 Representations for all known *catena*-phosphorus mono- (**A** – **C**) and dications (**D** – **G**) involving exclusively phosphine and phosphonium units.

Although mononuclear phosphorus compounds can support three[97-99] and up to five[98] positive charges with appropriate nitrogen-based substituents (for example **1.60** and **1.61**), no catenated phosphorus systems exist with a higher positive charge than +2. Unlike for the highly catenated phosphines or phosphorus anions (**Chapter 1.3**, **1.4**), no *catena*-phosphorus cation has been isolated with more than five phosphorus atoms. These limitations, and the unsystematic nature of the few reports on these cationic species, leave apparent holes in a broader understanding of fundamental *catena*-phosphorus chemistry.

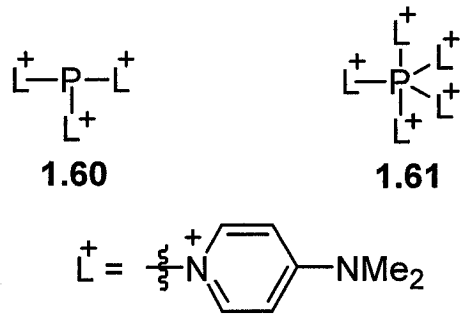

1.60 **1.61**

The following chapters provide an account of contributions towards a rational and systematic development of *catena*-phosphorus cations consisting of phosphine and phosphonium units. The synthesis, isolation, properties, and reactivity of these cations demonstrate their accessibility, and illustrate a potential for growth within this new realm of fundamentally relevant phosphorus chemistry.

Chapter 2.0: Cyclodiphosphinophosphonium Ions

2.1 Introduction

As illustrated previously in **Figure 1.2**, dicationic framework **D** is the only known representative of monocyclic *catena*-phosphorus cations. In the context of a rational development of *catena*-phosphorus cations, we sought to prepare the first examples in the series of small monocyclic phosphorus cations consisting of three, four, and five directly bonded phosphorus atoms. This chapter deals with the synthesis and characterization of cyclodiphosphinophosphonium ions (**H**).[100] Cyclotriphosphinophosphonium (**I**) and cyclotetraphosphinophosphonium (**J**) ions are discussed in **Chapter 3** and **Chapter 4**, respectively.

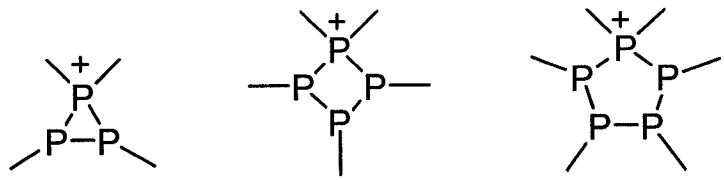

H **I** **J**

2.2 Alkylation of Cyclotriphosphines with Methyl Triflate

Knowing that simple phosphonium salts ([R_3PR'][X]) can be prepared from phosphines (R_3P) and alkyl halides (R'X), a logical synthesis of cations of type **H** presented itself via the alkylation of cyclotriphosphines. Phosphorus-31 NMR spectra of reaction mixtures containing (^{t}BuP)$_3$ **2.1a** and excess (1.5 – 2 molar equivalents) MeOTf showed the immediate and quantitative consumption of **2.1a** along with the concurrent formation of an approximate AMX spin system (**Figure 2.1**) for [(^{t}BuP)$_2$P^{t}BuMe][OTf] (**2.2a**[OTf]). Though some second-order effects were present at this field (101.3 MHz), indicated by the non-uniform peak intensities, each signal occured as a doublet of doublets, with the signals corresponding to the tetracoordinate phosphonium center at the lowest field (X part of AMX). All coupling constants were in the typical range for P-P single bonds ($^1J_{AM}$ = -123 Hz, $^1J_{AX}$ = -334 Hz, $^1J_{MX}$ = -317 Hz), and the largest values involved the phosphonium center.

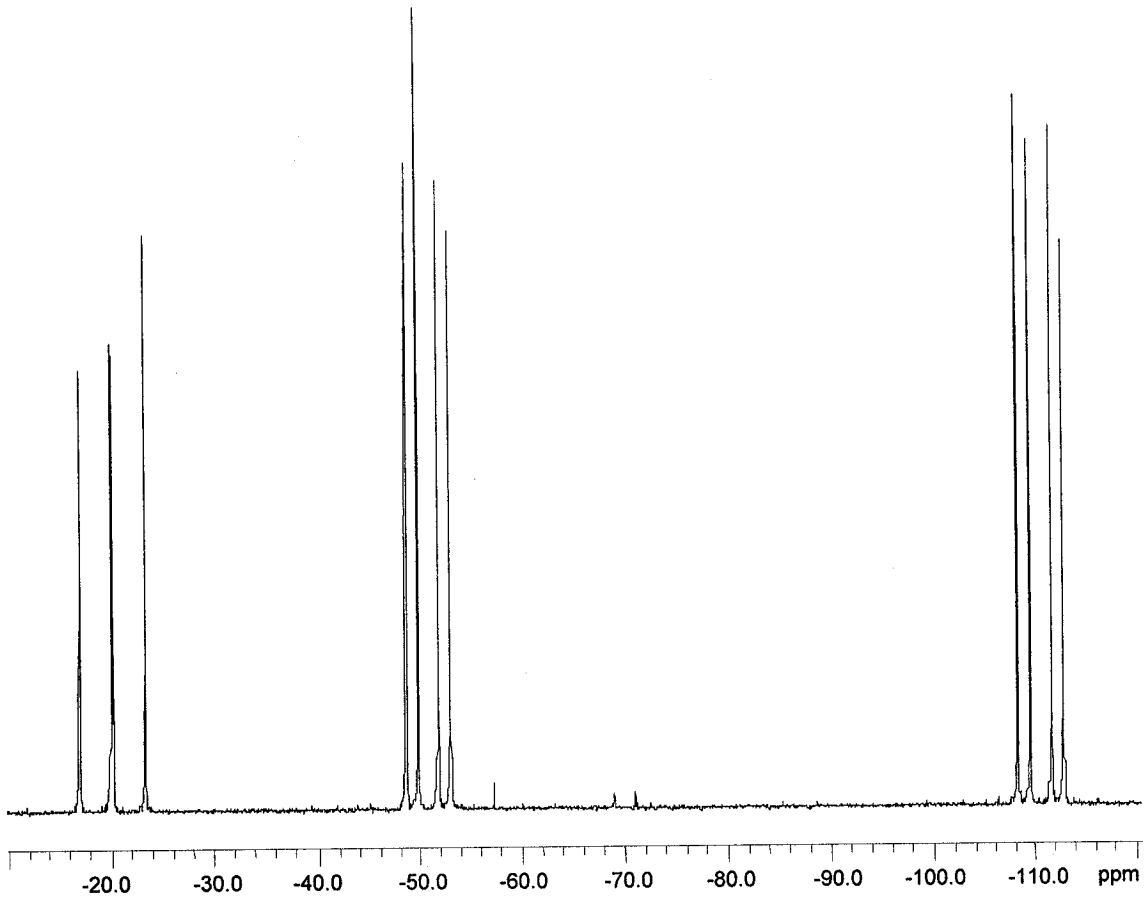

Figure 2.1 $^{31}P\{^{1}H\}$ NMR spectrum (101.3 MHz) for a reaction mixture containing (^{t}BuP)$_3$ and MeOTf, showing quantitative formation of **2.2a**[OTf].

The observation of only an AMX spin system from this reaction is interpreted in terms of stereoselective methylation of **2.1a** at either of the equivalent *cis* substituted phosphorus centers to give racemic **2.2a** with three distinct phosphorus nuclei (**Scheme 2.1**), rather than the potential *meso* isomer of C_s symmetry (potentially formed from methylation of the unique phosphorus center). This was confirmed by X-ray analysis, as crystals of **2.2a**[OTf] contained both enantiomers of the cation. The structure of one enantiomer of **2.2a** is shown in **Figure 2.2**.

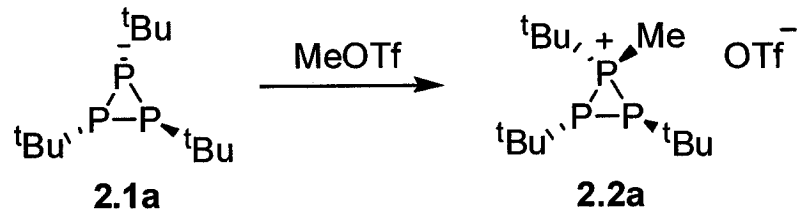

2.1a **2.2a**

Scheme 2.1 Synthesis of racemic **2.2a**[OTf] by methylation of (^{t}BuP)$_3$.

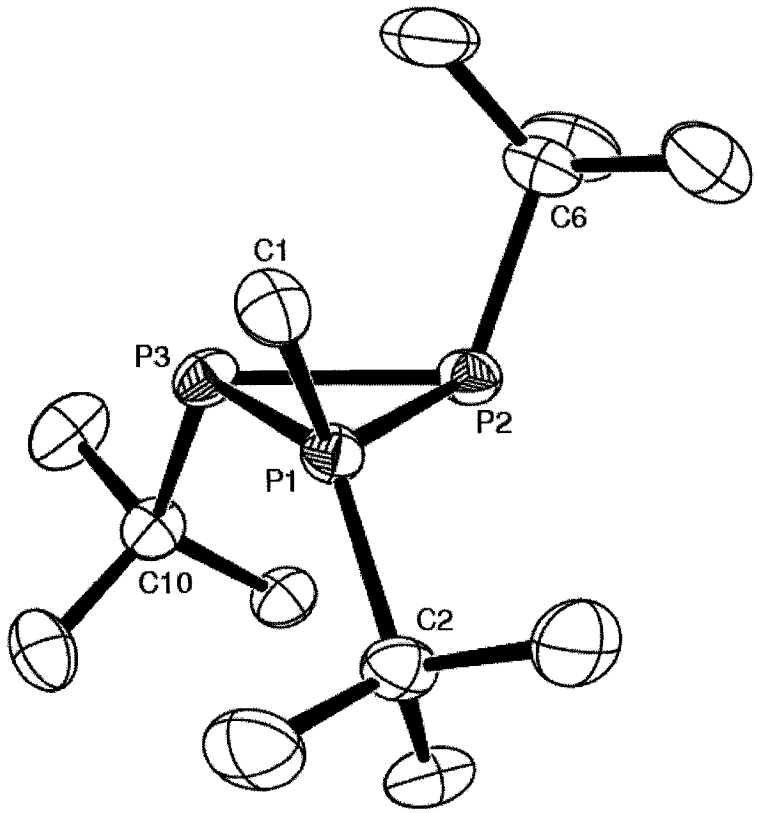

Figure 2.2 Solid state structure of one enantiomer of the cation in **2.2a**[OTf], with hydrogen atoms omitted for clarity and thermal ellipsoids at the 50% probability level.

The most notable structural features of **2.2a** are indicative of the high degree of steric strain within the molecule, resulting from unfavorable *cis* interactions between ^{t}Bu (at C6) and Me (C1) substituents on one face of the molecule, and two ^{t}Bu (C2 and C10) groups on the other. Thus, despite the similar endocyclic angles in **2.1a** and **2.2a**, the four coordinate P1 atom of **2.2a** is highly distorted with C-P1-P angles ranging from 108.6 – 133.2°. Also, the plane defined by C1, P1, C2 is twisted by 72.5° with respect to the plane containing the three phosphorus atoms (ideally 90°).

The bond distances and angles of catenated phosphorus systems generally show little dependence on the molecular charge. Although the shortest bonds in **2.2a** involve the tetracoordinate phosphonium center (**Table 2.1**), the observed P-P bond lengths (2.15 – 2.23 Å) are consistent with typical P-P single bonds found in neutral (eg. **2.1a**: P-P = 2.19 – 2.22 Å)[101] and anionic catenated systems. Similarly, the shortest P-C bond lengths (ranging from 1.81 – 1.89 Å) involve the phosphonium center (**Table 2.1**).

Table 2.1 Selected structural parameters for **2.2a**. Numbers in square brackets correspond to atom labels in **Figure 2.2**.

P-C (Å)	P-P (Å)	C-P-P (°)	C-P-C (°)	P-P-P (°)
1.858(2) [1,2]	2.1465(6) [1,2]	123.15(7) [1,1,2]	110.41(9) [1,1,2]	62.31(2) [2,1,3]
1.806(2) [1,1]	2.1652(6) [1,3]	108.62(7) [1,1,3]		59.26(2) [1,2,3]
1.886(2) [2,6]	2.2306(6) [2,3]	112.97(6) [2,1,2]		58.43(2) [1,3,2]
1.894(2) [3,10]		133.21(6) [2,1,3]		

The analogous reactions of $(CyP)_3$ **2.1b** and MeOTf were more complicated (**Scheme 2.2**). Although the cyclodiphosphinophosphonium ion in $[(CyP)_2PCyMe][OTf]$ (**2.2b**[OTf]) was observed by $^{31}P\{^1H\}$ NMR spectroscopy (AMX spin system, **Table 2.2**), it could not be isolated as it was formed in approximately equimolar amounts with the tetraphosphorus monocation $[(CyP)_3PCyMe][OTf]$ (**3.6b**[OTf]). Compound **3.6**[OTf] has been fully characterized from a more direct synthesis involving reactions of $(CyP)_4$ and MeOTf (see **Chapter 3**). Over time, the concentration of **3.6b** increased relative to that of **2.2b**, however the observation of other unidentified byproducts prevented the definitive identification of a direct conversion from **2.2b** to **3.6b**. This highlights the importance of the bulky ^{t}Bu substituents in the formation of **2.2a**[OTf] as the exclusive product from **2.1a** and MeOTf.

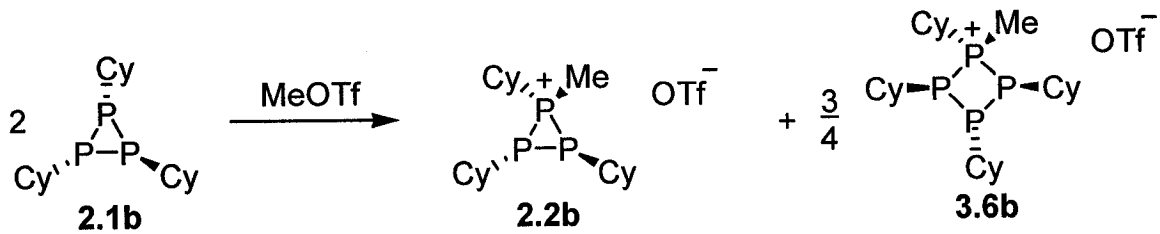

Scheme 2.2 Synthesis of **2.2b**[OTf] and **3.6b**[OTf] from $(CyP)_3$ and MeOTf.

Table 2.2 $^{31}P\{^{1}H\}$ NMR parameters for **2.2a**[OTf] and **2.2b**[OTf] in CH_2Cl_2.

Cation	P_A (ppm)	P_M (ppm)	P_X (ppm)	$^1J_{AM}$ (Hz)	$^1J_{AX}$ (Hz)	$^1J_{MX}$ (Hz)
2.2a	-110	-51	-20	-123	-334	-317
2.2b	-156	-129	-46	-97	-292	-292

Attempts at using other electrophiles in reactions with **2.1a** showed that the products depend on the nature of the electrophiles and the counterion. As illustrated in **Scheme 2.3a**, the reaction of **2.1a** and triflic acid afforded the ring expansion product **3.7a**, which has also been generated and fully characterized from the reaction of $(^tBuP)_4$ and triflic acid (**Chapter 3**). In contrast, the addition of equimolar amounts of hydrochloric acid to **2.1a** afforded the ring opened product **2.3** almost quantitatively. Compound **2.3** was identified by its characteristic $^{31}P\{^{1}H\}$, and ^{31}P NMR spectra.[19] Also, unlike MeOTf, iodomethane failed to react with **2.1a**.

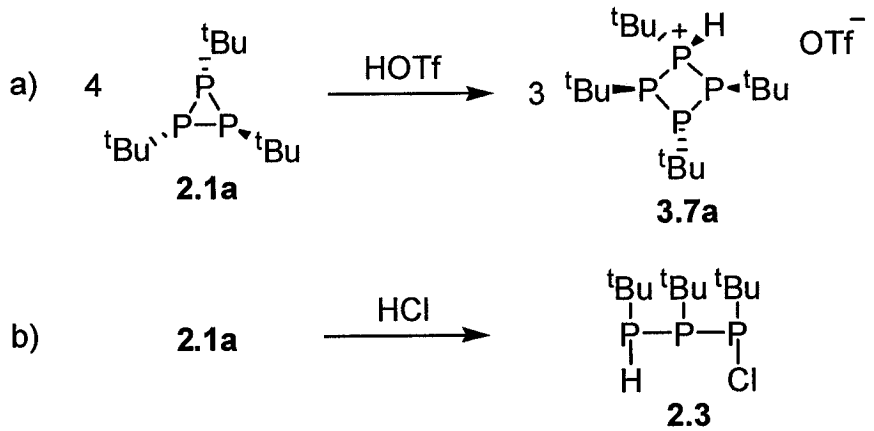

Scheme 2.3 Reactions of $(^tBuP)_3$ with a) HOTf and b) HCl.

2.3 Summary

The first example of a cyclic diphosphinophosphonium ion has been synthesized and isolated as $[(^tBuP)_2P^tBuMe][OTf]$ (**2.2a**[OTf]) from the quantitative reaction of cyclotriphosphine $(^tBuP)_3$ and excess MeOTf. This represents the smallest member of the family of cyclic polyphosphinophosphonium monocations, and is an important achievement in a systematic development of *catena*-phosphorus cations. It has also been demonstrated that the products from reactions of cyclopolyphosphines $[(RP)_n]$ and electrophiles are dependent on the choice of substituent (R), electrophile, and counterion.

Chapter 3.0: Cyclotriphosphinophosphonium Ions

3.1 Introduction

Based on elemental analysis data, Issleib *et al.* reported the formation of the cyclotriphosphinophosphonium iodide salts **3.1a**[I], **3.1b**[I] from the reaction of the corresponding cyclotetraphosphine and methyliodide.[36;102] An analogous salt **3.2**[Cl] was proposed, also based on combustion analysis, from the reaction of $(EtP)_4$ and CCl_4.[103] Without solid state structures or NMR data, the product assignments in these cases are ambiguous, as elemental analysis cannot be used to distinguish between the possible ionic (**3.3A**), ring opened (**3.3B**) and triphosphinophosphorane (**3.3C**) formulations.

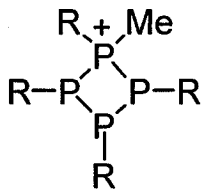

3.1

a: R = ^{t}Bu

b: R = Et

3.2

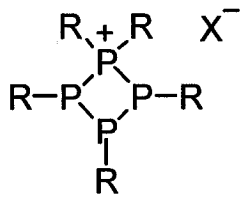

3.3A

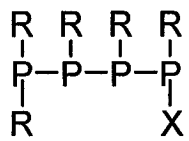

3.3B

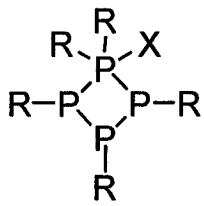

3.3C

More recently, alkylation, acylation, and protonation reactions with the unusual tricyclic tetraphosphine **3.4** have led to the observation of products concluded to be salts of type **3.3A** based on multinuclear NMR data.[104] Only the acylated derivative was isolated, and no yields were reported.

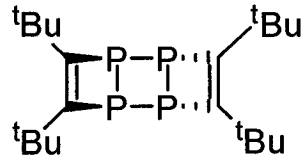

3.4

This chapter presents the synthesis, multinuclear NMR data, and crystallographic characterization of a number of isolable cyclotriphosphinophosphonium ions.[100]

3.2 Synthesis and Phosphorus-31 NMR Studies

In analogy to the synthesis of $[(^tBuP)_2P^tBuMe][OTf]$ (**2.2a**[OTf]), cyclotriphosphinophosphonium ions $[(RP)_3PRMe][OTf]$ (**3.6**[OTf]; **a**: R = ^{t}Bu; **b**: R = Cy) were prepared by methylation of the corresponding cyclotetraphosphines $(^tBuP)_4$ (**3.5a**) and $(CyP)_4$ (**3.5b**) with excess (1.5 – 2 molar equivalents) MeOTf (**Scheme 3.1a**). Triflic acid (HOTf) was used in a similar manner for the formation of protonated analogues **3.7a**[OTf] and **3.7b**[OTf] (**Scheme 3.1b**). In all cases the reactions were quantitative, and the electrophile (effectively Me^+ or H^+) added directly to one of the four equivalent phosphorus atoms of the all-*trans* cyclotetraphosphine, resulting in a *meso* product with C_s symmetry.

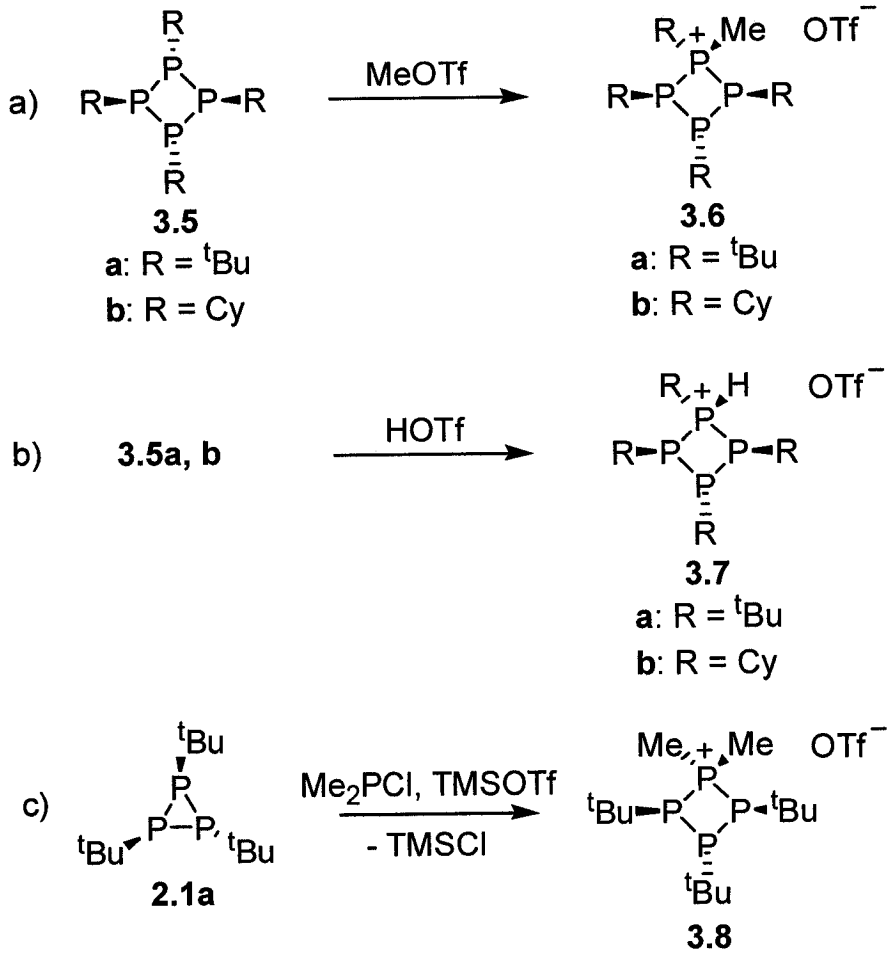

Scheme 3.1 Synthesis of derivatives of **3.6**[OTf], **3.7**[OTf] and **3.8**[OTf].

The reactions were monitored by $^{31}P\{^{1}H\}$ NMR spectroscopy, and the products were easily identified by their AB_2X (**3.6a**), A_2MX (**3.6b**, **3.7b**), A_2BX (**3.7a**) spin systems (**Table 3.1**). Representative examples of the simulated spectra are shown in **Figure 3.1 – 3.3**. In the proton coupled spectrum of **3.7a**, the low field triplet was split into an overlapping, five-line, doublet of triplets. This corresponded to a $^{1}J_{PH}$ value of 461 Hz, which was also observed in the ^{1}H NMR spectrum (7.71 ppm, d, $^{1}J_{PH}$ = 464 Hz). The complex second-order spin system of **3.7b** complicated the determination of the P-H coupling constant by use of ^{31}P NMR; however, it was easily observed in the ^{1}H NMR spectrum (7.84 ppm, d, $^{1}J_{PH}$ = 452 Hz).

Table 3.1 Simulated $^{31}P\{^{1}H\}$ NMR parameters for derivatives of **3.6**[OTf], **3.7**[OTf] and **3.8**[OTf].

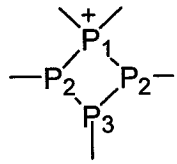

Cation	P_1 (ppm)	P_2 (ppm)	P_3 (ppm)	$^{1}J_{12}$ (Hz)	$^{1}J_{23}$ (Hz)	$^{2}J_{13}$ (Hz)
3.6a[a]	18	-39	-43	-275	-152	9
3.6b[a]	10	-70	-56	-230	-122	-17
3.7a[b]	-32	-57	-55	-260	-156	12
3.7b[b]	-23	-74	-64	-233	-126	16
3.8[a]	-2.1	-24	-28	-251	-143	28

[a] $CDCl_3$, 298 K; [b] CH_2Cl_2, 200 K.

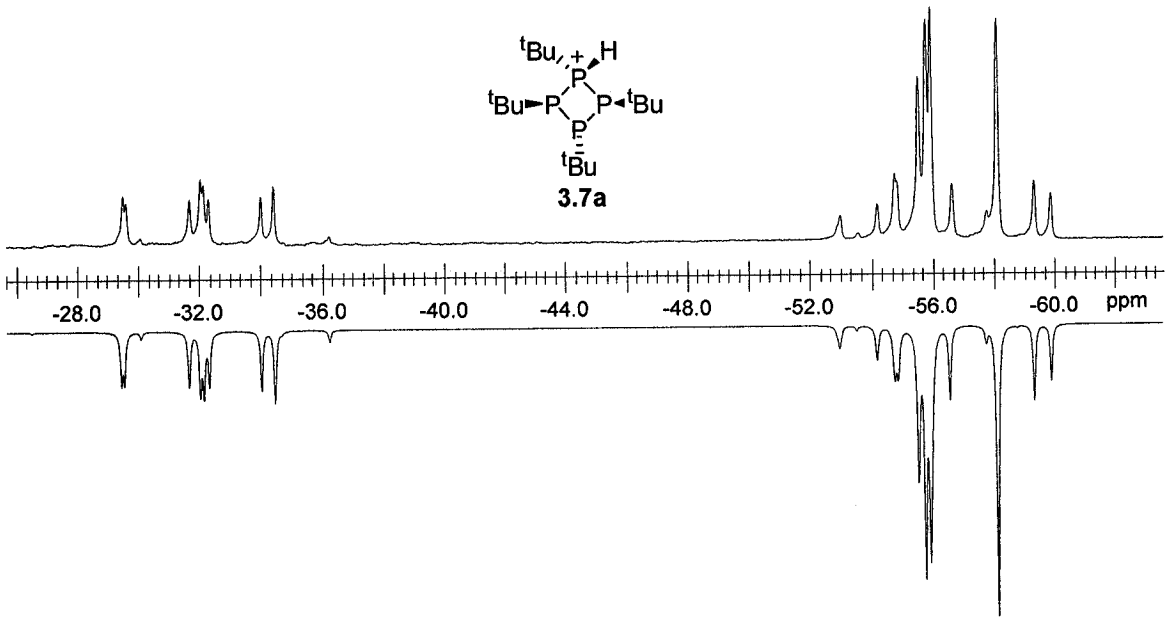

Figure 3.1 Experimental (top) and simulated (inverted) $^{31}P\{^{1}H\}$ NMR spectra (101.3 MHz, 200 K) of **3.7a**[OTf] (A_2BX spin system).

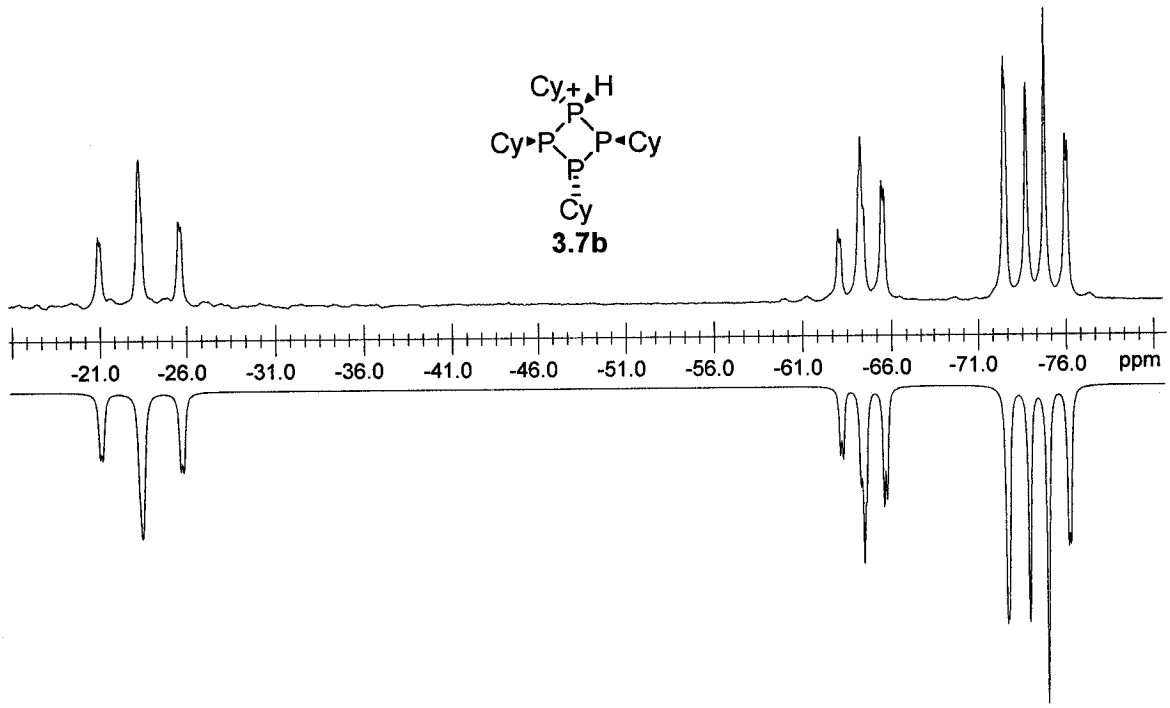

Figure 3.2 Experimental (top) and simulated (inverted) $^{31}P\{^{1}H\}$ NMR spectra (101.3 MHz, 200 K) of **3.7b**[OTf] (A_2MX spin system).

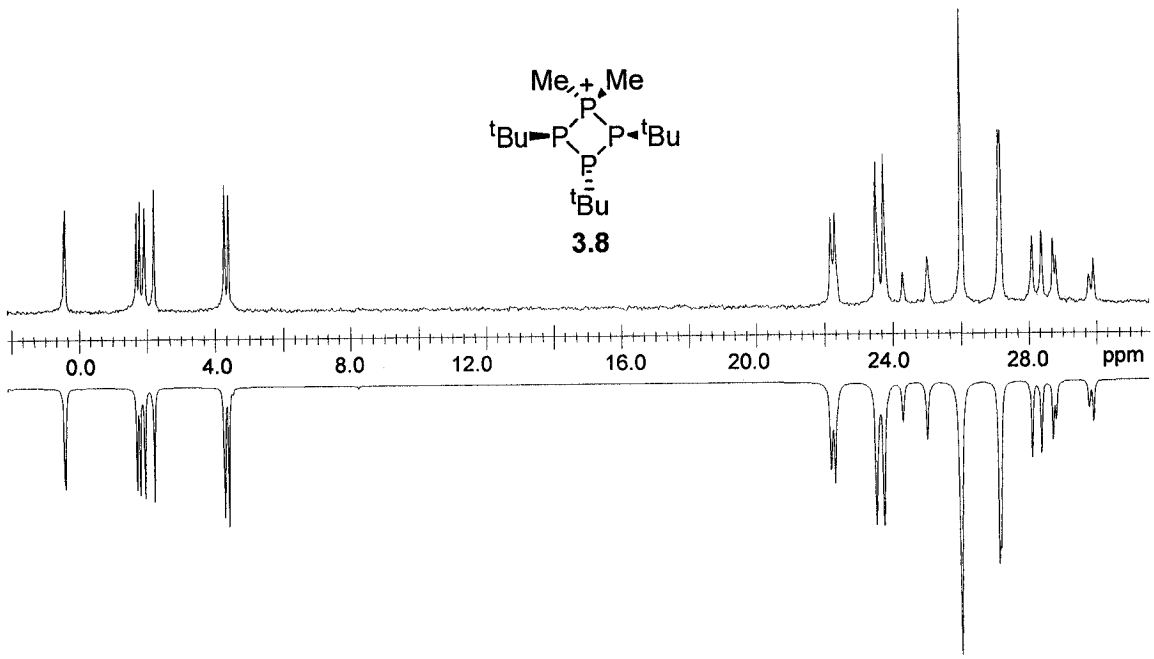

Figure 3.3 Experimental (top) and simulated (inverted) $^{31}P\{^{1}H\}$ NMR spectra (101.3 MHz) of **3.8**[OTf] (AB_2X spin system).

In contrast to H^+ and Me^+, the transient electrophilic phosphenium ion Me_2P^+, generated *in situ* from Me_2PCl and TMSOTf, attacked a P-P bond of ($^tBuP)_3$ (**2.1a**), rather than a phosphine lone pair (although this may be involved as a first step in the mechanism). This was clearly indicated by a simulation of the ^{31}P NMR spectrum for the major product (> 95%) from the reaction mixture (**Figure 3.3**, **Table 3.1**). The observed AB_2X spin system is indicative of ring expansion via the selective insertion of Me_2P^+ into the P-P bond between the two identical phosphorus atoms of **2.1a**, giving *meso*-[($^tBuP)_3PMe_2$][OTf] (**3.8**[OTf], **Scheme 3.1c**). No other diastereomeric forms of **3.8** were observed. Presumably, the *cis* nature of two of the three ^{t}Bu substituents of **2.1a** provides access to only one P-P bond via the face of the molecule opposite to the two substituents. An analogous insertion of "PX" (X = Cl, Br) has been observed for **2.1a**.[105]

3.3 X-Ray Structures

The solid state structures for derivatives **3.6a**[OTf], **3.6b**[OTf], **3.7a**[OTf], and **3.8**[OTf] were determined by X-ray crystallography, and the cations are shown in **Figure 3.4 – 3.7**. In all cases, the structures confirm the products as determined by $^{31}P\{^1H\}$ NMR spectroscopy. All compounds show ionic formulations in the solid state, with the shortest anion-cation interactions occurring through the substituents at phosphorus, making them clear examples of phosphonium ions (**3.3A**) rather than neutral phosphoranes (**3.3C**). Structural parameters for these cations are presented in **Table 3.2**.

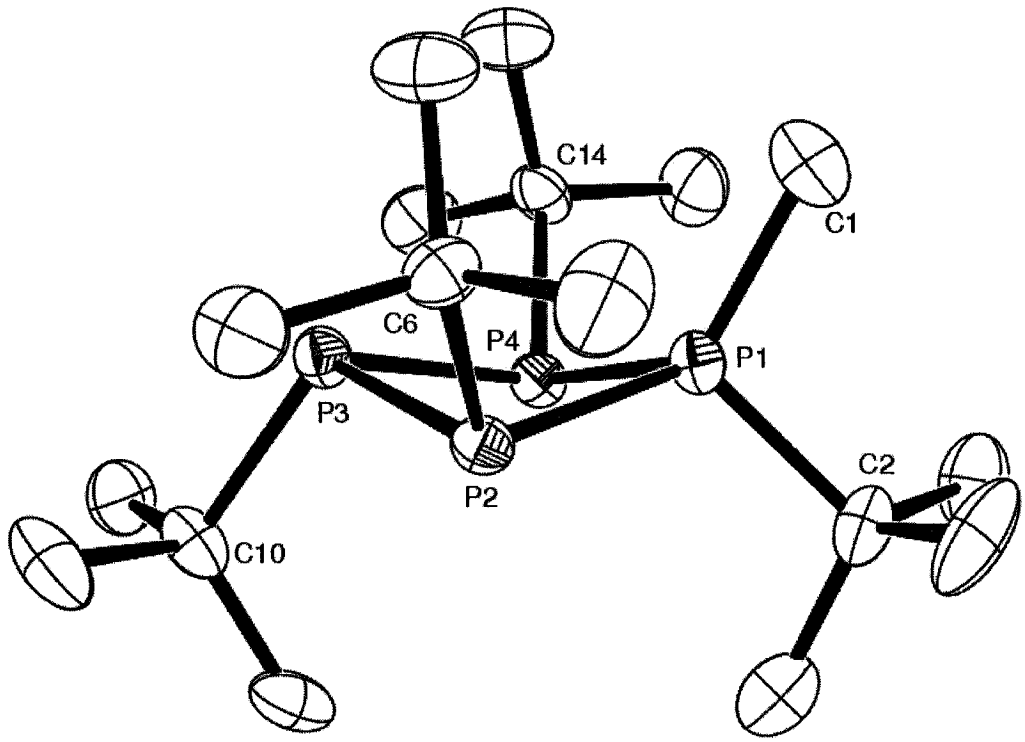

Figure 3.4 Solid state structure of the cation in [(^{t}BuP)$_3$P^{t}BuMe][OTf] (**3.6a**[OTf]) with hydrogen atoms omitted for clarity and thermal ellipsoids at the 50% probability level.

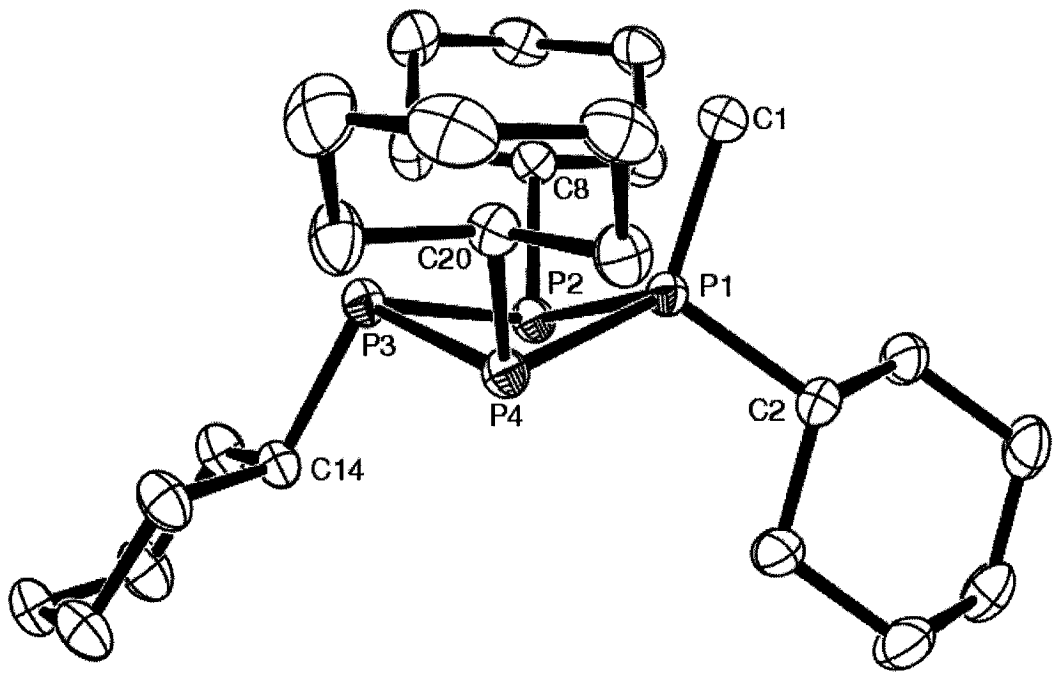

Figure 3.5 Solid state structure of the cation in [(CyP)$_3$PCyMe][OTf] (**3.6b**[OTf]) with hydrogen atoms omitted for clarity and thermal ellipsoids at the 50% probability level.

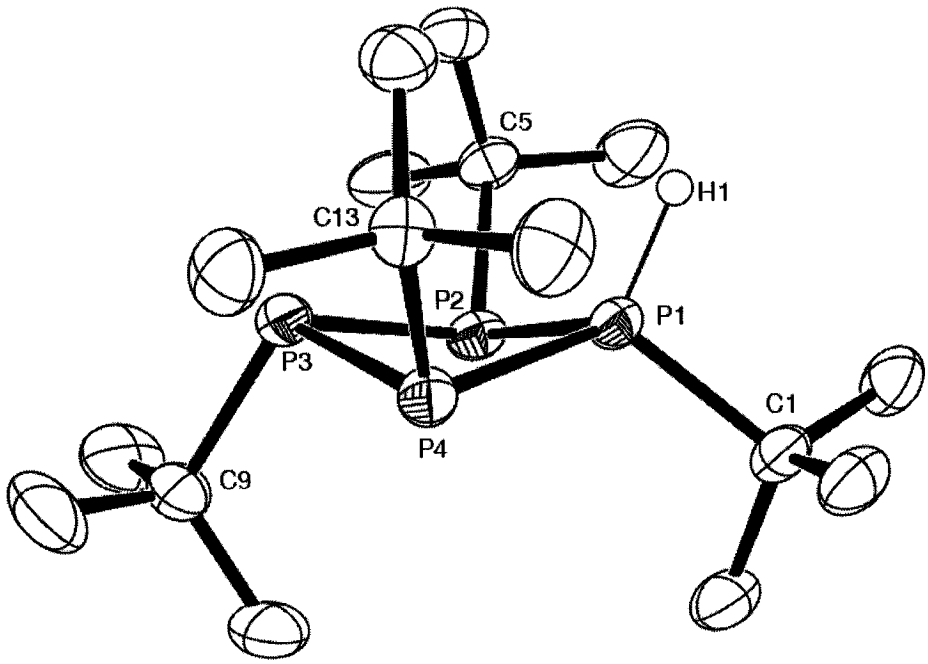

Figure 3.6 Solid state structure of the cation in [(^{t}BuP)$_3$P^{t}BuH][OTf] (**3.7a**[OTf]) with hydrogen atoms (except H1) omitted for clarity and thermal ellipsoids at the 50% probability level.

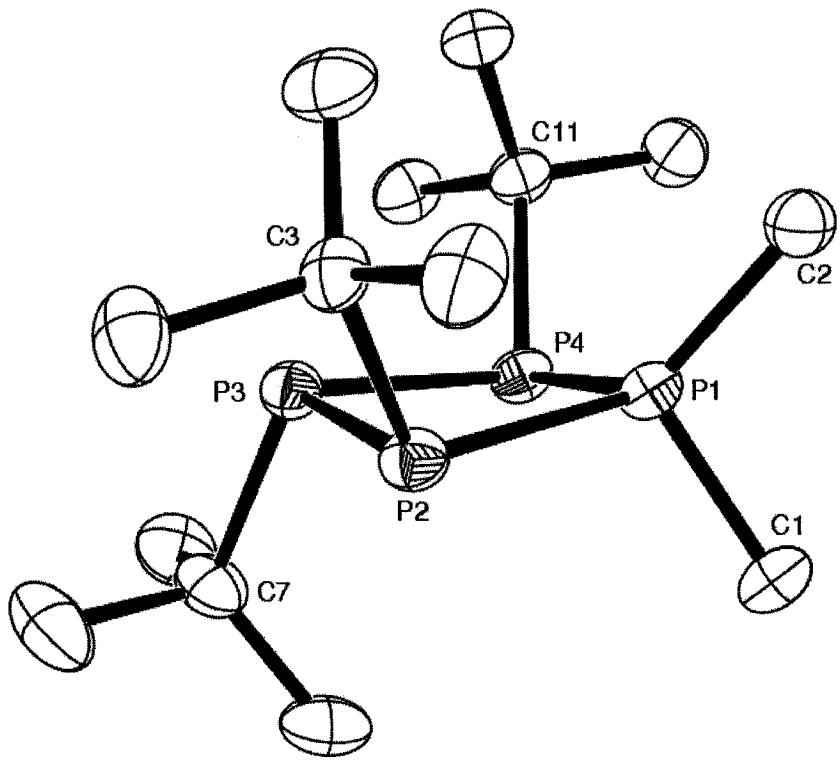

Figure 3.7 Solid state structure of the cation in [(^{t}BuP)$_3$PMe$_2$][OTf] (**3.8**[OTf]) with hydrogen atoms omitted for clarity and thermal ellipsoids at the 50% probability level.

Table 3.2 Selected structural parameters for derivatives of **3.6**[OTf], **3.7a**[OTf] and **3.8**[OTf]. Numbers in square brackets correspond to atom labels in **Figure 3.4 – 3.7.**

Cation	P-C (Å)	P-P (Å)	C-P-P (°)	C-P-C (°)	P-P-P (°)	τ^a (°)
3.6a	1.848(4) [1,2] 1.813(4) [1,1] 1.903(4) [2,6] 1.903(4) [3,10] 1.894(3) [4,14]	2.204(2) [1,2] 2.203(2) [1,4] 2.244 (2) [2,3] 2.246(2) [3,4]	118.6(2) [1,1,2] 119.1(2) [1,1,4] 109.8(2) [2,1,2] 110.1(2) [2,1,4]	106.5(2) [1,1,2]	92.04(6) [4,1,2] 85.10(5) [1,2,3] 89.85(6) [2,3,4] 85.08(6) [1,4,3]	21.09
3.6b	1.822(2) [1,2] 1.797(2) [1,1] 1.867(2) [2,8] 1.871(2) [3,14] 1.858(2) [4,20]	2.1952(6) [1,2] 2.1896(6) [1,4] 2.2387(6) [2,3] 2.2378(6) [3,4]	114.45(7) [1,1,2] 115.54(7) [1,1,4] 113.68(6) [2,1,2] 113.03(6) [2,1,4]	108.44(8) [1,1,2]	91.05(2) [4,1,2] 84.92(2) [1,2,3] 88.68(2) [4,3,2] 85.07(2) [1,4,3]	23.92
3.7a	1.850(2) [1,1] 1.32(2) [1,H1] 1.892(2) [2,5] 1.890(3) [3,9] 1.881(3) [4,13]	2.191(1) [1,2] 2.180(1) [1,4] 2.237(2) [2,3] 2.242(1) [3,4]	115.29(9) [1,1,2] 113.58(8) [1,1,4] 115.0(9) [H1,1,2] 115(1) [H1,1,4]	105.3(9) [1,1,H1]	92.68(5) [4,1,2] 85.17(4) [1,2,3] 89.83(4) [2,3,4] 85.30(4) [1,4,3]	19.86
3.8	1.800(2) [1,2] 1.802(2) [1,1] 1.890(2) [2,3] 1.890(2) [3,7] 1.885(2) [4,11]	2.2032(5) [1,2] 2.1983(6) [1,4] 2.2385(6) [2,3] 2.2307(6) [3,4]	106.33(6) [1,1,2] 105.12(6) [1,1,4] 122.72(6) [2,1,2] 120.56(6) [2,1,4]	105.99(9) [2,1,1]	94.33(2) [4,1,2] 85.50(2) [1,2,3] 92.47(2) [4,3,2] 85.80(2) [1,4,3]	10.43

[a] Average P-P-P-P torsional angle (τ).

Cyclotetraphophines occur as puckered rings in part to minimize the steric interaction between substituents on non-adjacent phosphorus atoms (**Figure 3.8**). The addition of a fifth substituent to the ring, as in the cyclotriphosphinophosphonium cations, creates a steric imposition between the new substituent and substituents on both adjacent phosphorus atoms (**Figure 3.8**). This unfavorable interaction is alleviated by a flattening of the ring, and as a result the cations **3.6a, 3.7a** and **3.6b** are found to be more planar [average P-P-P-P torsional angles (τ) are closer to 0°] than their neutral precursors (**Table 3.2**; cf. **3.5a:** $\tau = 24.5°$,[106] **3.5b:** $\tau = 31.4°$ [107]).

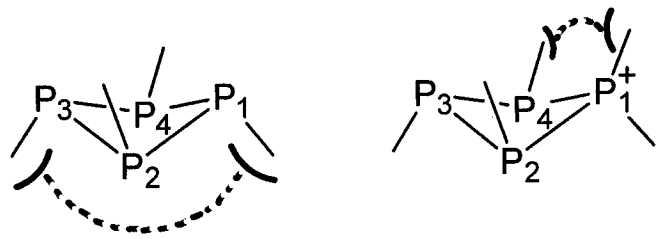

Figure 3.8 Schematic demonstrating some principal steric interactions in cyclotetraphospines (left) and cyclotetraphosphinophosphonium ions (right).

In **3.6b**, the less sterically bulky cyclohexyl substituents accommodate the most puckered ring because of relatively small Me(P1)-Cy(P2,P4) steric repulsions, which are reflected in the wide C1-P1-C2 angle [108.44(8)°] and narrow range of C-P-P angles [113.03(6)° – 115.54(7)°]. The protonated cation **3.7a** should allow for a more puckered ring than methylated **3.6a**, based on the reduced R(P1)-^{t}Bu(P2,P4) interactions, however the opposite is observed. This is likely due to packing effects in the crystal and the limited flexibility imposed by the four ^{t}Bu groups since τ values are approximately equal in **3.6a** and **3.7a**, and both rings are only slightly more planar than (^{t}BuP)$_4$ (**3.5a**). Finally, the cyclo-P_4 unit of **3.8** is more planar than that of both **3.6a** and **3.7a**. Thus the reduced Me1(P1)-^{t}Bu(P3) steric interaction allows for the relief of the Me2(P1)-^{t}Bu(P2,P4) interactions by flattening the tetraphosphorus ring. These interactions are also manifested in the narrow C2-P1-C1 angle [105.99(9)°], large C2-P-P angles [120.56(6)°, 122.72(6)°] and relatively small C1-P-P angles [105.12(6)° – 106.33(6)°].

3.4 Dependence of $^3J_{PH}$ on Phosphine Lone-Pair Orientation

The ^{1}H NMR data for the methyl groups in derivatives of **3.6**, **3.8** and **2.2a** is presented in **Table 3.3**. Each of these tetraphosphorus cations exibited one signal with doublet multiplicity, while in **3.8** the second methyl group was observed as a six-line doublet of triplets. The signal for the methyl group of cyclodiphosphinophosphonium **2.2a** was observed as a doublet of doublets. These multiplicities can be rationalized by considering the configurational arrangements for these cations. Thus, the methyl protons show coupling to the phosphorus atom to which they are bound ($^2J_{PH}$), and to adjacent phosphorus atoms ($^3J_{PH}$) only if the lone pair is in the *cis* position (on the same face of the ring), as illustrated in **Figure 5**. It should be noted that the effects of lone-pairs on coupling constants have been documented for many other systems,[108] and the observed trends have often been used to extract configurational information from coupling constant values.

Table 3.3 ^{1}H NMR characteristics for the methyl groups in deivatives of **3.6**[OTf], **3.8**[OTf], and **2.2a**[OTf].

Compound	δ (ppm)	Multiplicity	$^{2}J_{PH}$ (Hz)	$^{3}J_{PH}$ (Hz)
3.6a[OTf]	2.62	d	12	0
3.6b[OTf]	2.40	d	12	0
3.8[OTf]	2.66	d	14	0
	2.37	dt	13	8
2.2a[OTf]	2.36	dd	13	8

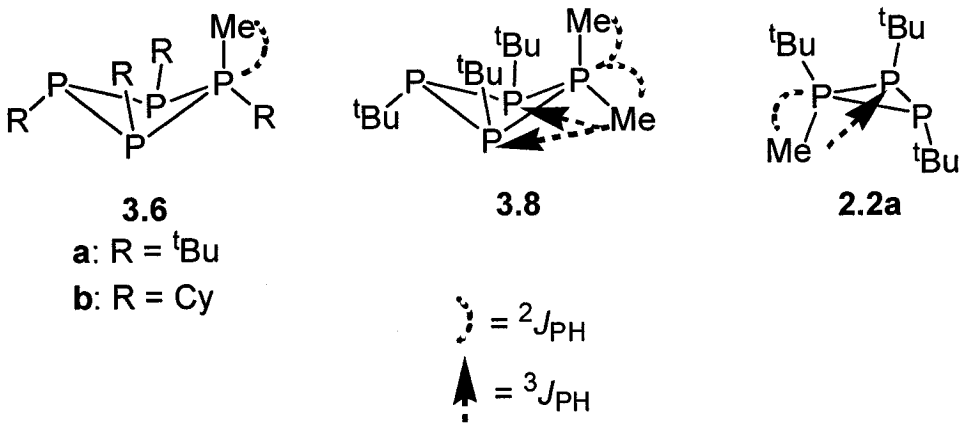

Figure 3.9 Schematic showing the phophorus centers involved in P-H coupling with the methyl groups in **3.6a**, **3.6b**, **3.8** and **2.2a**.

3.5 Reactivity Studies with Trimethylphosphine

As a preliminary study of the reactivity of these new cations, **3.6a**[OTf], **3.6b**[OTf], **3.7a**[OTf] and **3.8**[OTf] were reacted with the strong nucleophile Me_3P and the reaction mixture were monitored by $^{31}P\{^{1}H\}$ NMR. The observation of **2.1a** in the reaction of **3.8**[OTf] with Me_3P (**Scheme 3.2a**, incomplete conversion after 4 days) was accompanied by broad signals for the phosphinophosphonium ion $[Me_3P\text{-}PMe_2][OTf]$ (^{31}P: δ = 16, -60 ppm)[109] as well as a small signal for $(^{t}BuP)_4$ (**3.5a**). This demonstrates a nucleophile-induced reversibility of the phosphenium ion insertion reaction (**Scheme 3.1c**).

Similarly, in monitoring the analogous reaction involving **3.6b**[OTf] (**Scheme 3.2b**), two doublets (^{31}P: δ = 15, -38 ppm, $^{1}J_{PP}$ = -295 Hz), were observed (assigned to $[Me_3P\text{-}PCyMe][OTf]$) along with the characteristic A_2B spin system for $(CyP)_3$ (**2.1b**)[20]

and < 5% of $(CyP)_4$ (**3.5b**). In this case, the reaction was virtually complete within 24 hours. Coupled with the formation of **3.6b**[OTf] (**Scheme 3.1a**) this phosphenium ion abstraction and ring contraction represents a synthetically viable two-step conversion from cyclotetraphosphine **3.5b** to cyclotriphosphine **2.1b**. Derivative **3.6a**[OTf] showed no reaction, thus for non-protonated derivatives, the reactivity towards Me_3P decreases with increasing bulkiness of the substituents (reactivity of **3.6b**>**3.8**>**3.6a**).

In the case of **3.7a**[OTf], the reactivity with Me_3P was dominated by the acidity of the P-H bond of the cation. Therefore, rather than abtracting $PCyH^+$, the phosphine quantitatively deprotonated the cyclic monocation according to **Scheme 3.2c**. The formation of $[Me_3PH][OTf]$ was easily identified in the reaction mixture by the presence of a doublet of multiplets in the proton coupled ^{31}P NMR spectrum (^{31}P: δ = -3 ppm, $^1J_{PH}$ ~ 510 Hz).

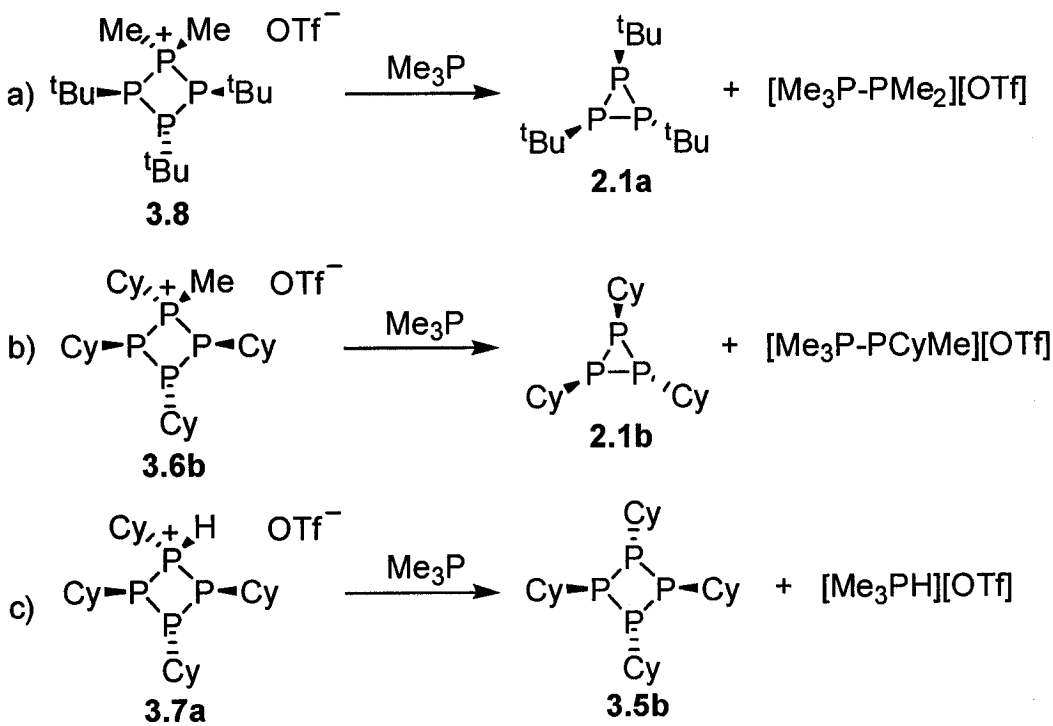

3.8 **2.1a** **3.6b** **2.1b** **3.7a** **3.5b**

Scheme 3.2 Reactions of **3.8**[OTf], **3.6b**[OTf] and **3.7a**[OTf] with Me_3P.

3.6 Summary

Derivatives of cyclotriphosphinophosphonium ions have been prepared by methylation of cyclotetraphosphines or by a new phosphenium ion insertion and ring expansion reaction with $(^{t}BuP)_3$. These compounds have been characterized by multinuclear NMR spectroscopy, including detailed $^{31}P\{^{1}H\}$ analysis, and in most cases by X-ray crystallography. They represent the first definitive examples of cyclic tetraphosphorus monocations and add a new member to the family of known cyclic polyphosphinophosphonium ions.

Chapter 4.0: Cyclotetraphosphinophosphonium Ions

4.1 Introduction

Cyclotriphosphinophosponium cations have been prepared by methylation or phosphenium ion insertion reactions (**Chapter 3**). Knowing the prevalence of five- and six-membered rings in neutral and anionic catenated phosphorus compounds (**Chapter 1.3, 1.4**), it was reasoned that these synthetic methods should be extendable to the preparation of cations involving larger rings.

Although cyclotetraphosphinophosphonium ions were first proposed on the basis of elemental analysis data,[102;103] this chapter presents the first definitive examples of these pentaphosphorus monocations,[109] characterized by multinuclear NMR spectroscopy and X-ray crystallography. The data presented also strongly supports pseudorotation for these species, as it best accounts for the high symmetries observed in solution despite the C_1 geometries found in the solid state. Although pseudorotation[110] has been commonly used in describing the facile exchange between envelope and twist conformations of five-membered rings involving various organic frameworks,[111] the concept has only been tentatively applied (**Chapter 4.4**) to inorganic ring systems featuring catenated phosphorus atoms.

4.2 Synthesis and Solution NMR Data

The reactions of cyclopentaphosphines **4.1a** and **4.1b**[112] with MeOTf were monitored by $^{31}P\{^1H\}$ NMR spectroscopy. In both cases the spectra of the reaction mixtures were identical to those of redissolved crystalline samples. For **4.1b**, simulation of the spectra revealed that, though many peaks were present, the reaction exclusively formed a single product with an ABCDX spin system (**Table 4.1**, **Figure 4.1**), assigned to racemic $[(PhP)_4PPhMe][OTf]$ (**4.2a**[OTf], **Scheme 4.1a**).

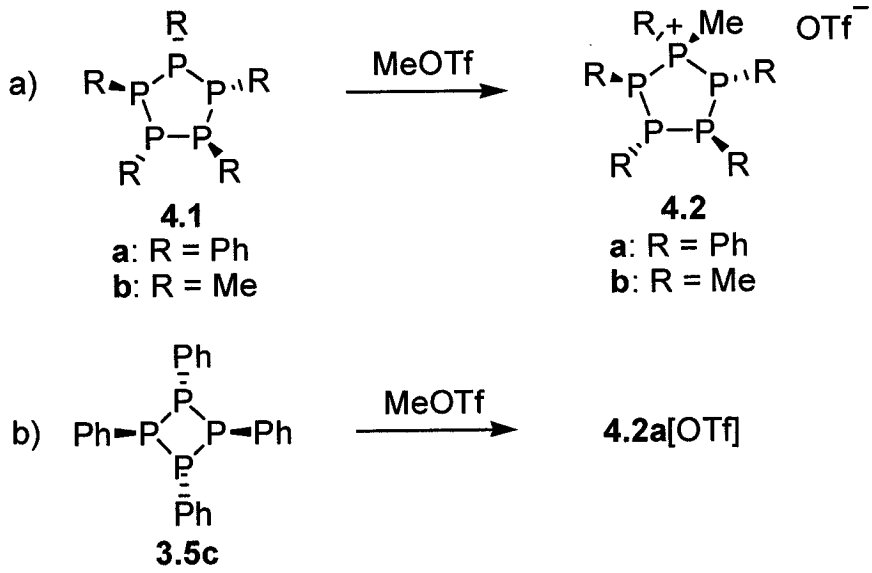

Scheme 4.1 Synthesis of racemic mixtures of **4.2a**[OTf] and **4.2b**[OTf] by methylation of a) cyclopentaphosphines or b) $(PhP)_4$.

It has been observed that $^1J_{PP}$ couplings between directly bonded phosphorus atoms of *cis* substitution are of higher magnitude (~ 60 – 100 Hz greater) than those involving *trans* substitution;[113;114] therefore, the coupling constants for **4.2a** are consistent with the sterically favored all-*trans* configuration of substituents about the phosphonium center. This assignment has also been supported by three separate and distinct X-ray structures. Unfortunately disorder in the crystals prevented the meaningful determination of structural information beyond molecular configuration and atom connectivities. No other diastereomers of **4.2a** were observed in solution, indicating stereoselective methylation of **4.1a** at one of the two directly bonded phosphorus atoms of *cis* substitution. Interestingly, in contrast to the four-membered monocations formed by methylation of other cyclotetraphosphines (**Chapter 3**), **4.2a**[OTf] was the exclusive polyphosphinophosphonium salt formed in the reaction of $(PhP)_4$ (**3.5c**) and MeOTf (**Scheme 4.1b**), demonstrating a preference for the five-membered cation involving phenyl substituents at the phosphine centers.

Table 4.1 Simulated $^{31}P\{^{1}H\}$ NMR parameters for the ABCDX spin system of $[(PhP)_4PPhMe][OTf]$ (**4.2a**[OTf]) in $CDCl_3$.

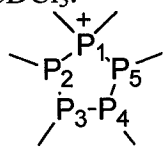

Chemical Shift (ppm)	^{1}J (Hz)	^{2}J (Hz)
22 [1]	-315 [1,2]	17 [1,3]
-25 [2]	-328 [1,5]	30 [1,4]
-32 [3]	-193 [2,3]	58 [2,4]
-34 [4]	-166 [3,4]	-15 [2,5]
-36 [5]	-162 [4,5]	71 [3,5]

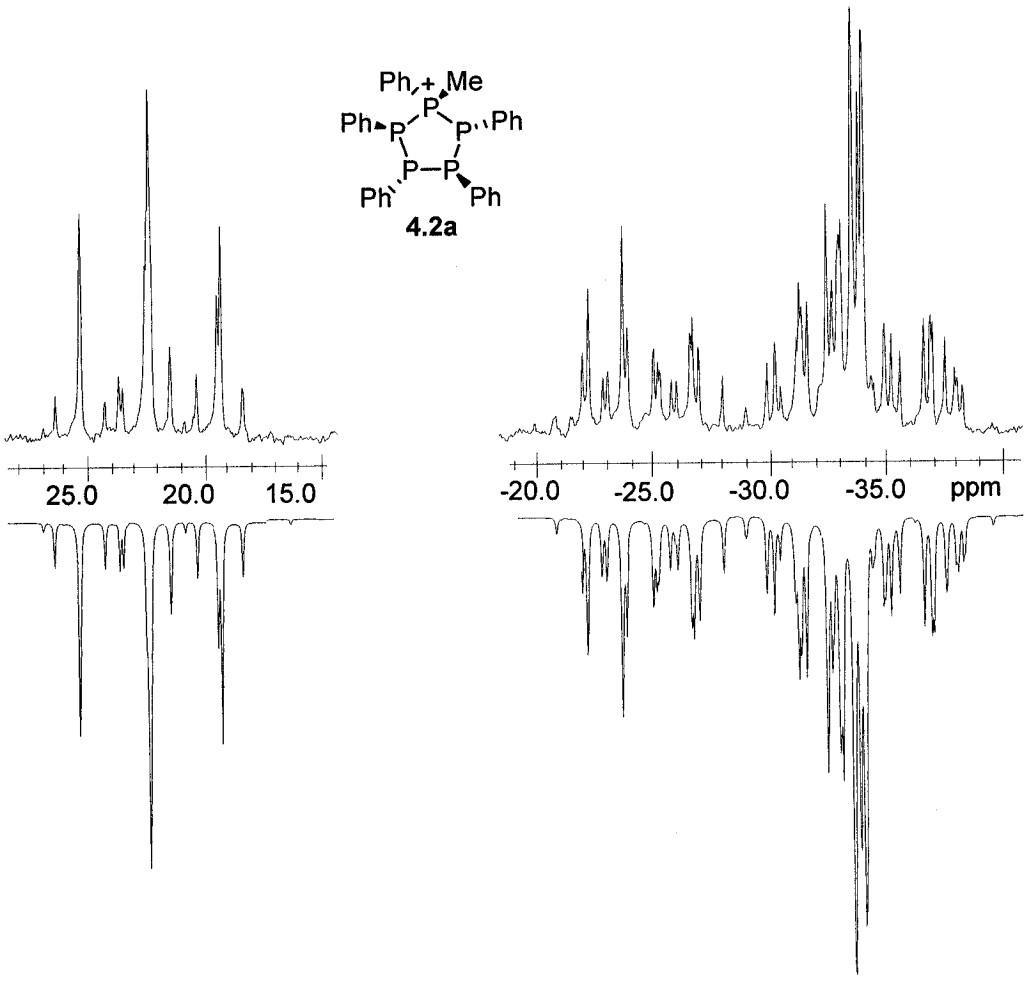

Figure 4.1 Expansions for experimental (top) and simulated (inverted) $^{31}P\{^{1}H\}$ NMR spectra (101.3 MHz) for $[(PhP)_4PPhMe][OTf]$ (**4.2a**[OTf]).

The hexamethyl derivative, $[(MeP)_4PMe_2][OTf]$ (**4.2b**[OTf], **Scheme 4.1a**),[112] has been assigned to the AA'BB'X spin system observed by $^{31}P\{^1H\}$ NMR spectroscopy (**Table 4.2**, **Figure 4.2**); however, spectra of both the reaction mixture and redissolved crystals showed significant amounts of other products (**Figure 4.2**). Based on the three diastereomers observed by Baudler in the oxidation of one phosphorus center in **4.1b** with oxygen,[115] these products likely include other stereoisomers of **4.2b**, which seem only accessible because of the small steric bulk of the methyl substituents. Again the coupling parameters are consistent with an all-*trans* configuration, and this has been verified in the solid state by X-ray crystallography (details to follow in **Chapter 4.3**).

Table 4.2 Simulated $^{31}P\{^1H\}$ NMR parameters for the AA'BB'X spin systems of **4.2b**[OTf] and derivatives of **4.3**[OTf].

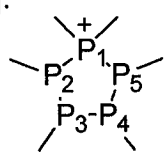

Cation	$(MeP)_4PMe_2^+$ **4.2b**[a]	$(CyP)_4PMe_2^+$ **4.3a**[b]	$(CyP)_4PPh_2^+$ **4.3b**[a]	$(PhP)_4PPh_2^+$ **4.3c**[b]	$(PhP)_4PMe_2^+$ **4.3d**[b]	$(MeP)_4PPh_2^+$ **4.3e**[a]
$\delta_3 = \delta_4$ (ppm)	24	-14	-15	-42	-26	28
$\delta_2 = \delta_5$ (ppm)	20	-8	-2	-36	-32	16
δ_1 (ppm)	101	42	52	22	27	110
$^1J_{34}$ (Hz)	-263	-255	-247	-142	-186	-248
$^1J_{32} = {}^1J_{45}$ (Hz)	-277	-264	-262	-160	-192	-272
$^1J_{21} = {}^1J_{51}$ (Hz)	-346	-332	-352	-325	-315	-364
$^2J_{31} = {}^2J_{41}$ (Hz)	-3	9	2	28	24	-1
$^2J_{35} = {}^2J_{42}$ (Hz)	16	0	0	79	50	24
$^2J_{25}$ (Hz)	-19	-21	-21	-14	-15	-15

[a] CH_2Cl_2; [b] $CDCl_3$.

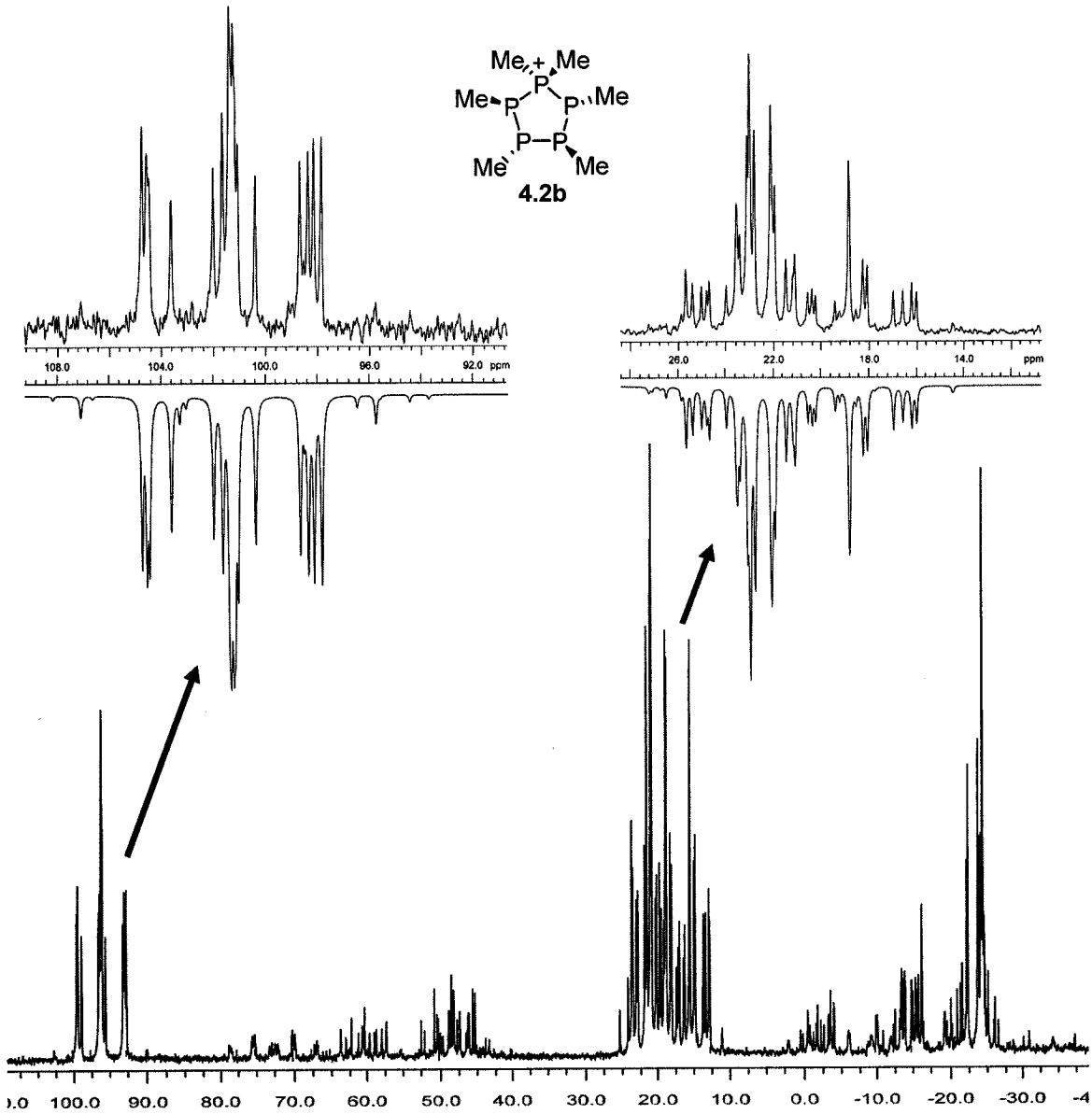

Figure 4.2 $^{31}P\{^{1}H\}$ NMR spectrum (101.3 MHz) for a reaction mixture containing $(MeP)_5$ and MeOTf, showing expansions for the AA'BB'X spin system of $[(MeP)_4PMe_2][OTf]$ (**4.2b**[OTf]) with the simulated spectrum (inverted).

In an attempt to effect phosphenium ion insertion reactions, cyclotetraphosphines $(^{t}BuP)_4$ (**3.5a**) and $(CyP)_4$ (**3.5b**) were each reacted with R'_2PCl (R' = Ph, Me) in the presence of TMSOTf. After stirring for 24 hours, $^{31}P\{^{1}H\}$ NMR spectra of reaction mixtures involving the more sterically encumbered **3.5a** with Ph_2PCl showed only starting materials, while reactions with Me_2PCl showed **3.5a**, $[Me_2ClP\text{-}PMe_2][OTf]$ ($^{31}P\{^{1}H\}$, δ = -31ppm and 102 ppm – broad peaks at room temperature), and only minor

amounts (<5%) of unidentified byproducts that were inconsistent with cyclotetraphosphinophosponium ions.

In contrast, $^{31}P\{^{1}H\}$ NMR spectra of analogous reaction mixtures containing $(CyP)_4$ (**3.5b**) and excess R'_2PCl (R' = Ph, Me) and TMSOTf showed complete consumption of **3.5b** within one hour. In the case of Me_2PCl, the reaction was nearly quantitative in the formation of $[(CyP)_4PMe_2][OTf]$ (**4.3a**[OTf], **Scheme 4.2**). The observed AA'BB'X spin system for **4.3a**[OTf] has been simulated (**Table 4.2**, **Figure 4.3**) and X-ray crystallography confirms the product assignment (**Chapter 4.3**). Though no pure compounds could be isolated from the reaction with Ph_2PCl (**Scheme 4.2**), simulation of the spectrum for the reaction mixture revealed a dominant AA'BB'X spin sytem (**Table 4.2**), and a minor (partially overlapping) AB_2X spin system (**Figure 4.4**). Based on chemical shifts and coupling constants, these spin systems are assigned to cyclopentaphosphorus $[(CyP)_4PPh_2][OTf]$ (**4.3b**[OTf]), and cyclotetraphosphorus $[(CyP)_3PPh_2][OTf]$ (**4.4**[OTf]), respectively.

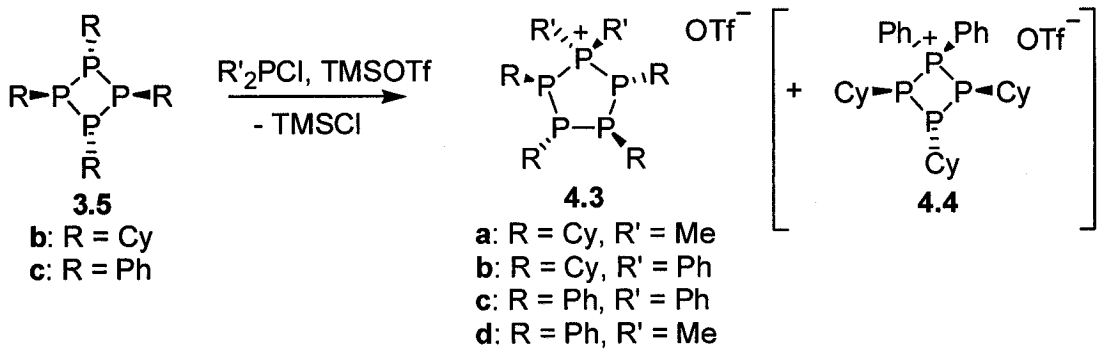

3.5
b: R = Cy
c: R = Ph

4.3
a: R = Cy, R' = Me
b: R = Cy, R' = Ph
c: R = Ph, R' = Ph
d: R = Ph, R' = Me

4.4

Scheme 4.2 Synthesis of racemic mixtures of **4.3a-d**[OTf] via insertion/ring expansion reactions of cyclotetraphosphines and R'_2PCl/TMSOTf.

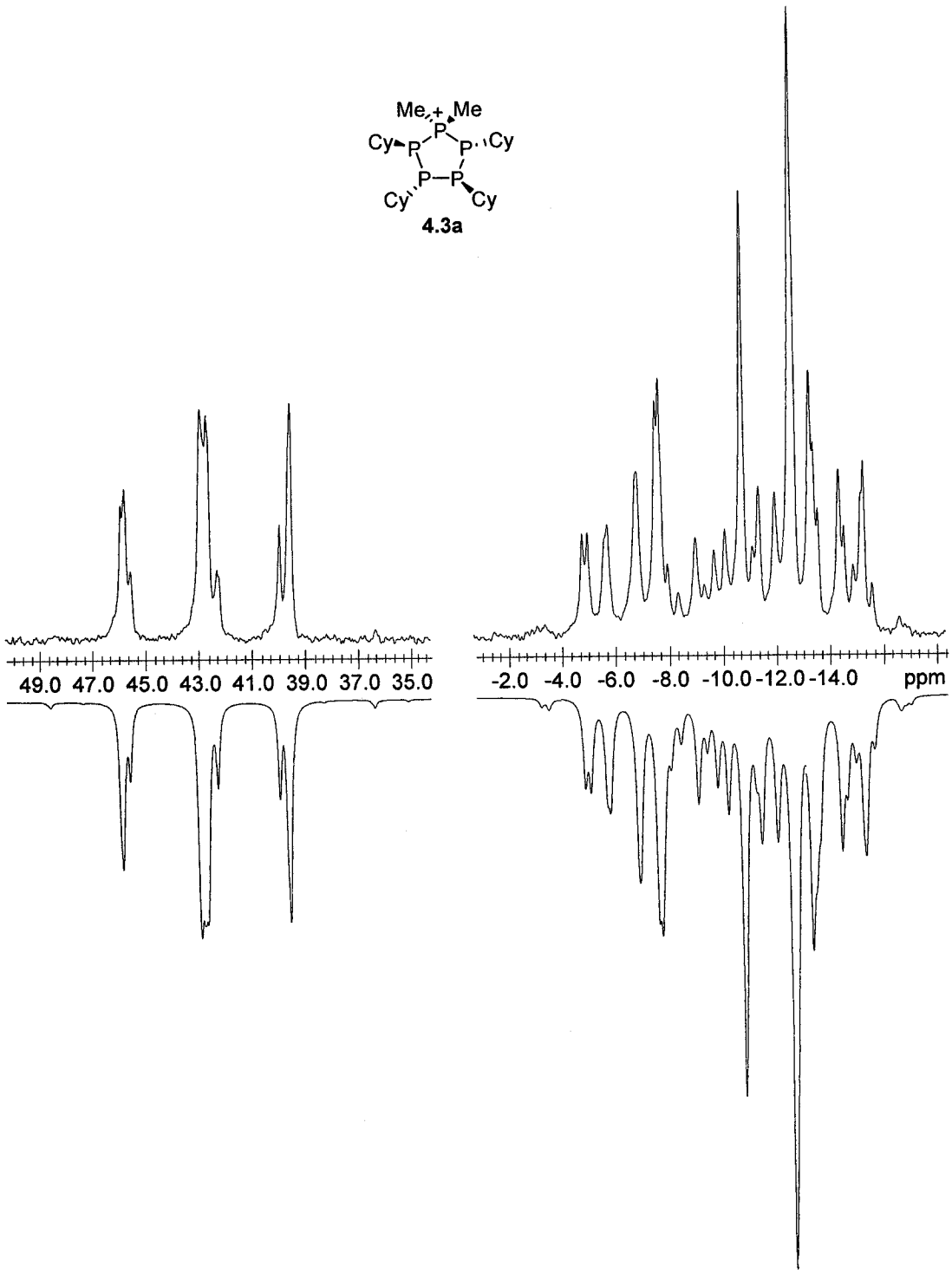

Figure 4.3 Expansions for experimental (top) and simulated (inverted) $^{31}P\{^{1}H\}$ NMR spectra (101.3 MHz) for $[(CyP)_4PMe_2][OTf]$ (**4.3a**[OTf]).

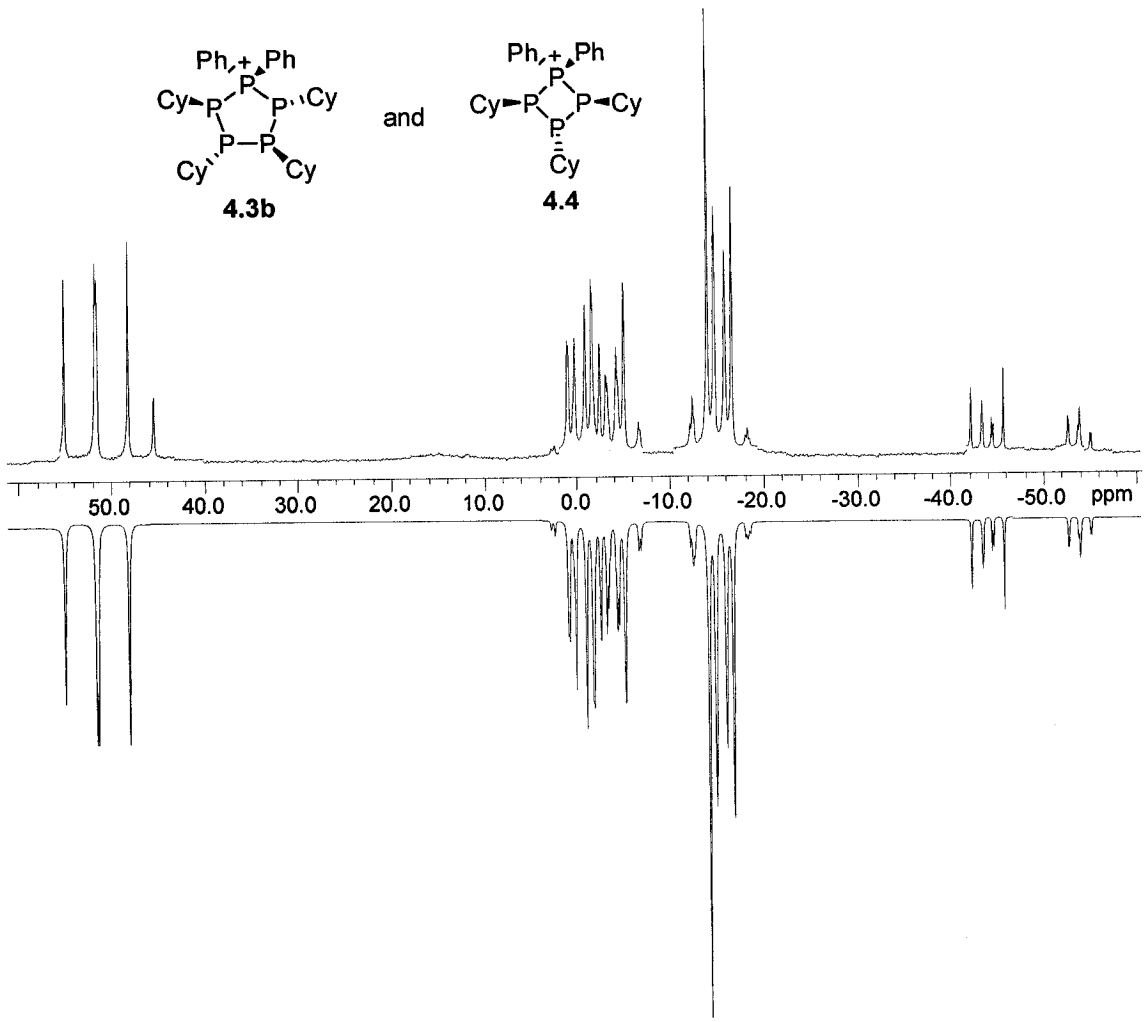

Figure 4.4 Experimental (top) and simulated (inverted) $^{31}P\{^{1}H\}$ NMR spectra (101.3 MHz) for a reaction mixture containing $(CyP)_4$, Ph_2PCl and TMSOTf, showing $[(CyP)_4PPh_2][OTf]$ (**4.3b**[OTf]) and $[(CyP)_3PPh_2][OTf]$ (**4.4**[OTf]).

Although triflate salts of the pentaphosphorus monocations **4.3c** and **4.3d** were formed cleanly in reactions involving $(PhP)_4$ (**3.5c**, **Scheme 4.2**), they were more conveniently prepared from the cyclopentaphosphine $(PhP)_5$ (**4.1a**). Thus, in contrast to the phosphenium ion insertion and concurrent ring expansion observed in reactions involving **3.5b** and **3.5c** (**Scheme 4.2**), reactions involving **4.1a** and R'_2PCl/TMSOTf (R' = Me, Ph) showed a selectivity for cyclotetraphosphinophosphonium ions (**Scheme 4.3a**) over the hexaphosphorus alternative **4.5**. The products have been confirmed by simulation of their $^{31}P\{^{1}H\}$ NMR spectra [**Table 4.2**, **Figure 4.5** (**4.3c**[OTf]) and **Figure 4.6** (**4.3d**[OTf])], and X-ray structures (**Chapter 4.3**).

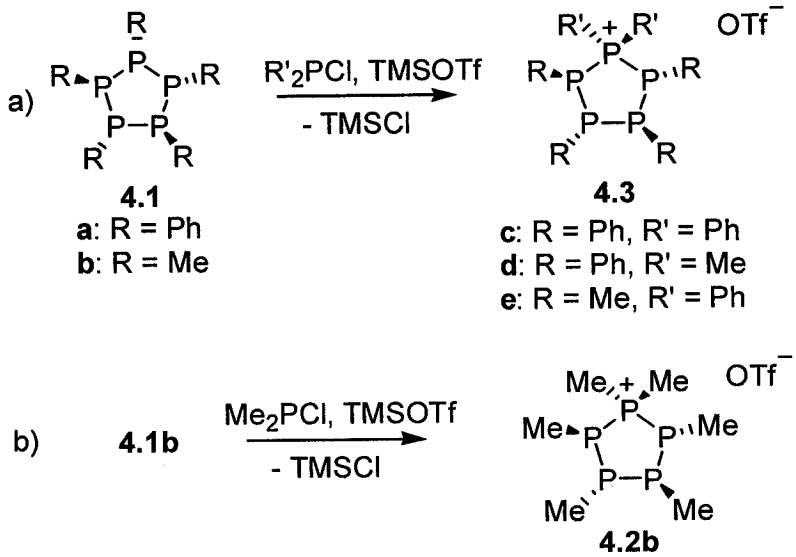

Scheme 4.3 Synthesis of racemic mixtures of **4.3c-e**[OTf] and **4.2b**[OTf] from reactions of cyclopentaphosphines with R'_2PCl/TMSOTf.

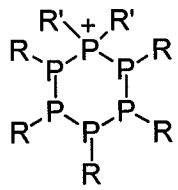

4.5

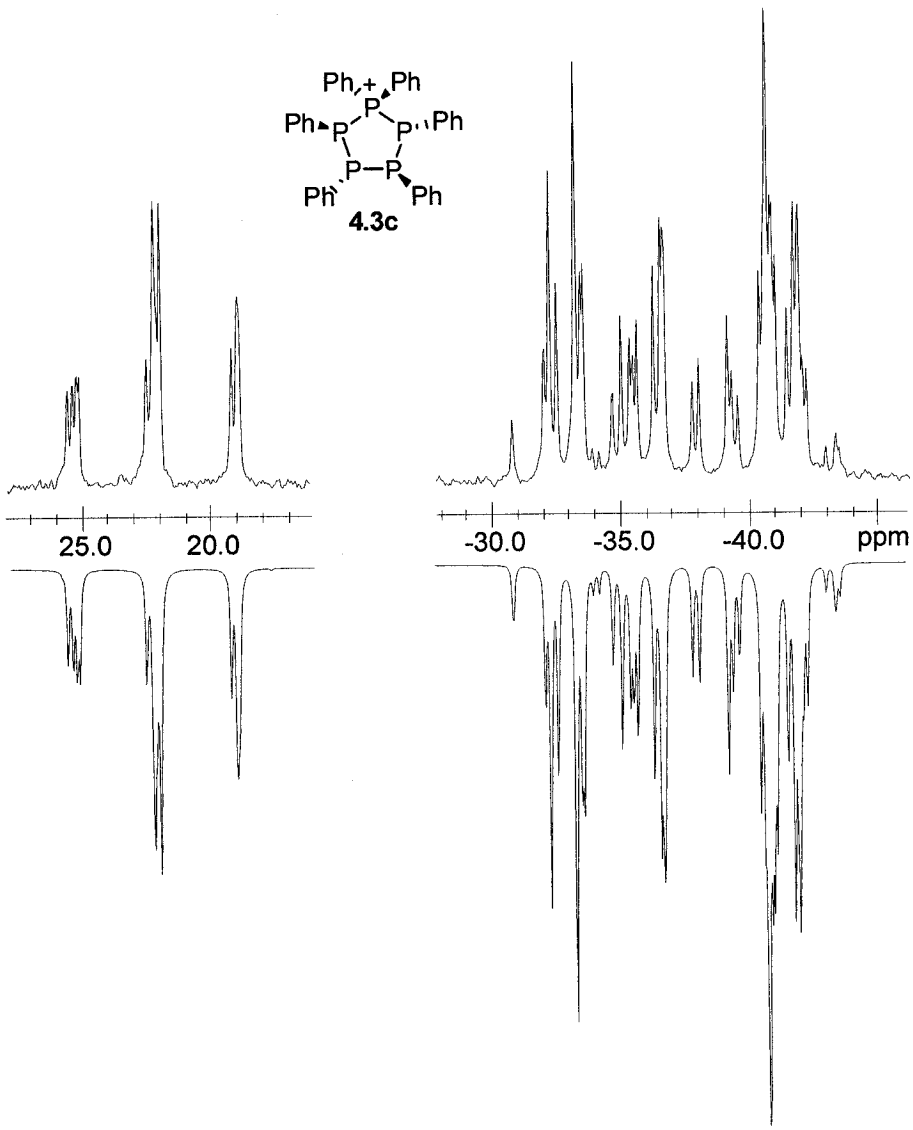

Figure 4.5 Expansions for experimental (top) and simulated (inverted) $^{31}P\{^{1}H\}$ NMR spectra (101.3 MHz) for $[(PhP)_4PPh_2][OTf]$ (**4.3c**[OTf]).

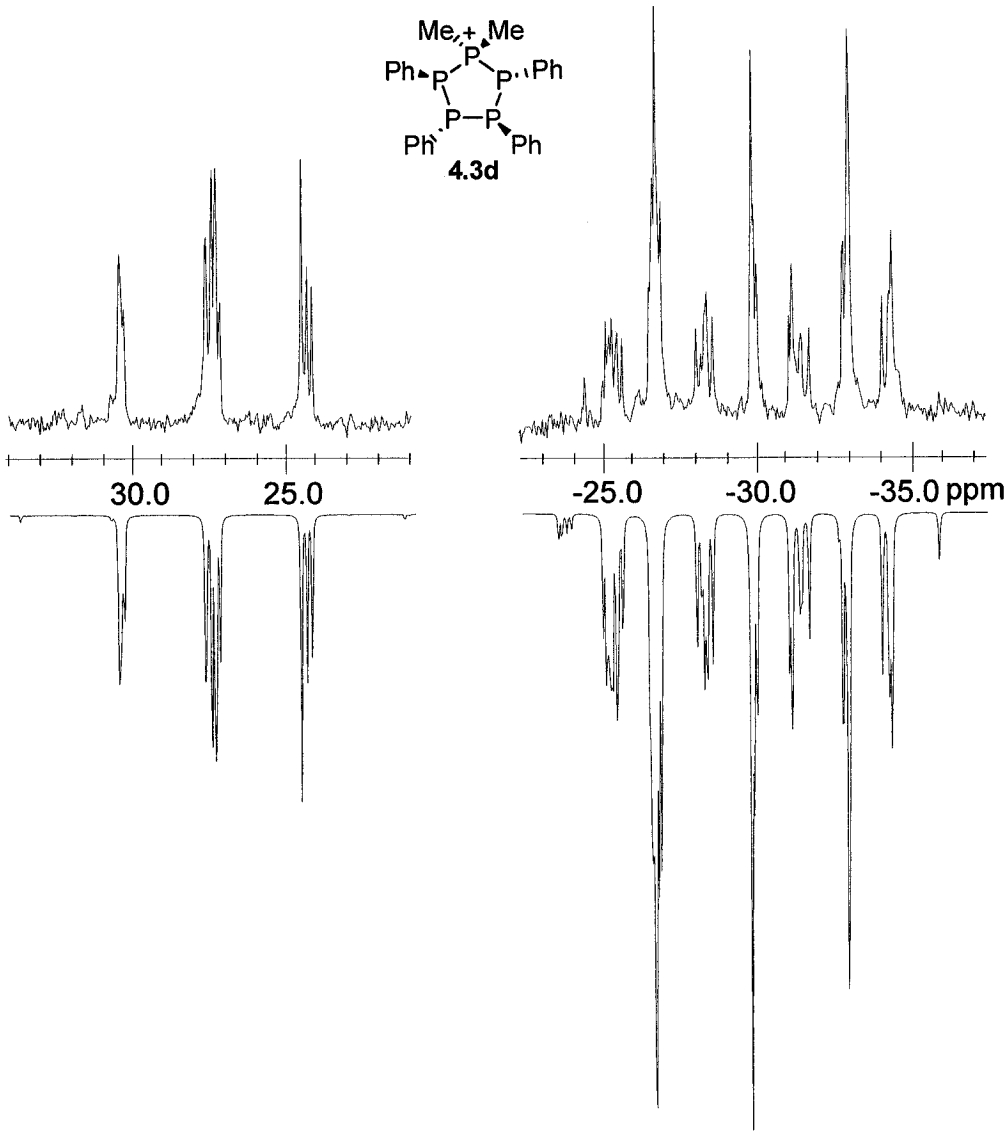

Figure 4.6 Expansions for experimental (top) and simulated (inverted) $^{31}P\{^{1}H\}$ NMR spectra (101.3 MHz)for $[(PhP)_4PMe_2][OTf]$ (**4.3d**[OTf]).

The analogous reactions with $(MeP)_5$ (**4.1b**) also showed pentaphosphorus products (**Scheme 4.3**). Interestingly, $^{31}P\{^{1}H\}$ NMR spectroscopy of reaction mixtures involving **4.1b** and Me_2PCl/TMSOTf (**Scheme 4.3b**) exibited virtually identical characteristics to that between **4.1b** and MeOTf (**Figure 4.2**).[112] The reaction involving the bulkier phosphine, Ph_2PCl, gave $[(MeP)_4PPh_2][OTf]$ (**4.3e**, **Scheme 4.3a**) and some by-products, as evidenced by simulation of the $^{31}P\{^{1}H\}$ NMR spectrum of the reaction mixture (**Figure 4.7**, **Table 4.2**), but **4.3e**[OTf] could not be isolated as a pure compound.[112]

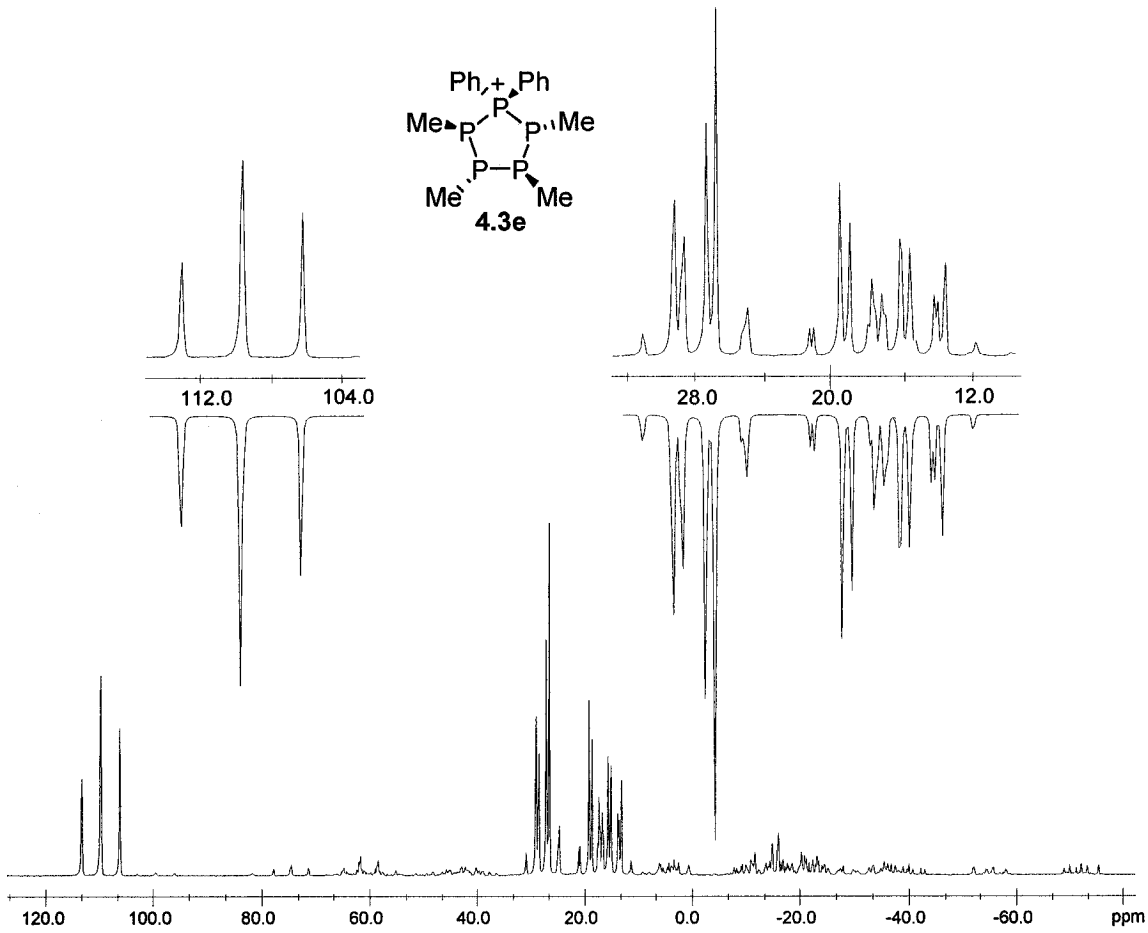

Figure 4.7 $^{31}P\{^{1}H\}$ NMR spectrum (101.3 MHz) for the reaction mixture containing $(MeP)_5$, Ph_2PCl and TMSOTf, showing expansions for the AA'BB'X spin system of $[(MeP)_4PPh_2][OTf]$ (**4.3e**[OTf]) with the simulated spectrum (inverted).

4.3 X-Ray Structures

Triflate salts of cyclotetraphosphinophosphonium ions **4.2b**,[112] **4.3a**, **4.3c** and **4.3d** were characterized in the solid-state by X-ray crystallography, and their structures are shown on the left side of **Figure 4.8** – **Figure 4.11**, respectively, with the tetracoordinate phosphorus center labeled as P1. All crystals are racemic, containing both enantiomers of the cations. The enantiomers in crystals of $[(PhP)_4PPh_2][OTf]$ (**4.3c**[OTf]) and $[(PhP)_4PMe_2][OTf]$ (**4.3d**[OTf]) are related by crystallographic symmetry. In crystals of $[(MeP)_4PMe_2][OTf]$ (**4.2b**[OTf]) and $[(CyP)_4PMe_2][OTf]$ (**4.3a**[OTf]) the two enantiomers are crystallographically independent. The metrical parameters of the two

enantiomeric cations in **4.2b**[OTf] are not significantly different, and for **4.3b**[OTf] they deviate only significantly in the orientation of the cyclohexyl groups. For convenience only one enantiomer, the *R,S,S,R* enantiomer, of each cation is discussed. Selected structural parameters for these cyclotetraphosphinophosphonium ions are presented in **Table 4.3**.

Although the cations **4.2a**, **4.3a**, **4.3c**, and **4.3d** adopt the most favorable all-*trans* configurations of the four phosphine centers, each derivative has a unique C_1 conformation in the solid state. An envelope (E) conformation is observed for the pentaphosphorus frameworks of **4.2a**, **4.3c**, and **4.3d**, while **4.3a** adopts a twist (T) conformation (right side of **Figure 4.8** – **Figure 4.11**). The best conformational descriptor (E or T) was determined using the free Platon program.[116] An envelope conformation is defined by four coplanar atoms and a twist conformation is defined by the coplanarity of three atoms and the midpoint of the opposite bond The conformations are named according to the numbered atoms outside of the plane (i.e. $^2T_3$ defines a twist conformation with atoms 2 and 3 above and below the plane, respectively). All conformations are unique in that there is only one twist conformation (**4.3a**), and only one envelope adjacent to the phosphonium center (**4.3d**). While there are two conformations where the envelope position is two bonds away from the phosphonium center, one has an axial (**4.2b**), and the other an equatorial (**4.3c**) substituent at the out-of-plane phosphorus.

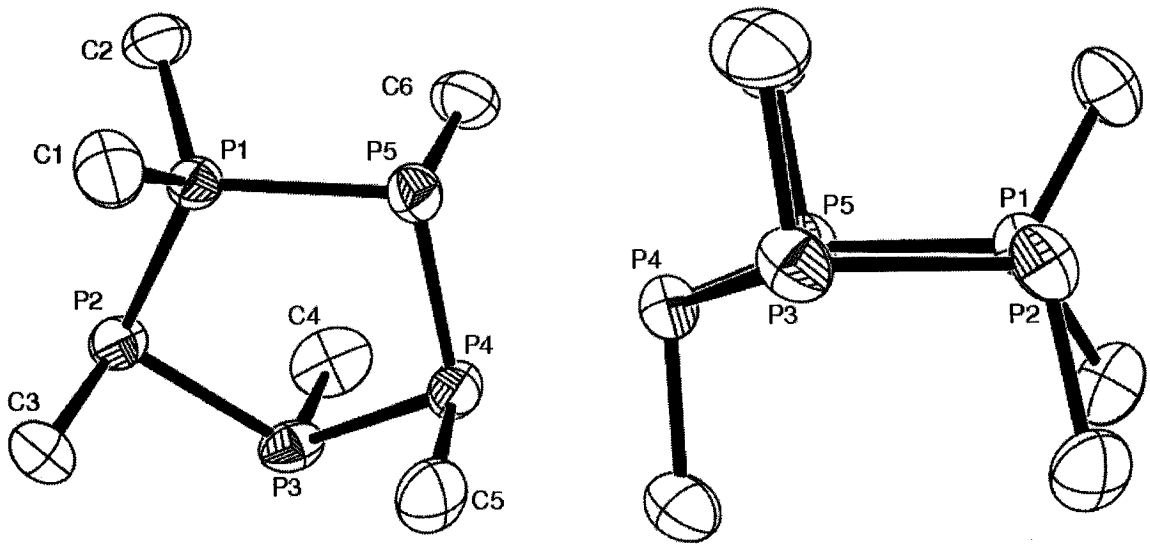

Figure 4.8 Left: solid state structure of one of the two crystallographically independent cations in racemic $[(MeP)_4PMe_2][OTf]$ (**4.2b**[OTf]) with hydrogen atoms omitted for clarity and thermal ellipsoids at the 50% probability level. Right: a side view illustrating the envelope conformation of the cation.

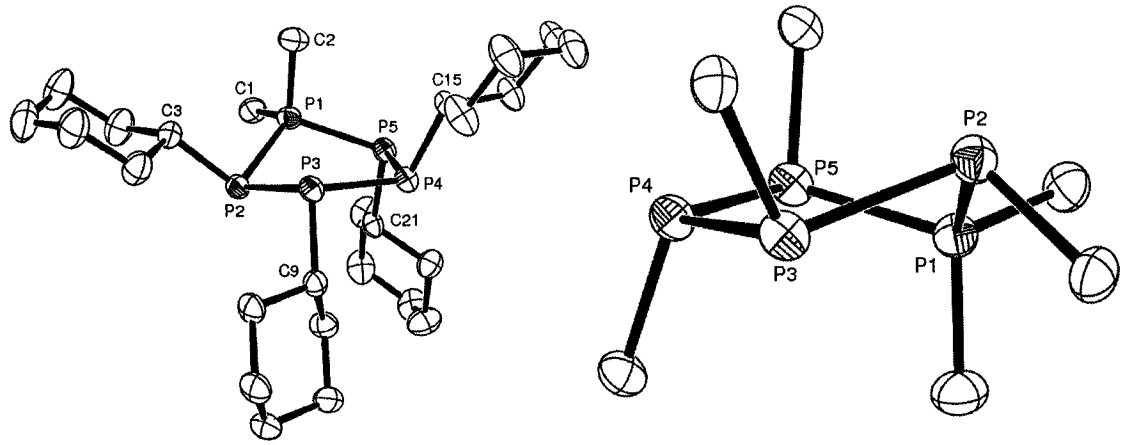

Figure 4.9 Left: solid state structure of one of the two crystallographically independent cations in racemic $[(CyP)_4PMe_2][OTf]$ (**4.3a**[OTf]) with hydrogen atoms omitted for clarity and thermal ellipsoids at the 50% probability level. Right: a side view illustrating the twist conformation of the cation with select carbon atoms omitted for clarity.

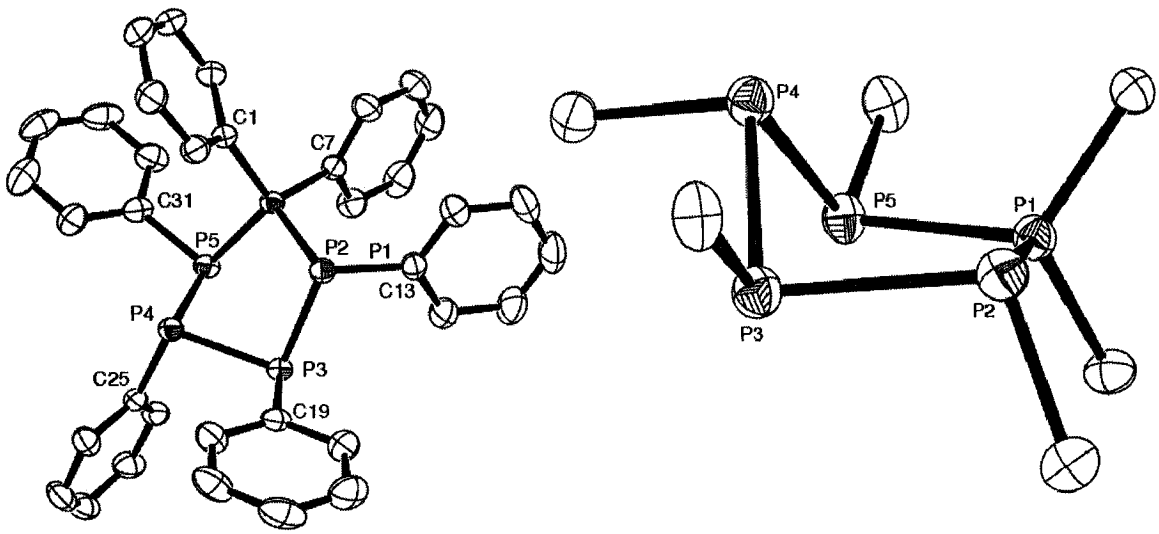

Figure 4.10 Left: solid state structure of one enantiomer of the cation in racemic $[(PhP)_4PPh_2][OTf]$ (**4.3c**[OTf]) with hydrogen atoms omitted for clarity and thermal ellipsoids at the 50% probability level. Right: a side view illustrating the envelope conformation of the cation with select carbon atoms omitted for clarity.

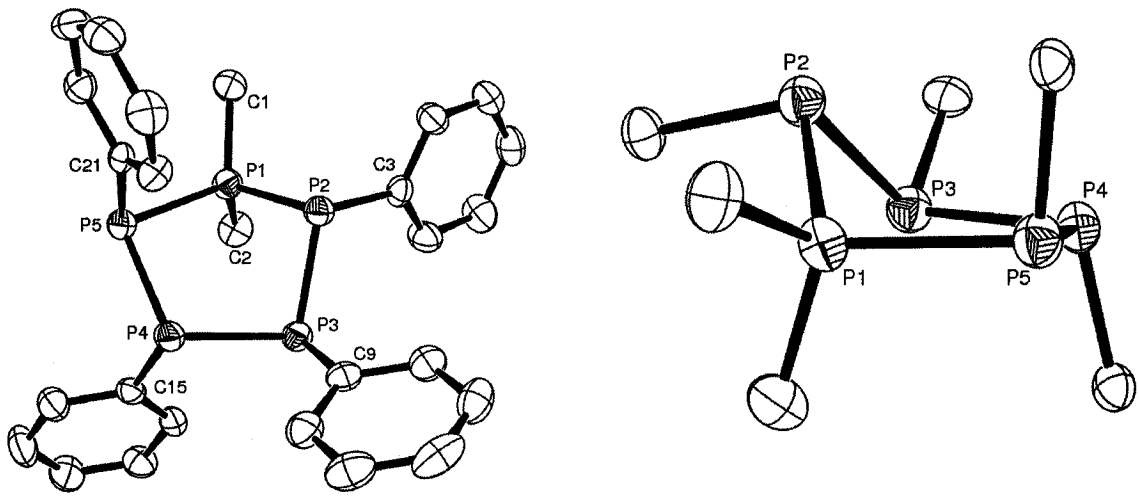

Figure 4.11 Left: solid state structure of one enantiomer of the cation in racemic $[(PhP)_4PMe_2][OTf]$ (**4.3d**[OTf]) with hydrogen atoms omitted for clarity and thermal ellipsoids at the 50% probability level. Right: a side view illustrating the envelope conformation of the cation with select carbon atoms omitted for clarity.

Table 4.3 Selected structural parameters for **4.2a**, **4.3a**, **4.3c**, **4.3d**. Numbers in square brackets correspond to atom labels in **Figure 4.8 – 4.11**.

Cation	P-C (Å)	P-P (Å)	C-P-C (°)	P-P-P (°)
4.2b	1.804(4) [1,1] 1.798(3) [1,2] 1.839(4) [2,3] 1.857(4) [3,4] 1.839(4) [4,5] 1.839(4) [5,6]	2.206(1) [1,2] 2.207(1) [1,5] 2.185(1) [2,3] 2.197(1) [3,4] 2.189(1) [4,5]	107.9(2) [1,1,2]	114.20(4) [2,1,5] 101.40(4) [1,2,3] 109.75(4) [2,3,4] 107.92(4) [3,4,5] 101.86(4) [4,5,1]
4.3a	1.794(3) [1,1] 1.804(3) [1,2] 1.876(3) [2,3] 1.885(3) [3,9] 1.862(3) [4,15] 1.876(3) [5,21]	2.192(1) [1,2] 2.183(1) [1,5] 2.223(1) [2,3] 2.220(1) [3,4] 2.202(1) [4,5]	106.6(1) [1,1,2]	107.87(4) [2,1,5] 95.54(4) [1,2,3] 104.56(4) [2,3,4] 109.08(4) [3,4,5] 97.46(4) [4,5,1]
4.3c	1.799(2) [1,1] 1.798(2) [1,7] 1.829(2) [2,13] 1.843(2) [3,19] 1.842(2) [4,25] 1.827(2) [5,31]	2.2221(6) [1,2] 2.2072(6) [1,5] 2.2318(6) [2,3] 2.2392(6) [3,4] 2.2251(6) [4,5]	111.59(8) [1,1,7]	107.36(2) [2,1,5] 96.52(2) [1,2,3] 93.59(2) [2,3,4] 89.56(2) [3,4,5] 91.64(2) [4,5,1]
4.3d	1.790(2) [1,1] 1.797(2) [1,2] 1.830(2) [2,3] 1.827(2) [3,9] 1.843(2) [4,15] 1.830(2) [5,21]	2.1864(9) [1,2] 2.1845(9) [1,5] 2.2187(9) [2,3] 2.2242(9) [3,4] 2.2115(9) [4,5]	107.9(1) [1,1,2]	102.79(4) [2,1,5] 91.91(3) [1,2,3] 96.78(3) [2,3,4] 108.47(3) [3,4,5] 96.41(4) [1,5,4]

4.4 Pseudorotation

Other than **4.2a**, all derivatives of cyclotetraphosphinophosphonium ions exhibit AA'BB'X spin systems according to $^{31}P\{^{1}H\}$ NMR spectroscopy (**Table 4.2**), implying C_2 symmetry in solution for each. This is inconsistent with the C_1 solid state conformations observed for **4.2a**, **4.3a**, **4.3c**, and **4.3d**. Analogous observations involving low solid state symmetry and high solution symmetry have been observed previously in five-membered rings with catenated or partially catenated phosphorus frameworks [C_1 solid state data: $(CF_3P)_5$ (**4.1c**),[117;118] $(PhP)_4CH_2$ (**4.6**),[119] $(^tBuP)_4CH^-$ (**4.7**)[120]; high symmetry solution NMR data: **4.1c**,[114] **4.6**,[28;121] **4.7**[120]]. No definitive rationale for these observations has been concluded, and a combination of (1) rapid inversion at phosphorus, which is known to have lower barriers in catenated systems,[122] (2) the adoption of a static C_2 twist or C_s envelope conformation, or (3) pseudorotation, have been suggested. Recent reports of $(^tBuP)_4P^-$ (**4.8**),[53] and $(CyP)_4E^-$ (**4.9a**: E = As,[123] **4.9b**: E = Sb[124]), offer no

explanation as to the discrepancies between C_1 solid state conformations for these compounds and the high symmetry they exhibit in solution.

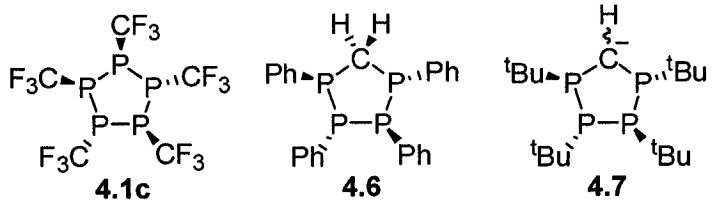

4.1c **4.6** **4.7**

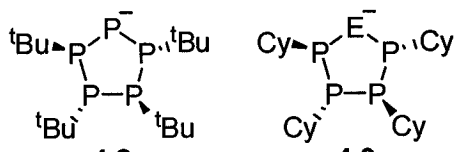

4.8 **4.9**

a: E = As
b: E = Sb

The observation of an ABCDX, rather than an AA'BB'X, spin system for **4.2a** implies that inversion at phosphorus, if it occurs at all, is slow on the NMR timescale. This is consistent with the conclusion that inversion occurs at the anionic carbon in **4.7**, where rapid inversion at phosphorus, though concluded to be less likely by the authors, could not be definitively excluded in accounting for the AA'BB' spin system observed by $^{31}P\{^1H\}$ NMR spectroscopy.[120] It is therefore unreasonable to invoke rapid inversion at phosphorus in monocations **4.2b** and derivatives of **4.3**. Moreover, the observation of four unique solid state C_1 structures for derivatives of **4.2b**, **4.3a**, **4.3c**, and **4.3d** contradicts the possibilty that in solution they each adopt a static twist conformation of C_2 symmetry ($^3\mathbf{T_4}$, or $^4\mathbf{T_3}$), as initially proposed for **4.6**.[28;125]

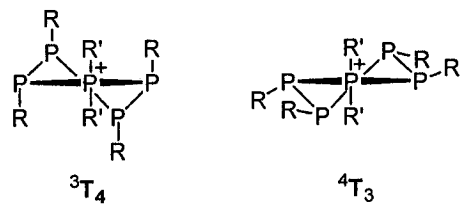

$^3T_4$ $^4T_3$

Ruling out inversion at phosphorus, and a static conformation of C_2 symmetry in solution, the higher symmetry observed for cyclotetraphosphinophosphonium cations in

solution over the solid state, can only be rationalized by pseudorotation in solution, as proposed for $(CF_3P)_5$ (**4.1c**).[114] Pseudorotation is a low energy ring puckering process that gives rise to a rapid conformational exchange, without requiring inversion, and it is well known in organic ring systems.[110;111] In this instance, the rapid (on the NMR time scale) conformational exchange must give a time-averaged structure where the core pentaphosphorus ring is rendered planar and the molecular symmetry is therefore governed by the substitution pattern (positions and types of substituents). This concept successfully colligates the AA'BB'X spin systems observed for **4.2b**, **4.3a**, **4.3c**, and **4.3d** with their asymmetric solid state structures, and also accounts for the ABCDX spin systems observed for derivative **4.2a**, which must remain in C_1 symmetry because of its asymmetric substitution pattern.

The "structural correlation principle" states that crystallization distorts a molecule from its gas-phase equilibrium geometry via a low-energy pathway.[126] This implies that the solid-state conformations of five-membered rings represent minima (not necessarily global minima) on the potential energy surface. In the case of five-membered rings, this is well supported for furanose rings of nucleosides and nucleotides.[127] Thus the four unique conformations for **4.2b**, **4.3a**, **4.3c**, and **4.3d** give indirect evidence for pseudorotation, as the skeletal conformations presented on the right side of **Figure 4.8 – 4.11** represent solid state snapshots of different molecular conformations within this dynamic solution process. This is somewhat analogous to the solid state evidence for bond-stretch isomerism in boron-phosphorus 1,3-diradicals,[128] and for Berry-Smith pseudorotation.[129]

Figure 4.12 presents a graphical representation of the conformations of all-*trans* substituted cyclotetraphosphinophosphonium ions, drawn as 1,1,2,3,4,5-hexasubstitued cyclopentanes for clarity, as a function of the phase angle of pseudorotation (φ).[130] Values of the phase angle and best conformational description of the ring in **4.2b**, **4.3a**, **4.3c**, and **4.3d** were found using the Platon program,[116] and are highlighted in boxes within the figure. It is important to note that for these crystallographically characterized derivatives, no absolute numbering of the atoms in the ring can be defined because of the achiral phosphonium center, and as such a change in numbering sense (direction) interconvert s atom 2 with 5, and 3 with 4. The highlighted conformations in **Figure 4.12**

correspond to the numbering scheme used for the *R,S,S,R* enantiomer of each derivative as shown in **Figure 4.8 – Figure 4.11**. Of the twenty possible conformations shown in **Figure 4.12**, only eleven are unique (five envelope and six twist), with all but $^{4}T_{3}$ and $^{3}T_{4}$ belonging to an equivalent pair related by 180 - φ (equivalent to a change in numbering sense). It is also worth noting that the pseudorotation process does not need to encompass all possible conformations (in this case only resultant C_2 symmetry is required), and further structurally characterized examples may help in determining the pseudorotation pathway for these cations. Perhaps even more direct evidence may be gained by structurally characterizing **4.2b**, **4.3a**, **4.3c**, and/or **4.3d** with different anions, in the hopes of observing different conformations for a given cation.

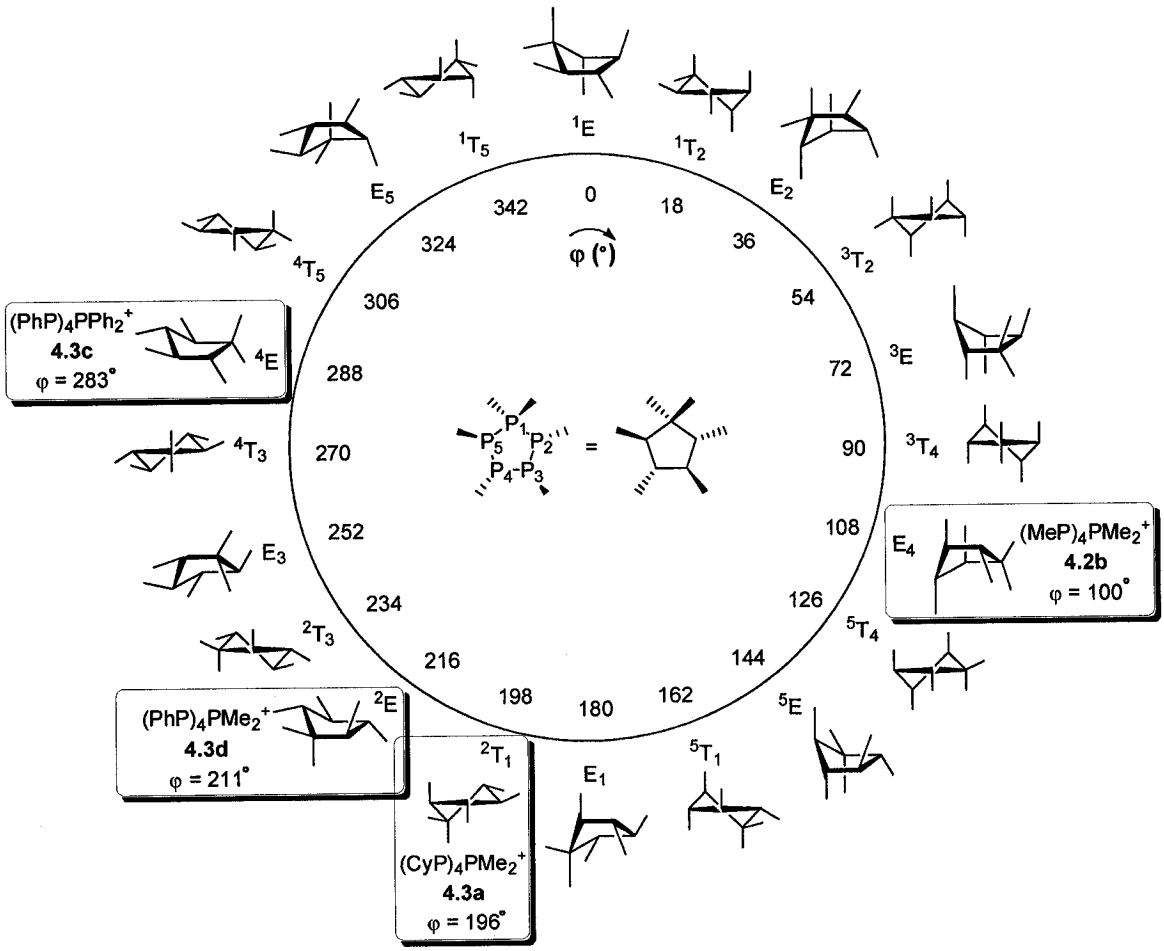

Figure 4.12 Graphical representation of the conformations of all-*trans* substituted cyclotetraphosphinophosphonium ions as a function of the phase angle of pseudorotation (φ, inside circle), with the best representations of the crystallographically characterized cations highlighted in boxes. Envelope (E) or twist (T) conformations are labeled outside the circle, where an envelope is defined by four coplanar atoms, and a twist by the coplanarity of three atoms and the midpoint of the opposite bond. The supercripts and subscripts represent the atoms above and below the plane respectively.

4.5 Summary

The first derivatives of cyclotetraphosphinophosponium cations have been isolated, and they represent the largest members in the family of monocyclic *catena*-phosphorus monocations. They can be prepared by the insertion of phosphenium ions (Ph_2P^+ or Me_2P^+ generated *in situ* from the chlorophosphine and TMSOTf) into the P-P bonds cyclopolyphosphines $(PhP)_4$, $(CyP)_4$, $(PhP)_5$ and $(MeP)_5$, or by methylation of

$(PhP)_4$, $(PhP)_5$, and $(MeP)_5$. The cations have been definitively characterized by simulation of their $^{31}P\{^1H\}$ NMR spectra and by X-ray crystallography for four derivatives. The crystal structures for each cation demonstrate unique C_1 conformations with all-*trans* configurations of substituents about the phosphonium center.

Rather than inversion at phosphorus or a static structure in solution, the concept of pseudorotation better colligates the observation of four unique C_1 structures in the solid state with effective C_2 symmetry in solution. It can be assumed that pseudorotation applies not only to cyclotetraphosphinophosphonium cations, but also to all related species mentioned in this chapter (**4.6** – **4.9**), and should be considered when dealing with other compounds containing five-membered rings. Moreover, pseudorotation is indirectly supported by the unique solid state structures of **4.2b**, **4.3a**, **4.3c**, and **4.3d**.

Chapter 5.0: The Diverse Reactivity of [(^{t}BuP)$_2$P^{t}BuMe][OTf]

5.1 Introduction

Although phosphenium ion abstraction or deprotonation products were observed in reactions of cyclotriphosphinophosphonium ions with Me_3P (**Chapter 3.5**), it is found that the high degree of strain in cyclodiphosphinophosphonium ion [(^{t}BuP)$_2$P^{t}BuMe][OTf] (**2.2a**[OTf]) imparts a much more diverse reactivity. This chapter presents the synthesis and characterization of new examples of acyclic and cyclic tetraphosphorus cations, formed from reactions of **2.2a**[OTf] with phosphines featuring zero (R_3P), one (Me_2PCl) or two ($MePCl_2$) chlorine substituents.

5.2 Acyclic 2,3,4-Triphosphino-1-Phosphonium Ions

Reactions involving various triorganophosphines and **2.2a**[OTf] were monitored by $^{31}P\{^1H\}$ NMR spectroscopy. Although the bulky and relatively weak donor Ph_3P showed no reactivity towards **2.2a**, reaction mixtures involving $^nPr_3P$, Me_3P, and Ph_2MeP displayed very complex NMR spectra. At room temperature, broad featureless peaks were observed, but low temperature studies revealed highly coupled multiplets. Simulated spectra for these mixtures demonstrate clean and virtually quantitative reactions (**Figure 5.1 – 5.3**). The simulated parameters (**Table 5.1**) are interpreted in terms of the formation of acyclic tetraphosphorus products. Intriguingly, one such species was formed in reactions with $^nPr_3P$ (minor unidentified by-products were also observed), but 50:50 mixtures of two acyclic tetraphosphorus products were found in reactions involving Me_3P or $PhMe_2P$. These products are assigned to diastereomers of acyclic tetraphosphorus monocations **5.1** (**Scheme 5.1**), which represent the first 2,3,4-triphosphino-1-phosphonium ions (**K**).

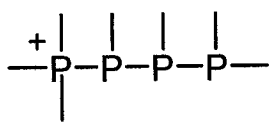

K

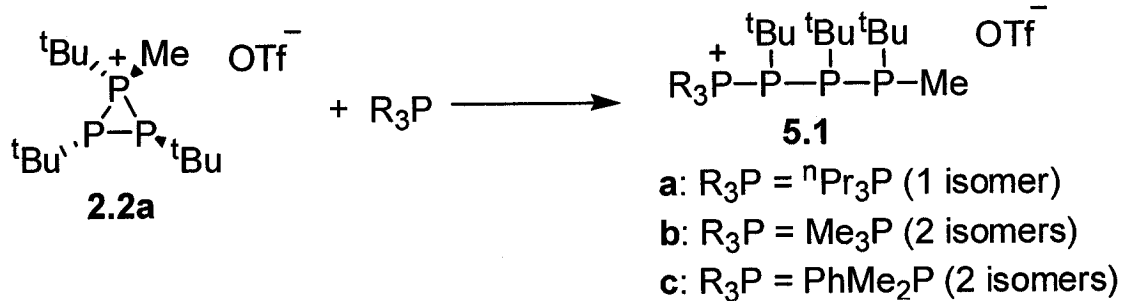

Scheme 5.1 Synthesis of derivatives of **5.1**[OTf] from **2.2a**[OTf].

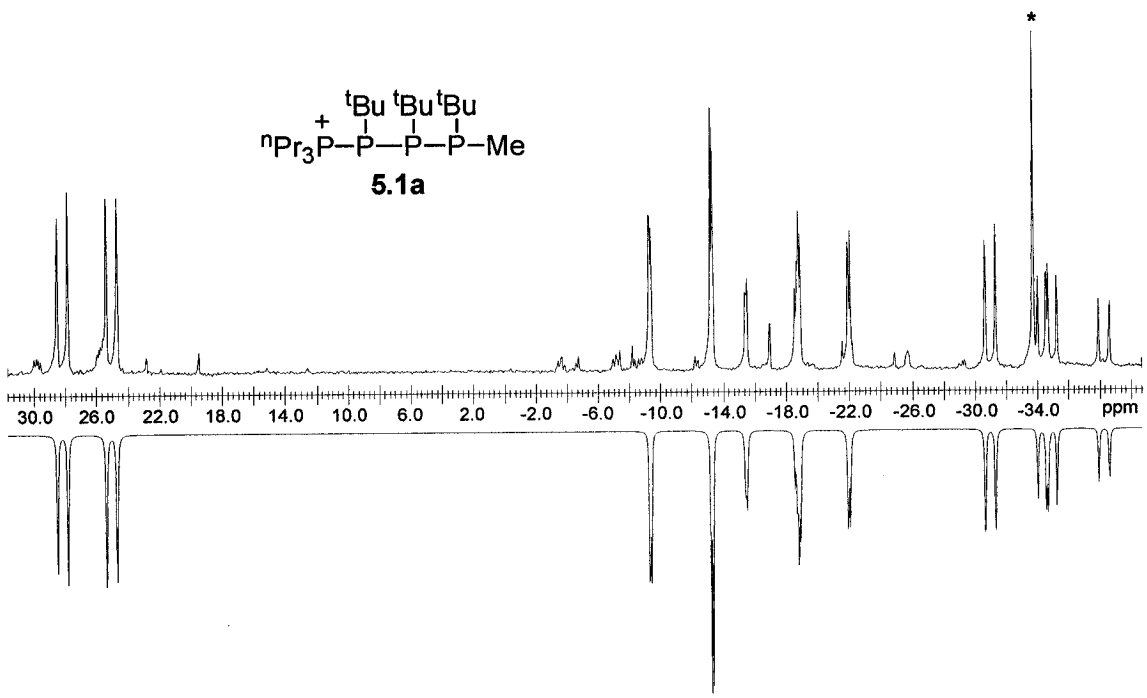

Figure 5.1 Experimental (top) and simulated (inverted) $^{31}P\{^{1}H\}$ NMR spectra (101.3 MHz, 193 K) of the reaction mixture between **2.2a**[OTf] and excess $^{n}Pr_3P$ (peak labelled *) showing only one diastereomer of **5.1a**.

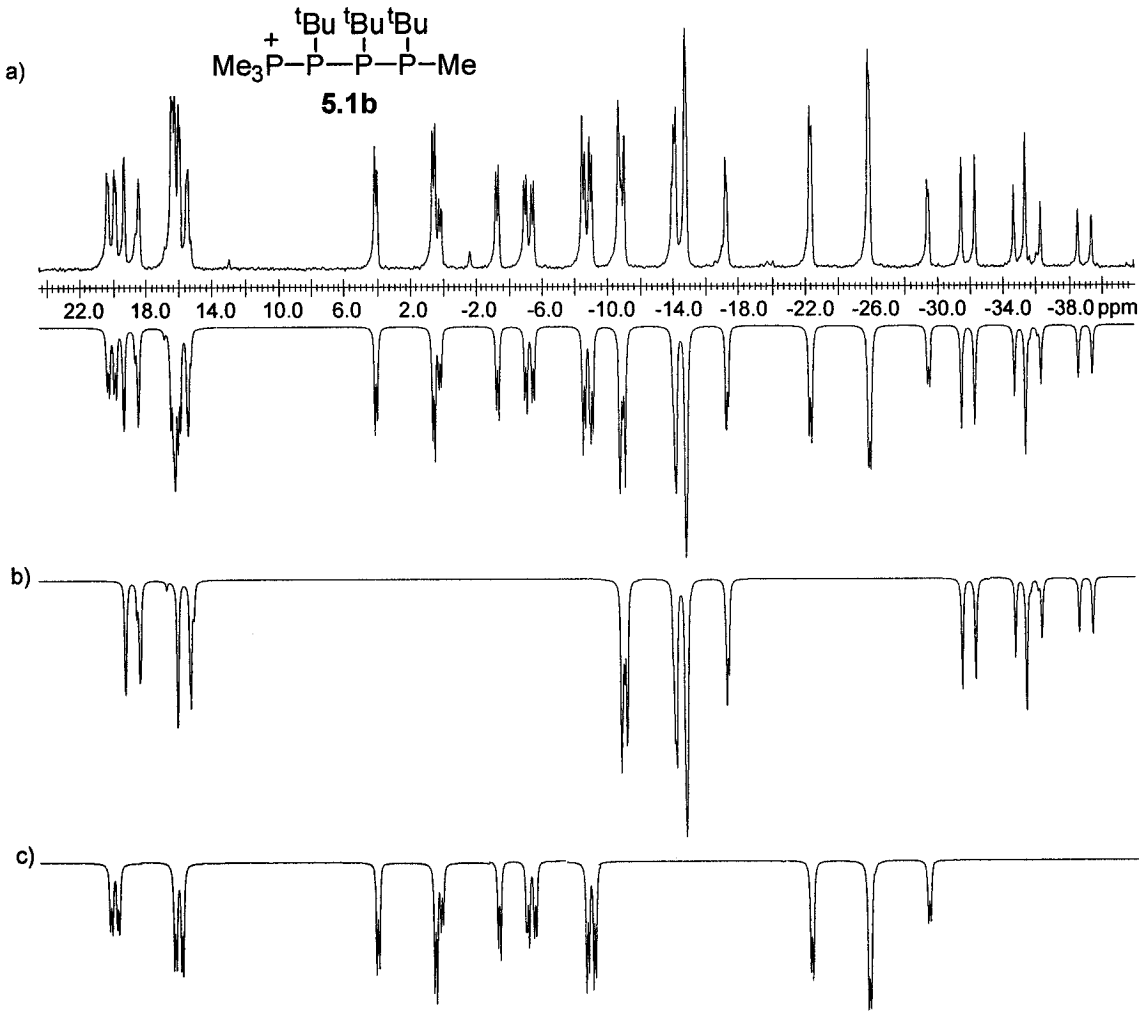

Figure 5.2 a) Experimental (top) and simulated (inverted) $^{31}P\{^{1}H\}$ NMR spectra (101.3 MHz, 193 K) of the reaction mixture between **2.2a**[OTf] and excess Me_3P (singlet at -60 ppm not shown). Simulated spectra for individual isomers of **5.1b** are shown in b) (Isomer 1) and c) (Isomer 2).

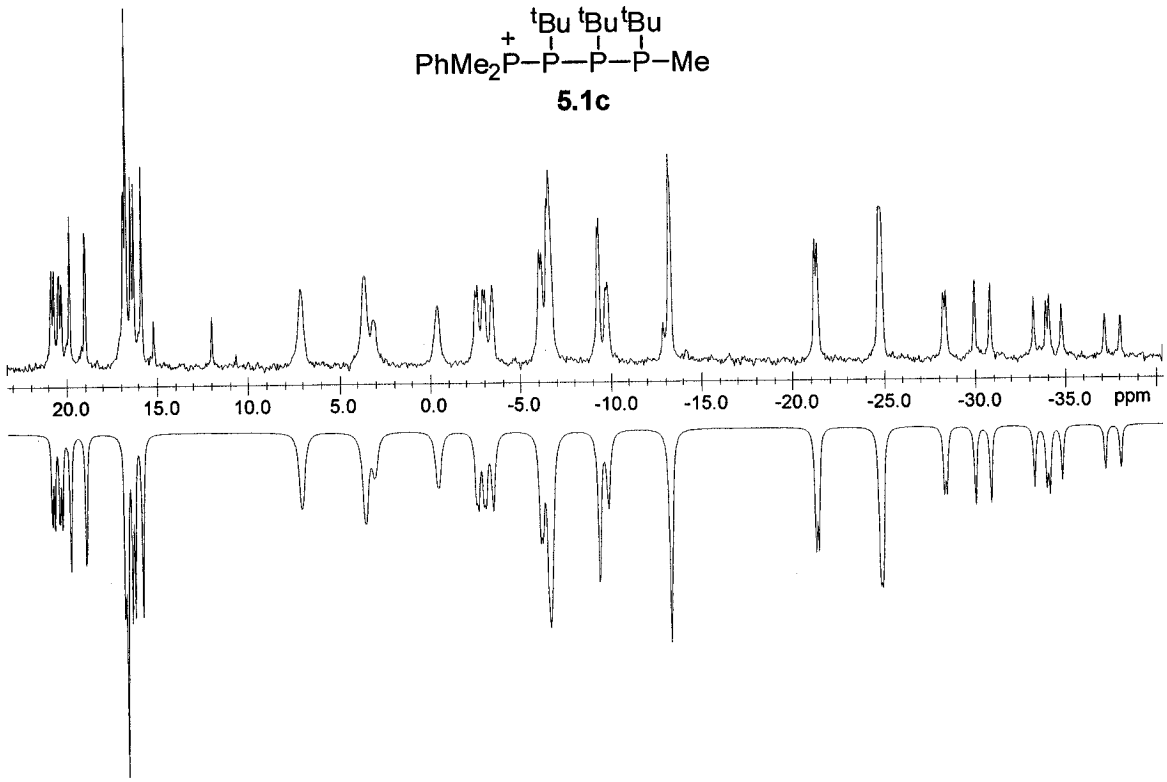

Figure 5.3 Experimental (top) and simulated (inverted) $^{31}P\{^{1}H\}$ NMR spectra (101.3 MHz, 213 K) of a reaction mixture containing **2.2a**[OTf] and excess $PhMe_2P$ (singlet at -45 ppm not shown) showing two diastereomers of **5.1c**.

Table 5.1 Simulated $^{31}P\{^{1}H\}$ NMR parameters for the AMNX spin systems of derivatives of **5.1**[OTf].

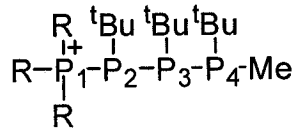

Compound	**5.1a**[OTf][a]	**5.1b**[OTf][a]		**5.1c**[OTf][b]	
		Isomer 1	**Isomer 2**	**Isomer 1**	**Isomer 2**
δ_4 **(ppm)**	-11	-13	-7	-11	-5
δ_3 **(ppm)**	-34	-35	-26	-34	-24
δ_2 **(ppm)**	-19	-14	0	-7	4
δ_1 **(ppm)**	27	17	18	18	18
$^{1}J_{34}$ **(Hz)**	-403	-399	-363	-401	-361
$^{1}J_{23}$ **(Hz)**	-345	-331	-365	-335	-362
$^{1}J_{12}$ **(Hz)**	-324	-315	-397	-318	-407
$^{2}J_{24}$ **(Hz)**	-5	-8	-11	1	-11
$^{2}J_{13}$ **(Hz)**	75	88	-9	92	-8
$^{3}J_{14}$ **(Hz)**	-2	-1	46	-1	44

[a] CH_2Cl_2, 193 K; [b] $CDCl_3$, 213 K.

Although the exact nature of these diastereomers is not known, the data (**Figure 5.1 – 5.3, Table 5.1**) demonstrates that **5.1a** and Isomer 1 of both **5.1b** and **5.1c** have similar chemical shifts and coupling constants. The same is true for Isomer 2 of both **5.1b** and **5.1c**. This suggests that only two stereochemical configurations, out of the four possible (**5.1i – 5.1iv**), are represented in solution at low temperature.

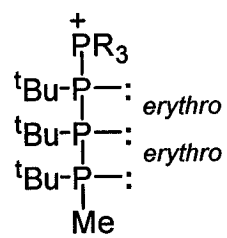

5.1i

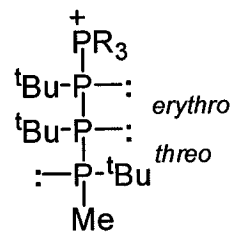

5.1ii

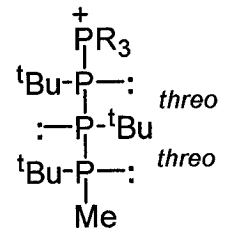

5.1iii

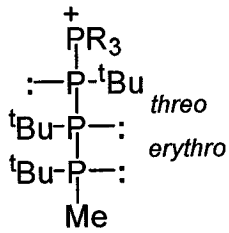

5.1iv

A concerted ring-opening mechanism for **Scheme 5.1** seems most likely, and considering the chiral configuration (*threo*; *R,R* or *S,S*) of racemic **2.2a**, the observed stereospecificity could result from phosphine attack at P^a and/or P^b to give **5.1i** and/or **5.1ii**, respectively. However, further inversion at any of the chiral phosphorus centers (as observed in tetraphosphine **5.2**)[131] to give one or two low energy isomers cannot be ruled out. Considering the dative nature of the bonds in acyclic phosphinophosphonium ions,[62] inversion at the phosphine center bound to the tetracoordinate phosphorus is available via bond dissociation/reassociation. In fact, these latter possibilities are supported by a preliminary X-ray structure of **5.1b**[OTf] (**Figure 5.4**) which demonstrates *threo*, *erythro* stereochemistry (i.e. **5.1iv**).

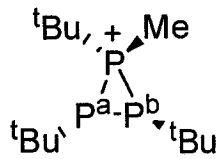

2.2a

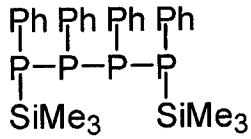

5.2

Interestingly, the molecule possesses a folded-in structure, perhaps because of a favorable interaction between the lone pair of P4 and the phosphonium center (P1). The

poor quality of the data does not allow for the meaningful determination of detailed structural parameters.

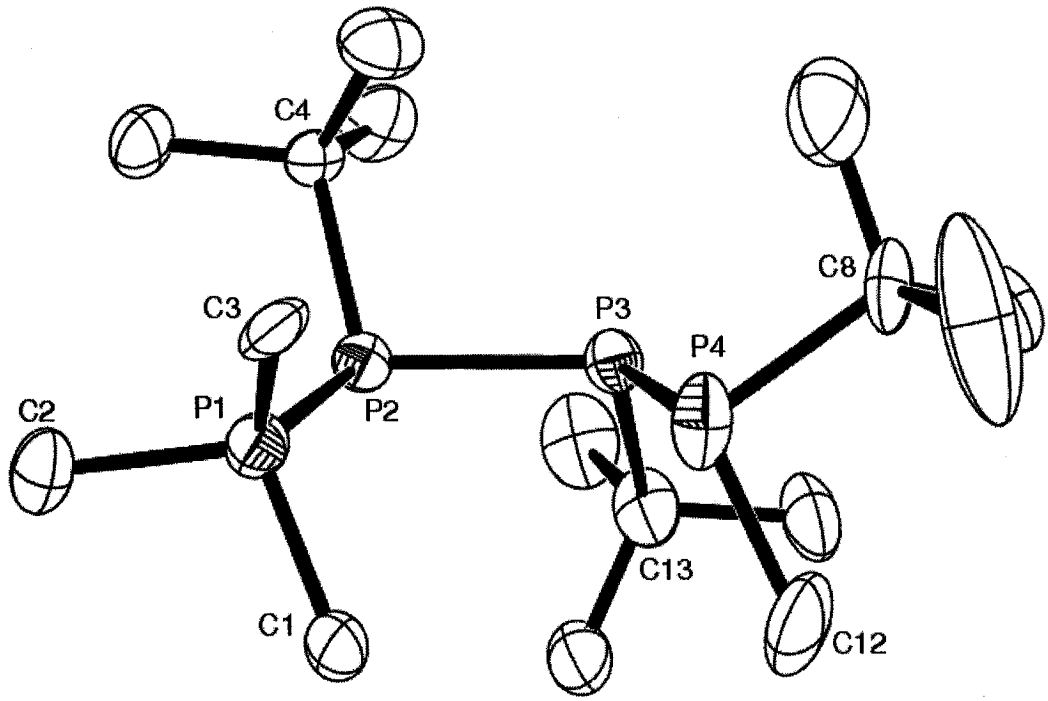

Figure 5.4 Preliminary X-ray structure showing the cation of **5.1b**[OTf], demonstrating a *threo, erythro* configuration (**5.1iv**). Hydrogen atoms are omitted for clarity and thermal ellipsoids are at the 50% probability level.

5.3 A Cyclic 3,4-Diphosphino-1,2-Diphosphonium Ion

The addition of Me_2PCl and TMSOTf to a solution of **2.2a**[OTf] in CH_2Cl_2 resulted in multiple phosphorus containing species, as indicated by $^{31}P\{^1H\}$ NMR spectroscopy of the reaction mixture. Surprisingly, after precipitation of a white solid from the reation mixture, recrystallization afforded single crystals of $[(^tBuP)_2(PMe_2)_2][OTf]_2$ (**5.3**$[OTf]_2$), the first example of a 3,4-diphosphino-1,2-diphosphonium ion (**L**).

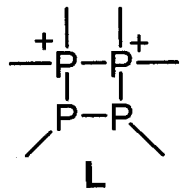

L

The reaction pathway is not yet understood, but one is proposed in **Scheme 5.2**. In support of the proposed steps, the $^{31}P\{^{1}H\}$ NMR spectrum of a reaction mixture containing two equivalents of Me_2PCl and **2.2a**[OTf] showed a singlet at 119 ppm, and A_2B spin system (δA = -109 pm, δB = -49 ppm, $^{1}J_{AB}$ = 313 Hz), which are assigned to ^{t}BuMePCl (cf. Me_2PCl: 93 ppm;[132] $^{t}Bu_2PCl$: 144 ppm[133]) and [(^{t}BuP)$_2$PMe_2][OTf] (**5.4**[OTf]), respectively. A number of broad signals centered at 136 ppm, 114 ppm, 10 ppm, -12 ppm, -42 ppm, and -54 ppm were also observed which could correspond to the *rac*- and *meso*- forms of **5.5**.

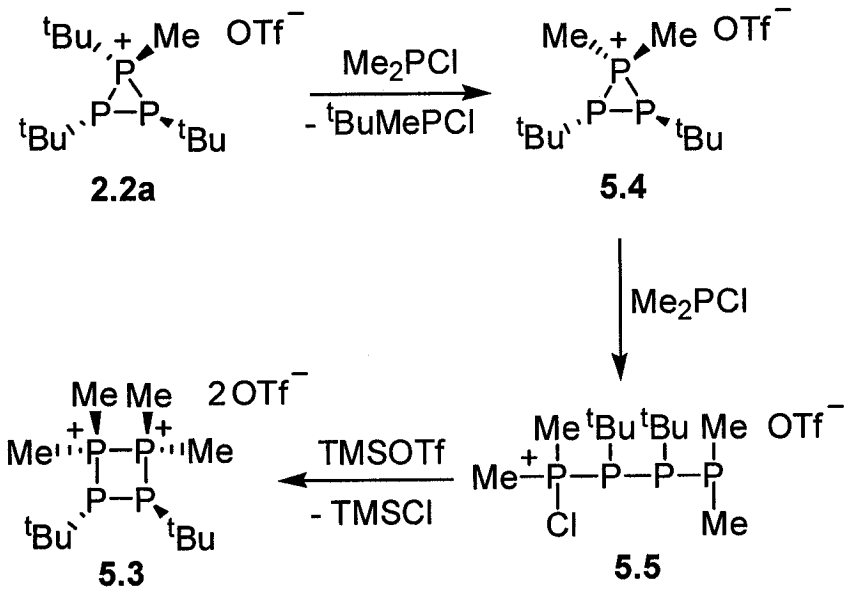

Scheme 5.2 Proposed pathway for the formation of **5.3**[OTf]$_2$ from **2.2a**[OTf].

The dication in **5.3**[OTf]$_2$ crystallized as a racemic mixture and is the first crystallographically characterized monocyclic 1,2-diphosphonium ion (**Figure 5.5**). The most striking feature of **5.3** is the presence of two directly bound phosphonium units (P1-P2). The four methyl groups are slightly staggered and the P1-P2 bond [2.207(1) Å] is

found to be slightly shorter than the bond between the phosphine centers [P3-P4 = 2.256(1) Å] (**Table 5.2**), with all P-P distances being consistent with single bonds.

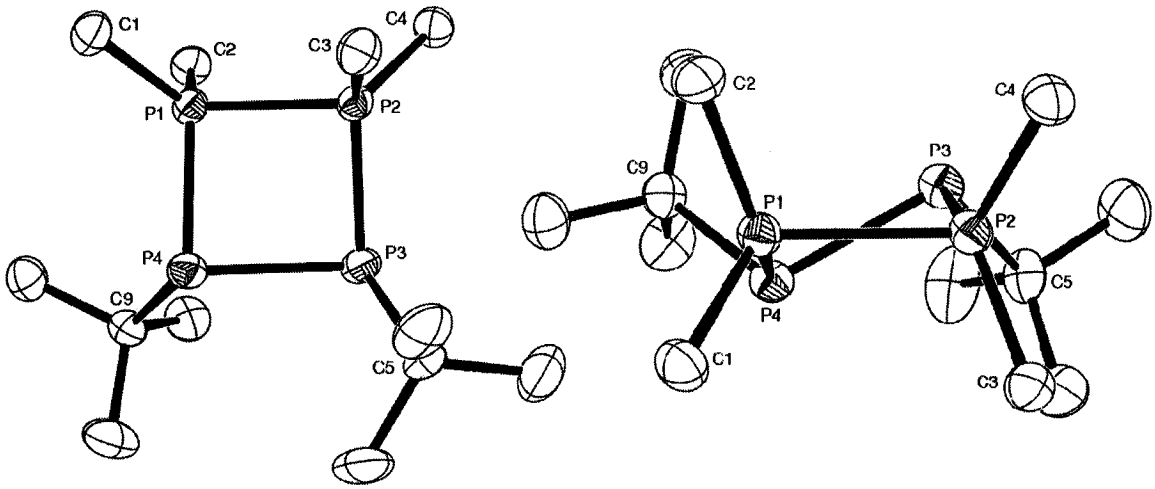

Figure 5.5 Two views of one enantiomer of the dication in **5.3**$[OTf]_2$ with hydrogen atoms omitted for clarity and thermal ellipsoids at the 50% probability level.

Table 5.2 Selected structural parameters for **5.3**. Numbers in square brackets correspond to atom labels in **Figure 5.5**.

P-P (Å)	P-C (Å)	C-P-P (°)	C-P-C (°)	P-P-P (°)
2.207(1) [1,2] 2.193(1) [1,4] 2.217(1) [2,3] 2.256(1) [3,4]	1.801(2) [1,1] 1.798(2) [1,2] 1.800(2) [2,3] 1.790(2) [2,4] 1.897(2) [3,5] 1.889(2) [4,9]	115.41(9) [1,1,2] 110.69(8) [1,1,4] 109.35(8) [2,1,2] 122.46(8) [2,1,4] 106.97(8) [3,2,1] 124.88(8) [3,2,3] 112.98(8) [4,2,1] 111.07(8) [4,2,3] 112.05(8) [5,3,2] 103.61(8) [5,3,4] 106.99(8) [9,4,1] 108.69(7) [9,4,3]	110.3(1) [1,1,2] 111.3(1) [3,2,4]	86.99(4) [2,1,4] 86.84(4) [1,2,3] 85.20(4) [2,3,4] 86.21(4) [1,4,3]

Only three other crystallographically characterized examples of 1,2-diphosphonium ions have been reported: acyclic **1.51a** (P-P = 2.364(3) Å),[86] bicyclic **1.51b** (P-P = 2.189 Å),[84] and tricyclic **1.51c** (P-P = 2.165(2) Å).[87] The longer P-P bond length in **1.51a** seems to suggest that the cyclic frameworks of **5.3**, **1.51b**, **1.51c** prevent bond lengthening caused by Coulombic repulsions; however, the recent structural characterization of acyclic **1.51d** (P-P = 2.198(2) Å)[134] suggests that the bond is lengthened primarily because of steric interactions between the bulky NEt_2 groups.

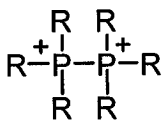

1.51
a: R = NEt_2
d: R = Me

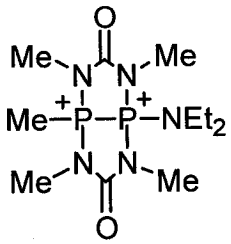

1.51b

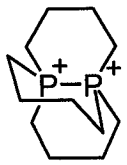

1.51c

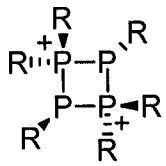

5.6
R = 2,6-dimethoxyphenyl

Dication **5.3** is a topological isomer of the only other cyclic *catena*-tetraphosphorus dication to be reported (**5.6**). Unlike the planar tetraphosphorus ring in the centrosymmetric 1,3-dication **5.6**,[83] the four *cis* interactions between substituents in the less symmetric (~C_2) 1,2-dication **5.3** result in even more ring puckering (average τ = 28.45°) than found in cyclotriphosphinophosphonium ions (**Table 3.3**, average τ = 10.41° - 21.09°).

Phosphorus, proton, and carbon NMR spectra of redissolved crystals of **5.3**$[OTf]_2$ were consistent with C_2 symmetry in solution. A new AA'BB' spin system, which has been simulated (**Figure 5.6**), was revealed by $^{31}P\{^1H\}$ NMR spectroscopy. The derived $^{31}P\{^1H\}$ NMR parameters are presented in **Table 5.3**. The $^1J_{PP}$ values corresponding to phosphine-phosphonium bonds (-284 Hz) or the *trans* substituted phosphine-phosphine bond (-169 Hz) are comparable to those found in cyclotriphosphinophosphonium ions (**Table 3.1**, e.g. $(^tBuP)_3PMe_2^+$ (**3.8**): -251 Hz and -143 Hz, respectively). In contrast, the $^1J_{PP}$ value for the two phosphonium centers in **5.3** seems very small (-40 Hz) in light of the much larger magnitude observed for **1.51b** ($^1J_{PP}$ = 219 Hz);[84] however, it is known that one-bond phosphorus-phosphorus coupling constants can be dependant on a number of factors, such as relative conformations and bond angles at the nuclei.[108] Recently, electron-donating or withdrawing effects of the substituents (R) in

phosphoranophosphonium monocations **1.59** have been invoked to describe the large variation in $^{1}J_{PP}$ magnitudes (**1.59a**: 23 Hz; **1.59b**: 13 Hz; **1.59c**: 277 Hz; **1.59d**: 324 Hz).[96]

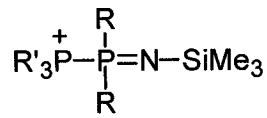

1.59

a: R = Me, R' = ^{n}Bu

b: R = R' = Me

c: R = OCH_2CF_3, R' = ^{n}Bu

d: R = OCH_2CF_3, R' = Me

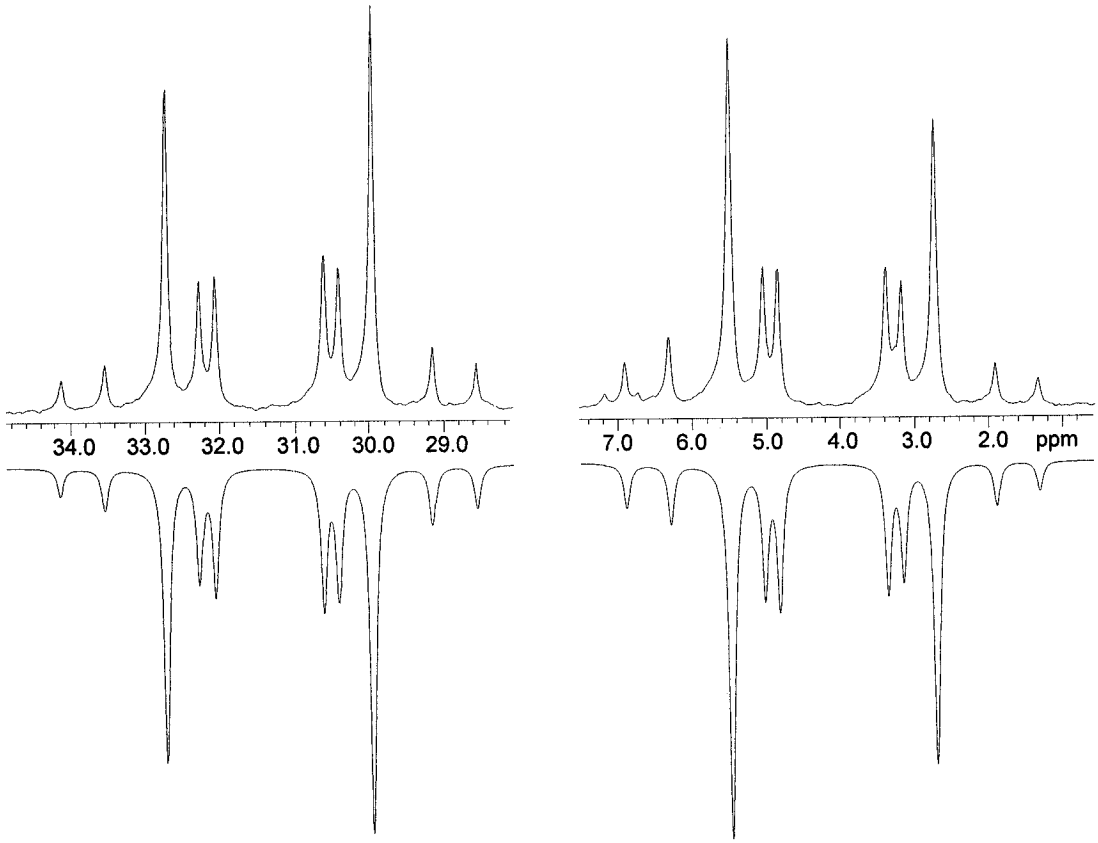

Figure 5.6 Expansions for experimental (top) and simulated (inverted) $^{31}P\{^{1}H\}$ NMR spectra (101.3 MHz) for **5.3**$[OTf]_2$.

Table 5.3 Simulated $^{31}P\{^{1}H\}$ NMR parameters for the AA'BB' spin system of **5.3**$[OTf]_2$ in CH_2Cl_2.

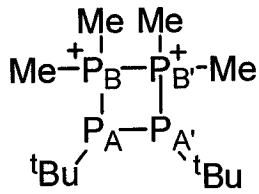

δ (ppm)	^1J (Hz)	^2J (Hz)
31 (B = B')	-284 (AB = A'B')	5 (A'B = AB')
4 (A= A')	-169 (AA')	
	-40 (BB')	

The ^1H NMR spectrum of **5.3**$[OTf]_2$ showed three second-order multiplets of relative integration 3:1:1 at 1.54 ppm, 2.73 ppm and 2.82 ppm, respectively. Thus, the ^{t}Bu substituents (1.54 ppm) are equivalent, and there are two spectroscopically distinct pairs of methyl substituents. Based on the dependence of $^3J_{PH}$ coupling on a *cis* orientation of the phosphine lone-pair and methyl group, as observed in cyclodi- and cyclotriphosphinophosphinium cations (**Chapter 3.4**), the six-line multiplet at 2.73 ppm is assigned to protons on C1 and C4 (**Figure 5.5**), and the less coupled four-line multiplet is assigned to protons on C2 and C3. Three multiplets were also observed in the ^{13}C NMR spectrum (quaternary carbons not observed), and an HSQC experiment showed correlation between a highly coupled multiplet at 13.5 ppm and the assigned C1/C4 pair, and between a less coupled signal at 9.7 ppm and the C2/C3 pair. The methyl groups on the ^{t}Bu substituents were observed at 29.5 ppm.

5.4 An Asymmetric Cyclotriphosphinophosphonium Ion

The substitution of $MePCl_2$ for Me_2PCl in reactions with **2.2a**[OTf] demonstrated further complexity in the reactivity of **2.2a**[OTf]. In monitoring the reactions by $^{31}P\{^{1}H\}$ NMR spectroscopy, it was found that ~1.2 equivalents of $MePCl_2$ were required for the complete consumption of **2.2a**[OTf]. Although, many unidentified products were initially observed, precipitation followed by recrystallization lead to a white solid, determined by NMR spectroscopy (see below) to be the new asymmetric cyclotriphosphinophosphonium ion **5.7**[OTf]. This monocation formally results from insertion of "MeP" into **2.2a**.

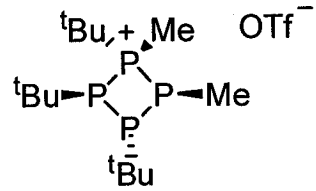

5.7

The $^{31}P\{^{1}H\}$ NMR spectrum of redissolved precipitate exhibited an AMNX spin system. Though line intensities are affected by second-order effects, each signal occurred as an eight-line doublet of doublet of doublets. The simulated spectrum is shown in **Figure 5.7** and the parameters are presented in **Table 5.4**.

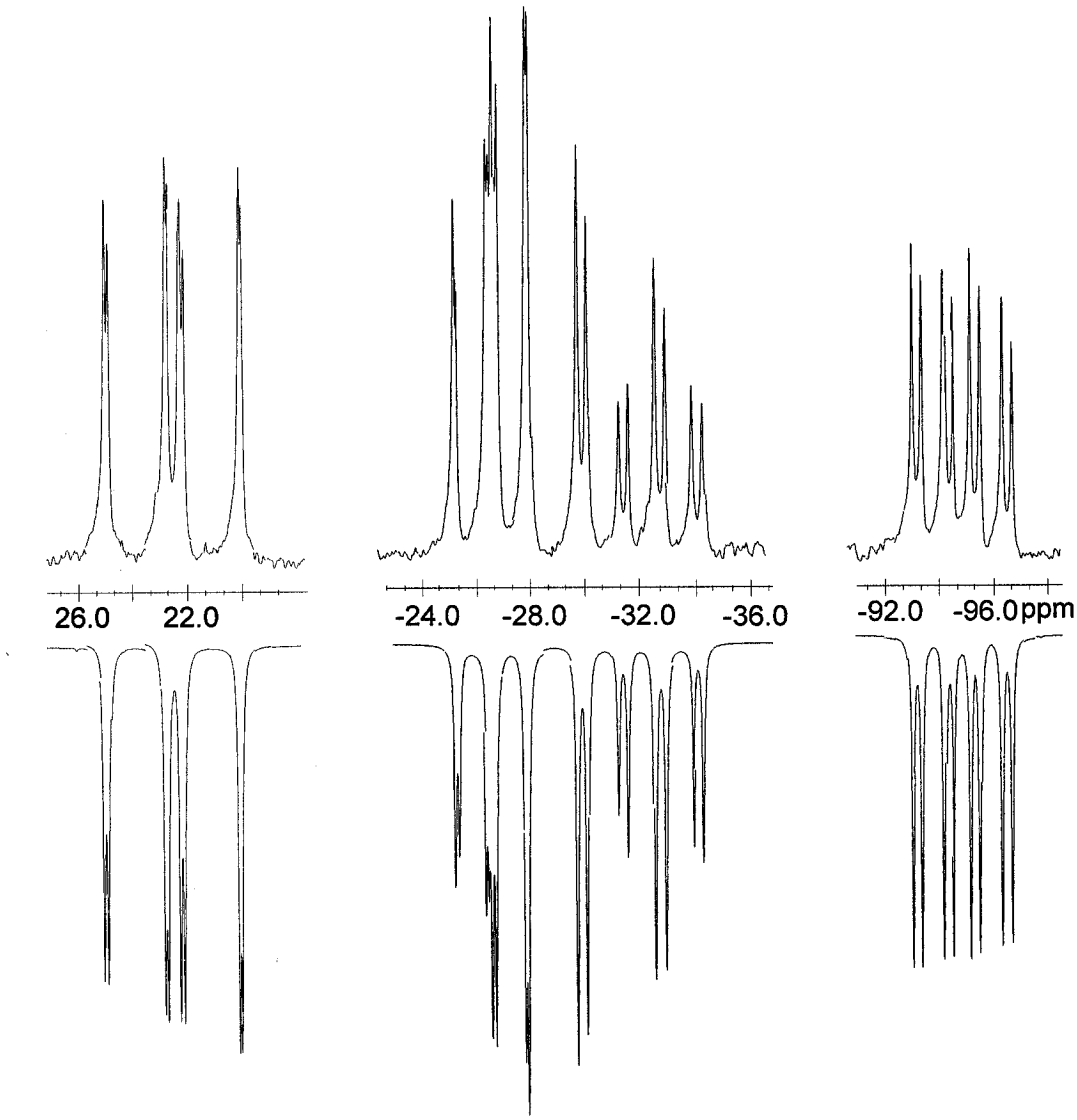

Figure 5.7 Expansions for experimental (top) and simulated (inverted) $^{31}P\{^{1}H\}$ NMR spectra (101.3 MHz) for **5.7**[OTf].

Table 5.4 Simulated $^{31}P\{^{1}H\}$ NMR parameters for the AMNX spin system of **5.7**[OTf] in $CDCl_3$.

δ (ppm)	**^{1}J (Hz)**	**^{2}J (Hz)**
22 (X)	-123 (AN)	41 (AM)
-26 (N)	-221 (AX)	19 (NX)
-31 (M)	-145 (MN)	
-95 (A)	-283 (MX)	

Based on comparison with the data in **Table 3.1** and **Table 5.4**, the presence of coupling constants over 200 Hz in magnitude are associated with coupling between a phosphine and a phosphonium unit, while coupling constants with magnitudes smaller

than 200 Hz signify coupling between two (*trans* substituted) phosphine centers. This, together with the chemical shifts of the phosphorus nuclei, indicates that **5.7** contains one phosphonium unit (X) and three unique phosphine centers (A, M, N). Moreover, the presence of four coupling constants consistent with $^{1}J_{PP}$ values, and two others consistent with $^{2}J_{PP}$ values, defines a cyclo-P_4 core of four unique phosphorus atoms.

Based on integrations, proton NMR data revealed that **5.7** contains three ^{t}Bu groups and two methyl groups. Importantly, the low field chemical shift (2.47 ppm) of one methyl group (Me1) and relatively high field shift (1.80 ppm) of the other (Me2), specify their positions on phosphonium and phosphine centers respectively. Moreover, the observed doublet for Me1 indicates no long range P-H coupling, and confirms that it is *cis* to two substituents on adjacent phosphorus atoms (cf. **Chapter 3.4**). The signal for Me2 occurs as a second-order eight-line multiplet, signifying $^{3}J_{PP}$ couplings, and places the methyl group *cis* to the lone pair of at least one adjacent phosphorus atom. Thus, the structure of **5.7**, expected to be a racemic mixture, is established by multinuclear NMR spectroscopy. In terms of the AMNX spin system observed in the $^{31}P\{^{1}H\}$ NMR spectrum, the phosphonium center can be assigned to X, and the opposing phosphorus atom to N. However, the assignment of A or M to the remaining P-^{t}Bu or P-Me phosphorus nuclei remains undefined (**Figure 5.8**).

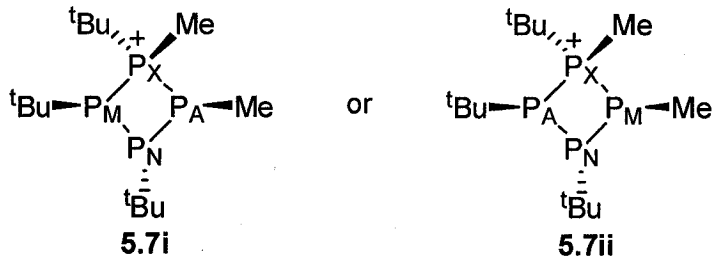

5.7i **5.7ii**

Figure 5.8 Two possible assignments of the AMNX spin system for **5.7**[OTf].

5.5 Summary

In reactions with triorganophosphines, the cyclodiphosphinophosphonium ion **2.2a**[OTf] was found to be a precursor to the first examples of acyclic tetraphosphorus monocations (**5.1**) via a phosphine-induced ring-opening reaction. Depending on the particular phosphine used, these cations were formed with varying degrees of

diastereoselectivity (one diastereomer with $^{n}Pr_3P$; two diastereomers with Me_3P or $PhMe_2P$), as confirmed by $^{31}P\{^{1}H\}$ NMR simulations.

Surprisingly, the use of chloro-substituted phosphines resulted in markedly different products. The first monocyclic 1,2-diphosphonium cation, crystallographically characterized as $[(^{t}BuP)_2(PMe)_2][OTf]_2$ (**5.3**$[OTf]_2$), has been prepared from **2.2a**[OTf], Me_2PCl and TMSOTf. This compound represents a topological isomer of the 1,3-dication **5.6**, the only other *catena*-tetraphosphorus dication.

It was also found that $MePCl_2$ reacted with **2.2a**[OTf] to give the assymetrical cyclotriphosphinophosphonium ion **5.7**[OTf]. The composition and configuration of this new tetraphosphorus moncation was established by multinuclear NMR spectroscopy and by the use of trends established for other cyclic di- and triphosphinophosphonium cations.

Though the mechanisms for these reactions are not well understood, they highlight the importance of **2.2a**[OTf] as a precursor to new *catena*-phosphorus cations. The observation of acyclic tetraphosphorus monocations, and cyclic tetraphosphorus mono- and dications from **2.2a**[OTf], prompts mechanistic investigations and further reactivity studies, and makes other such triphosphorus monocations important synthetic targets.

Chapter 6.0: Acyclic 1,3-Diphosphino-2-phosphonium Ions

6.1 Introduction

Besides monocationic derivatives of diphosphorus **A**, and tetraphosphorus **K** (**Chapter 5.2**), triphosphorus **1.41a**[69] is the only known acyclic monocation involving phosphine and phosphonium building units. As a contribution to this area, this chapter presents the first acyclic 1,3-diphosphinophosphonium ions (**B**) featuring organic substituents at phosphorus,[109] synthesized by a systematic extension of the effective P-P bond formation reactions recently developed for **A** (i.e. **Scheme 1.5c**).[61;62]

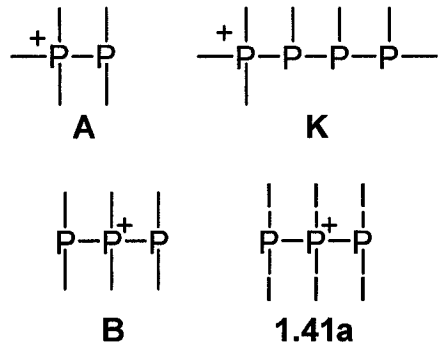

6.2 Synthesis and Characterization

Reactions of tetramethyldiphosphine **6.1a** or tetraphenyldiphosphine **6.1b** with Me_2PCl/TMSOTf or Ph_2PCl/TMSOTf, respectively, were monitored by $^{31}P\{^1H\}$ NMR spectroscopy. In both cases, although broad doublet and triplet signals were observed at room temperature, an 8-line A_2B spin system was observed at low temperature. This observation is consistent with the two equivalent phosphine centers (A, high field resonance) and single tetracordinate phosphonium center (B, low field resonance) of $[Me_2P\text{-}PMe_2\text{-}PMe_2][OTf]$ (**6.2a**[OTf]) and $[Ph_2P\text{-}PPh_2\text{-}PPh_2][OTf]$ (**6.2b**[OTf]). The reactions (**Scheme 6.1**) were rapid and virtually quantitative, and the $^{31}P\{^1H\}$ NMR spectrum of a representative reaction mixture between **6.1b** and Ph_2PCl/TMSOTf is shown in **Figure 6.1**.

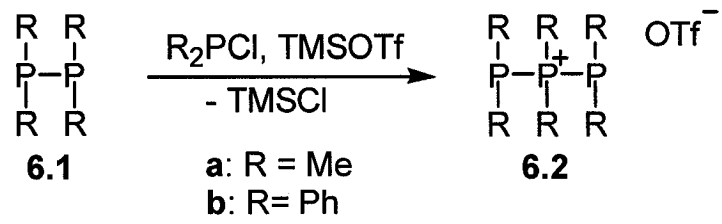

Scheme 6.1 Synthesis of **6.2a**[OTf] and **6.2b**[OTf].

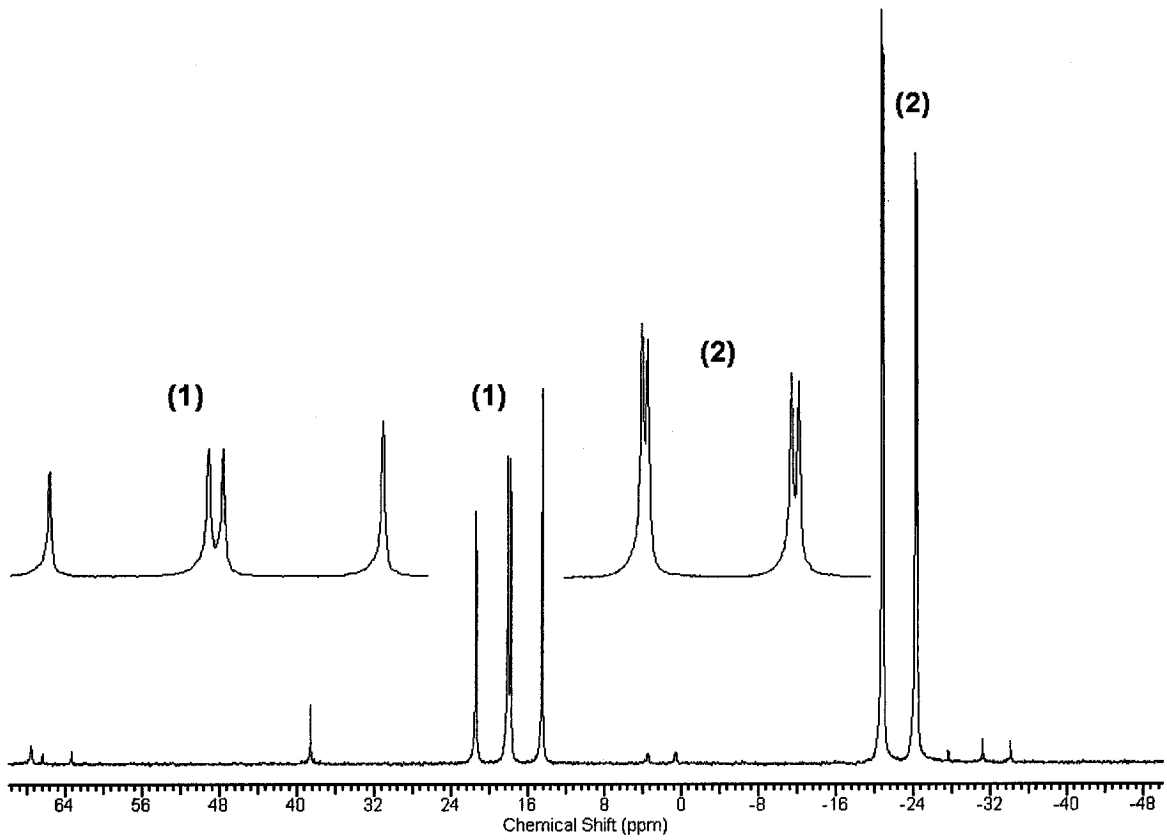

Figure 6.1 $^{31}P\{^{1}H\}$ NMR spectrum (101.3 MHz, 193 K) of a reaction mixture containing Ph_2P-PPh_2, Ph_2PCl and TMSOTf showing quantitative formation of **6.2b**[OTf].

Compound **6.2a**[OTf] has been crystallographically characterized, and the cation is observed in an eclipsed/staggered (C_s) conformation (**Figure 6.2**). The A_2B spin system observed by $^{31}P\{^{1}H\}$ spectroscopy is indicative of free rotation about the P-P bonds in solution (effective C_{2v} symmetry).

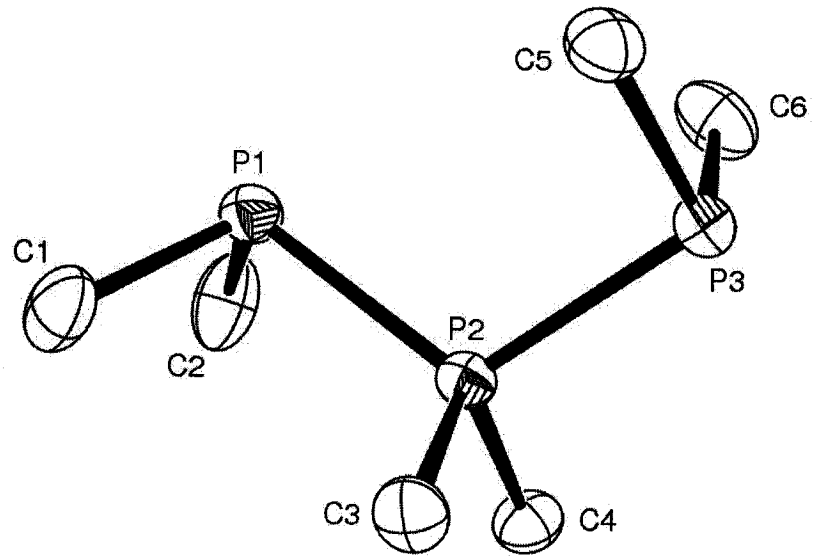

Figure 6.2 Solid state structure of the cation in the of **6.2a**[OTf], with hydrogen atoms omitted and thermal ellipsoids at the 50% probability level. P1-P2 = 2.2160(6) Å; P2-P3 = 2.1883(6) Å; P-P-P = 111.56(3)°.

Attempts to form diphosphinophosphonium ions with mixed substituents resulted in more complicated reaction mixtures. Low temperature (193 K) $^{31}P\{^{1}H\}$ NMR spectroscopy of reaction mixtures involving **6.1a**, Ph_2PCl and TMSOTf revealed a new AMX spin system along with the signals for **6.2a**, **6.1b**, Ph_2PCl, and some minor unidentified peaks. The spin system and chemical shifts of the new product suggest a linear, triphosphorus compound which is assigned to **6.2c**[OTf] (**Table 6.1**). Based on the approximate integrations in the $^{31}P\{^{1}H\}$ NMR spectra, **Scheme 5.2a** is proposed as a balanced equation. Some of the competing reactions which could account for the observed products are also presented (**Scheme 6.2b**). Compound **6.2c**[OTf] could not be isolated.

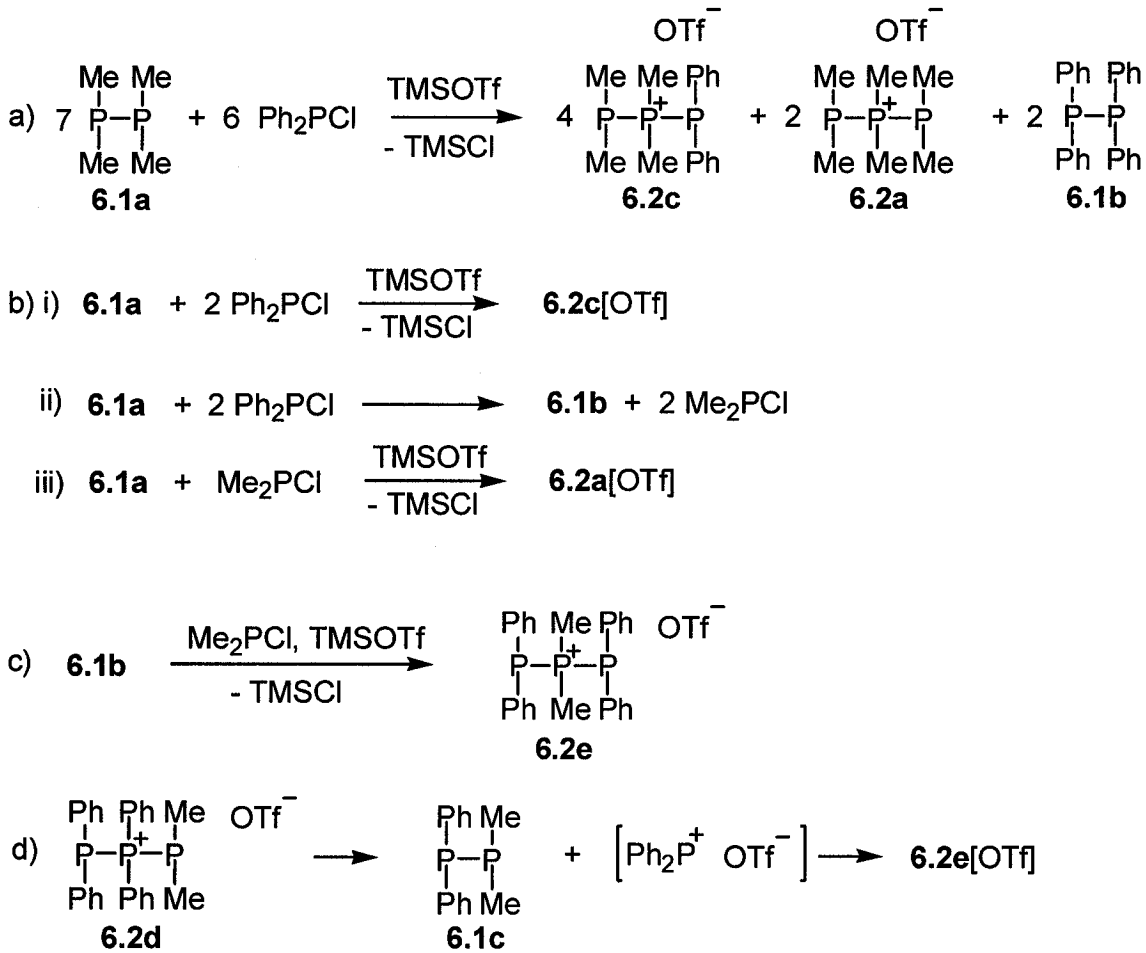

Scheme 6.2 Proposed reactions involved in the synthesis of **6.2c**[OTf] and **6.2e**[OTf].

Table 6.1 $^{31}P\{^{1}H\}$ NMR parameters for derivatives of **6.2**[OTf].

Compound	Spin System	$\delta_{phosphine}$ (ppm)	$\delta_{phosphonium}$ (ppm)	$^{1}J_{PP}$ (Hz)	$^{2}J_{PP}$ (Hz)
6.2a[OTf][a]	A_2B	-62	12	-298	-
6.2b[OTf][b]	A_2B	-22	18	-351	-
6.2c[OTf][b]	AMX	-52, -28	8	-331 (AX) -296 (MX)	13 (AM)
6.2e[OTf][a]	A_2B	-20	5	-337	-

[a] $CDCl_3$, 220 K; [b] CH_2Cl_2, 193 K.

Interestingly, the corresponding reactions involving **6.1b** and Me_2PCl resulted in a new A_2B spin system (> 80% by $^{31}P\{^{1}H\}$ NMR, with unidentified byproducts) which is assigned to **6.2e**[OTf] (**Table 6.1**). As discussed previously in **Chapter 3** and **Chapter 4**, phosphenium ion insertion into P-P bonds is not unexpected (**Scheme 6.2c**); however, the

observation of **6.2c** opens up the possibility that **6.2d** is formed as a first step, and subsequent rearrangement leads to **6.2e**. Considering, based on electronic arguments, that Me_2P-R is a better donor and Me_2P^+ a better acceptor than Ph_2P-R and Ph_2P^+ respectively, the rearrangement can be envisioned by breaking the most labile bond in **6.2d** to give Ph_2P-PMe_2 (**6.1c**) and Ph_2P^+, which reassociate to give isomer **6.2e** (**Scheme 6.2d**). Isomer **6.2e** is also expected to be sterically preferred over **6.2d**. This proposed scheme is consistent with the dative nature of phosphinophosphonium ions (**A**) and prompts an analogous description of the bonding in diphosphinophosphonium ions (**B**, **B'**).

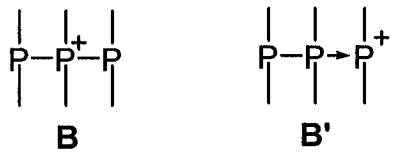

B **B'**

6.3 Summary

The first homoleptic, organo-substituted acyclic diphosphinophosphonium salts **6.2a**[OTf] and **6.2b**[OTf] have been prepared from diphosphines and chlorophosphines in the presence of TMSOTf. These cations were formed quantitatively, and have been characterized by $^{31}P\{^1H\}$ NMR spectroscopy and X-ray crystallography in the case of **6.2a**[OTf]. Cations **6.2c** and **6.2e**, featuring mixed organo-substituents, were observed in solution ($^{31}P\{^1H\}$ NMR), but could not be isolated.

Chapter 7.0: Acyclic 2,3-Diphosphino-1,4-Diphosphonium Ions

7.1 Introduction

Acyclic *catena*-phosphorus dications involving two (**E**)[86] and three (**F**)[90] phosphorus atoms are known. Some related tetraphosphorus dications have been reported, and crystallographically characterized as **1.53**[91] and **1.54.**[92] Although the phosphorus atoms in these examples are connected in linear chains, these systems are not truly acyclic as each contains bridging ligands. The relative position of the bridges (between phosphine centers in **1.53**, or phosphine and phosphonium centers in **1.54**) suggests that they are not essential to the stability of the compounds, and that 2,3-diphosphino-1,4-diphosphonium ions (**G**) with truly acyclic topologies should be accessible. This chapter presents the first examples of such acyclic tetraphosphorus dications prepared by a new reductive coupling reaction between phosphinophosphonium monocations.[135]

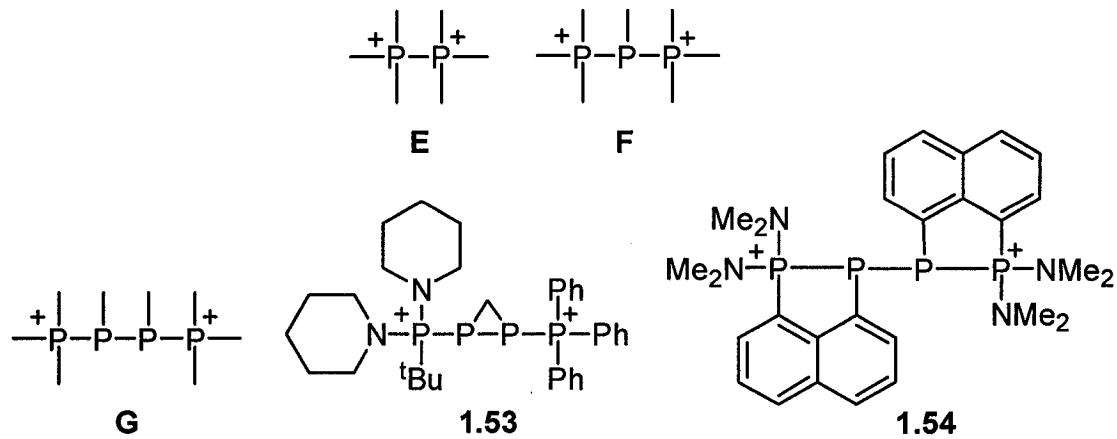

7.2 Synthesis and Characterization

The addition of Ph_3P to equimolar amounts of $RPCl_2$ (R = Ph, Me), and TMSOTf resulted in the rapid and quantitative formation of the chlorophosphinophosphonium salts (**7.1**[OTf]; **a**: R = Ph; **b**: R = Me; **Scheme 7.1a**). Surprisingly, these monocations were observed by $^{31}P\{^1H\}$ NMR spectroscopy as sharp singlets at room temperature (**7.1a**: 22, 55 ppm; **7.1b**: 21, 70 ppm), with low field shifts corresponding to the chloro-substituted

phosphine center. At 213 K, the spectrum for **7.1a** contained the expected doublets ($^1J_{PP}$ = 333 Hz) at 22 and 49 ppm. Single crystals of **7.1a**[OTf] were found to be racemic and the solid state structure of one enantiomer of the cation is shown in **Figure 7.1**.

a) $RPCl_2 + Ph_3P + TMSOTf \xrightarrow[-TMSCl]{rapid} Ph_3P{-}\overset{R}{\underset{|}{P}}{-}Cl^{+}\ OTf^{-}$ **7.1**

b) 2 **7.1**[OTf] + Ph_3P + TMSOTf $\xrightarrow[-\ TMSCl]{slow}$ $Ph_3P{-}\overset{R}{\underset{|}{P}}{-}\overset{R}{\underset{|}{P}}{-}PPh_3^{+}\ 2OTf^{-}$ + $[Ph_3PCl][OTf]$ **7.2**

---

c) 2 $RPCl_2$ + 3 Ph_3P + 3 TMSOTf $\xrightarrow[-3\ TMSCl]{}$ **7.2**$[OTf]_2$ + $[Ph_3PCl][OTf]$

a: R = Ph
b: R = Me

Scheme 7.1 a) Synthesis of derivatives of **7.1**[OTf]; b) Synthesis of derivatives of **7.2**$[OTf]_2$ by the reductive coupling of **7.1**[OTf]; c) Balanced equation for the one-pot synthesis of derivatives of **7.2**$[OTf]_2$.

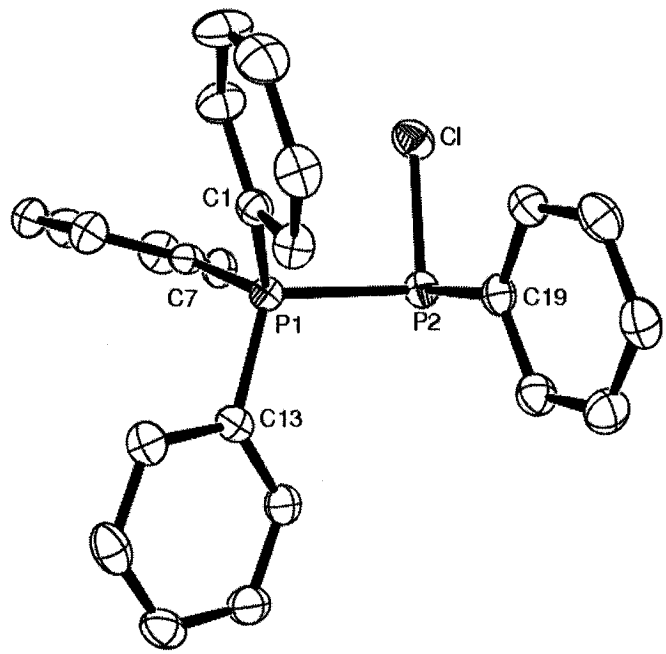

Figure 7.1 Solid state structure of one enantiomer of the cation in **7.1a**[OTf] with hydrogen atoms omitted for clarity and thermal ellipsoids at the 50% probability level.

After days of stirring at room temperature, $^{31}P\{^{1}H\}$ NMR spectroscopy showed that reactions involving excess Ph_3P and TMSOTf resulted in the consumption of initially formed **7.1**[OTf], with the concurrent appearance of $[Ph_3PCl][OTf]$ (singlet at 66 ppm; ^{19}F NMR: -80 ppm) and new AA'BB' spin systems (**Table 7.1**) corresponding to the acyclic tetraphosphorus dications $[Ph_3P\text{-}PR\text{-}PR\text{-}PPh_3][OTf]_2$ (**7.2**$[OTf]_2$; **a**: R = Ph; **b**: R = Me). Thus, the excess phosphine present in solution effects the reductive coupling of chlorophosphinophosphonium ions (**7.1**[OTf]) according to **Scheme 7.1b**. Derivatives of **7.2** were not observed if only one equivalent of TMSOTf was used, suggesting that the formation of $[Ph_3PCl][OTf]$, rather than simply Ph_3PCl_2, is an important driving force in the coupling reaction. A balanced equation for this one-pot synthesis is shown in **Scheme 7.1c**. Significantly, this reaction contrasts the formation of $[Ph_3P\text{-}PPh\text{-}PPh_3][AlCl_4]_2$ (**7.3**$[AlCl_4]_2$) from $PhPCl_2$, Ph_3P and $AlCl_3$,[90] where displacement of the second chloride ion in the supposed intermediate **7.1a**$[AlCl_4]$ is preferred over reductive coupling. Both derivatives of **7.2** have been structurally characterized in the solid state (**Figure 7.2 – 7.3**), and selected structural parameters are presented in **Table 7.2**.

Table 7.1 Simulated $^{31}P\{^{1}H\}$ NMR parameters for derivatives of **7.2**$[OTf]_2$ and **7.4**$[OTf]_2$.

Dication	7.2a[a]		7.2b[a]	7.4a[b]		7.4b[b]
	Isomer 1	Isomer 2[c]		Isomer 1	Isomer 2[c]	
$\delta_A = \delta_{A'}$	-33	-42	-71	-52	-56	-73
$\delta_B = \delta_{B'}$	24	22	26	25	23	26
$^1J_{AA'}$	-124	-	-278	-105	-	-238
$^1J_{AB} = {}^1J_{A'B'}$	-343	-	-282	-305	-	-269
$^2J_{AB'} = {}^2J_{A'B}$	69	-	78	66	-	80
$^3J_{BB'}$	51	-	62	56	-	58

[a] CH_2Cl_2 solution; [b] CD_3CN solution; [c] Minor isomer could not be simulated.

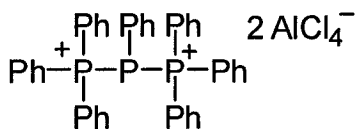

7.3

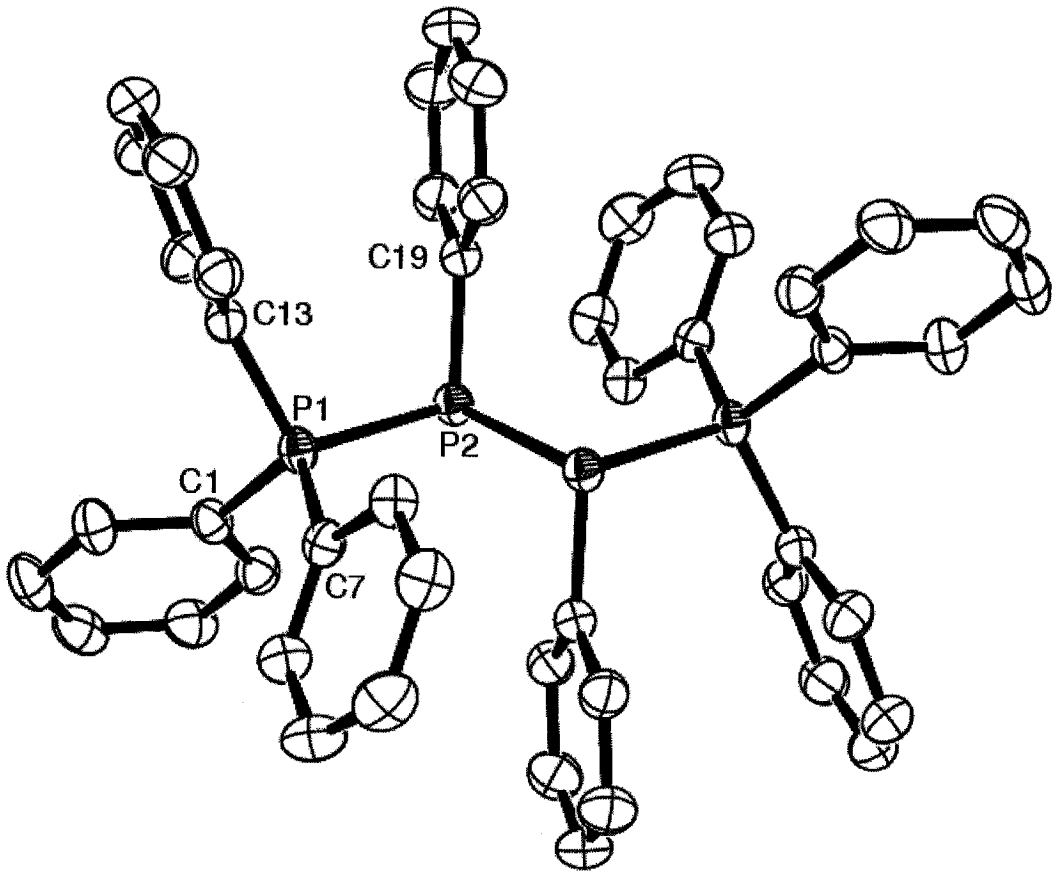

Figure 7.2 Solid state structure of the centrosymmetric *meso*- dication in **7.2a**$[OTf]_2$ with hydrogen atoms omitted for clarity and thermal ellipsoids at the 50% probability level.

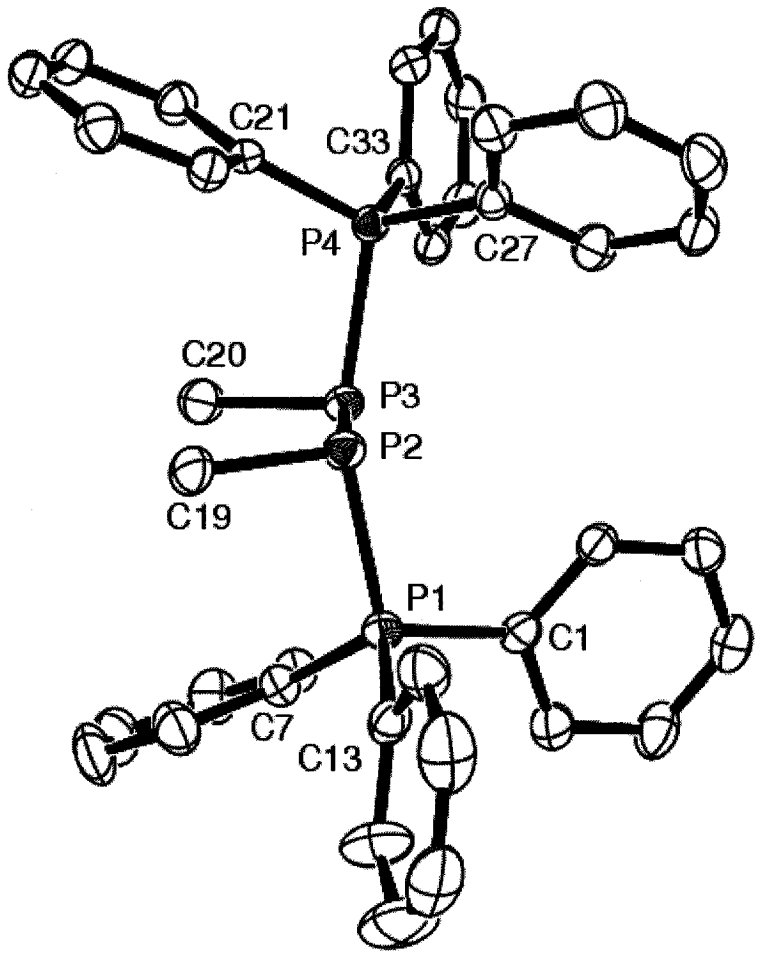

Figure 7.3 Solid state structure of one enantiomer of the dication in **7.2b**$[OTf]_2$ with hydrogen atoms omitted for clarity and thermal ellipsoids at the 50% probability level.

Table 7.2 Selected structural parameters for **7.1a** and derivatives of **7.2** and **7.4**. Numbers in square brackets correspond to atom labels in **Figure 7.1 - 7.3**, and **Figure 7.5 - 7.6**.

Cation	P-P (Å)	C-P-P (°)	C-P-P-C (°)	P1-P2-P3-P4 (°)
7.1a	2.2471(8) [1,2]	-	-	-
7.2a	2.258(1) [1,2] 2.221(1) [2,2']	101.65(8) [19,2,2']	180 [19,2,2',19']	180
7.2b	2.206(1) [1,2] 2.228(1) [2,3] 2.212(1) [3,4]	109.3(1) [19,2,3] 107.9(1) [20,3,2]	0.96 [19,2,3,20]	159.98
7.4a	2.2041(9) [1,2] 2.232(2) [2,2']	101.02(8) [19,2,2']	180 [19,2,2',19']	180
7.4b	2.192(2) [1,2] 2.243(2) [2,3] 2.191(2) [3,4]	102.1(2) [4,2,3] 102.8(2) [5,3,2]	31.26 [4,2,3,5]	126.72

Crystals of **7.2a**$[OTf]_2$ contain the *meso*-isomer of the dication, which itself is centrosymmetric with phenyl groups and Ph_3P units at torsional angles of 180°. It is important to note, however, that solid state ^{31}P CP/MAS NMR spectroscopy on a bulk sample of crystals revealed four distinct doublet-like signals, two of which were of much larger integration (greater than 10:1). This observation is interpreted in terms of two chemical species in the solid state, with peaks for the major component centered at 24 ppm and -40 ppm, and peaks for the minor component centered at 19 ppm and -31 ppm. Solution NMR studies on redissolved crystalline samples and reaction mixtures were consistent with the presence of both possible diastereomers (*meso*- and *rac*-). The $^{31}P\{^1H\}$ NMR spectrum for the major isomer (δ = 24 ppm and -33 ppm) has been simulated; however, the peaks for the minor constituent (δ = 22 ppm and -42 ppm) were not sufficiently resolved to allow for a meaningful determination of parameters (**Figure 7.4**). The diasteriomeric excess (d.e.) was found to be 62% from ^1H NMR integrations, but the preferred diastereomer in solution has not yet been definitively identified. In fact, from the the solution and solid state phosphorus chemical shifts, it cannot even be determined that the major isomer in solution is the major isomer in the solid state.

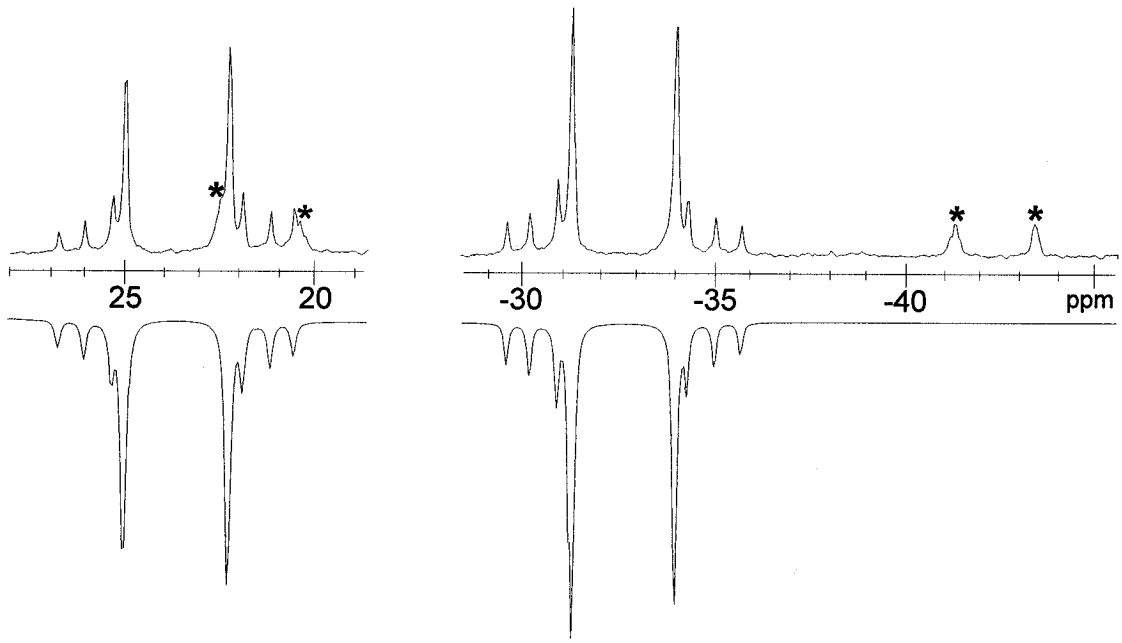

Figure 7.4 Expansions for the experimental (top) and simulated (inverted) $^{31}P\{^1H\}$ NMR spectra (101.3 MHz) for the major diastereomer in solutions of **7.2a**$[OTf]_2$. Peaks labeled "*" are assigned to the minor diastereomer.

The dication in compound **7.2b**$[OTf]_2$ crystallized in the racemic form and both enantiomers were present in the crystal. Interestingly, the methyl substituents are virtually eclipsed, with a C19-P2-P3-C20 torsional angle of 0.96°. Unlike **7.2a**[OTf], NMR analysis of redissolved solid and reaction mixtures showed only one diastereomer. Thus, the racemic form of **7.2b**$[OTf]_2$ is concluded to be formed exclusively in the reductive coupling of racemic **7.1b**[OTf]. It is noteworthy that crystals of **1.54** also contained both enantiomers of the racemic dication, and no other diastereomers were observed upon redissolution.[92]

It was found that the terminal phosphonium units could be exchanged in reactions of derivatives of **7.2**$[OTf]_2$ with Me_3P (**Scheme 7.2**). By use of $^{31}P\{^1H\}$ NMR spectroscopy, dications $[Me_3P\text{-}PR\text{-}PR\text{-}PMe_3][OTf]_2$ (**7.4**$[OTf]_2$; **a**: R = Ph; **b**: R = Me) were observed quantitatively as new AA'BB' spin systems (**Table 7.1**) in the reaction mixtures if an excess of Me_3P was used. Interestingly, the addition of one equivalent of Me_3P to a solution of **7.2a**$[OTf]_2$ afforded a 50:50 mixture of unreacted starting material and **7.4a**$[OTf]_2$, and monosubstitution was not observed. This ligand exchange reactivity is consistent with a coordinative bonding model (**G'**) for dications of type **G**, and they can be described as bisphosphine complexes of a *catena*-diphosphenium ion.

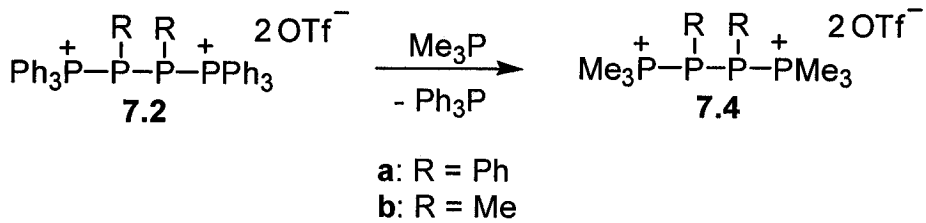

Scheme 7.2 Synthesis of **7.4**$[OTf]_2$ by ligand exchange involving **7.2**$[OTf]_2$.

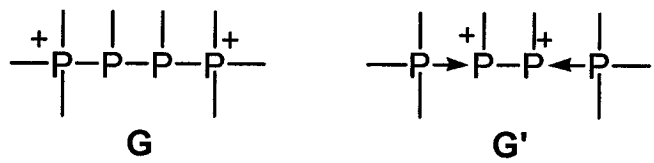

Derivatives of **7.4**$[OTf]_2$ were found to be much like the corresponding derivatives of **7.2**$[OTf]_2$. In solution, **7.4a**$[OTf]_2$ occured as a mixture of distereomers

(d.e. = 72%), and in the solid state a centrosymmetric *meso*-compound was observed (**Figure 7.5**, **Table 7.2**). For **7.4b**$[OTf]_2$ only one diastereomer was observed in solution, and the cation crystallized in the racemic form (**Figure 7.6**, **Table 7.2**). The methyl groups on the phosphine centers in **7.4b** were found to be much less eclipsed [τ(C4-P2-P3-C5) = 31.26°] than those in **7.2b**. In this case, the smaller bulk of the Me_3P groups, versus Ph_3P in **7.2b**, accommodates a smaller P1-P2-P3-P4 torsional angle (126.72° vs. 159.98°) and allows for a corresponding increase in the C-P2-P3-C torsional angle (**Table 7.2**). Consistent with the more eclipsed conformation, the C-P2-P3 angles in **7.2b** are larger [109.3(1)° and 107.9(1)°] than those in **7.4b** [102.1(1)° and 102.8(1)°].

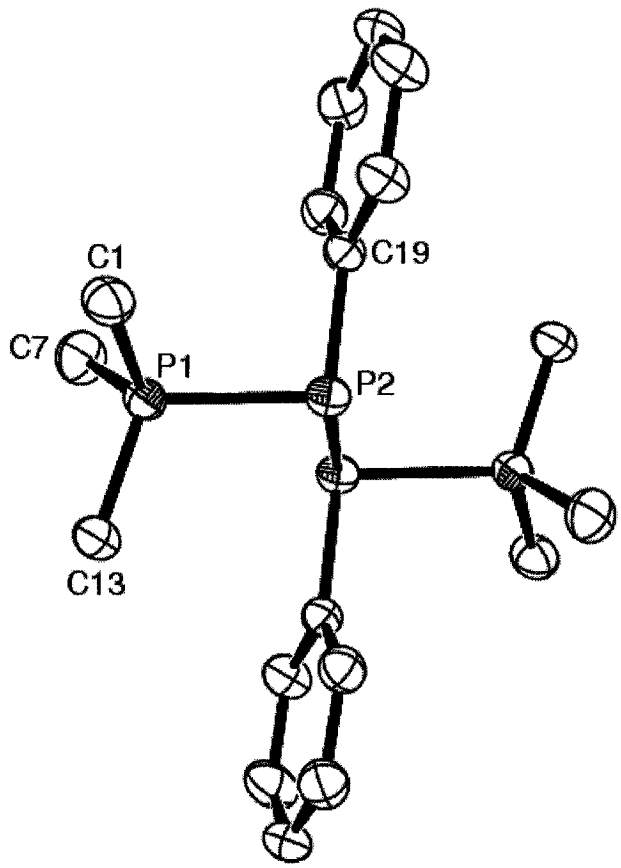

Figure 7.5 Solid state structure of the centrosymmetric *meso*- dication in **7.4a**$[OTf]_2$ with hydrogen atoms omitted for clarity and thermal ellipsoids at the 50% probability level.

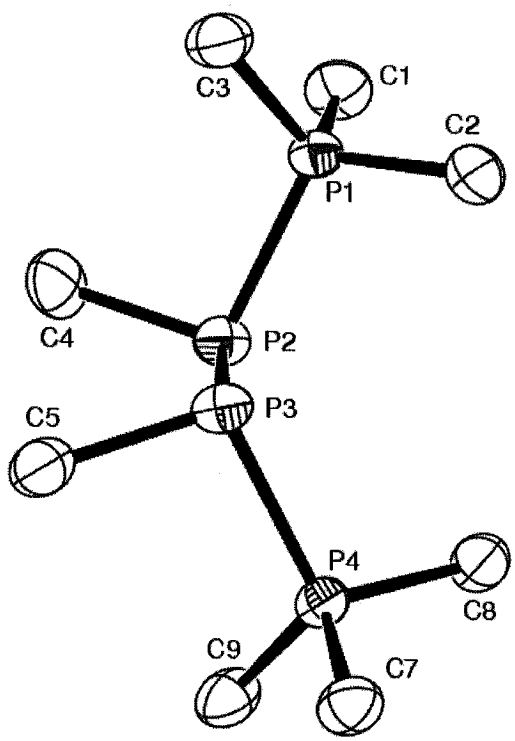

Figure 7.6 Solid state structure of one enantiomer of the dication in **7.4b**$[OTf]_2$ with hydrogen atoms omitted for clarity and thermal ellipsoids at the 50% probability level.

7.3 Summary

A new one-pot reductive coupling reaction, involving intermediate chlorophosphinophosphonium ions, has allowed the for the synthesis of the first derivatives of acyclic 2,3-diphosphino-1,4-diphosphonium ions. These dications represent new members in the limited series of acyclic *catena*-phosphorus dications, complementing the known diphosphonium,[86] and 2-phosphino-1,3-diphosphonium derivatives.[90]

Importantly, quantitative ligand exchange reactions of $[Ph_3P\text{-}PR\text{-}PR\text{-}PPh_3][OTf]_2$ (**7.2**$[OTf]_2$; **a**: R = Ph; **b**: R = Me) with Me_3P has provided access to derivatives $[Me_3P\text{-}PR\text{-}PR\text{-}PMe_3][OTf]_2$ (**7.4**$[OTf]_2$; **a**: R = Ph; **b**: R = Me) and has demonstrated the dative nature of the phosphine-phosphonium bonds in **7.2**. Both the reductive coupling and ligand exchange reactions presented here should be valuable in further diversifying the chemistry *catena*-phosphorus cations.

Chapter 8.0: Conclusion

8.1 Conclusion

Thirteen different arrangements of catenated phosphine and phosphonium units have now been realized (**Figure 8.1**). Contributions from this thesis include the first definitive examples of a family of monocyclic monocations (**H** – **J**),[100;109] the first derivatives acyclic tetraphosphorus monocations (**K**), and the only known cyclotetraphosphorus 1,2-dication (**L**). Of the examples reported prior to this thesis (**A** – **G**), the work presented here has added the first organo-substituted derivatives of **B**[109] and the first fully acyclic examples of **G**.[135] In addition, our group has recently reported on the thermal conversion of monocations of type **J** to the first examples *catena*-hexaphosphorus dications of form **M**.[136]

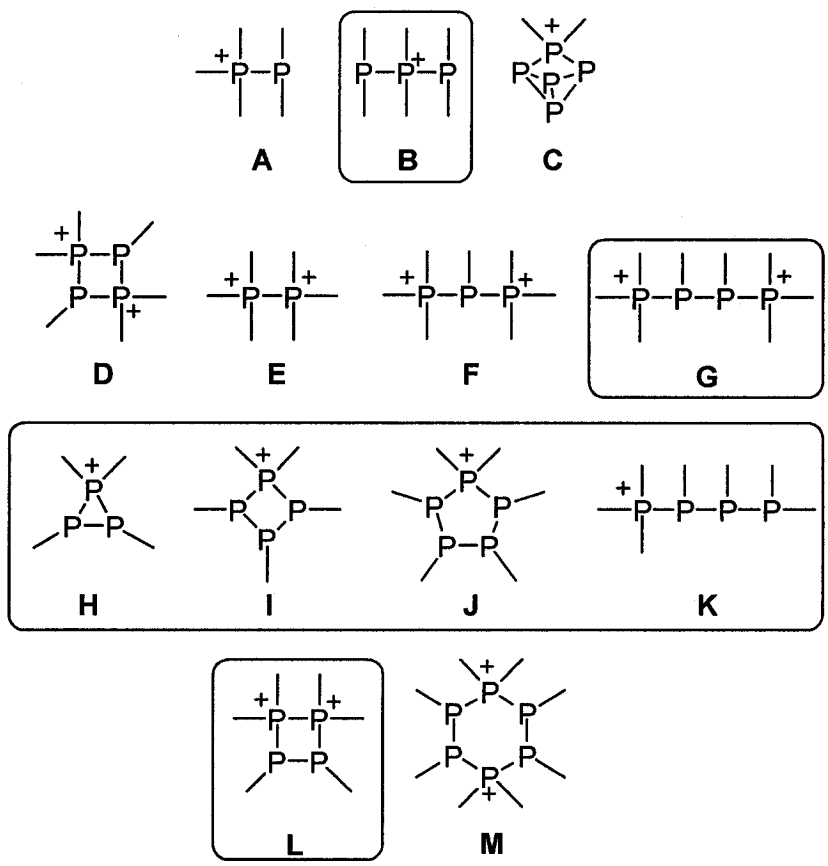

Figure 8.1 Representations for all currently known forms of *catena*-phosphorus cations involving exclusively phosphine and phosphonium units. Systems developed within this thesis are highlighted in boxes.

As for carbon, catenation makes up a significant component of the fundamental chemistry of phosphorus. The new synthetic methods and *catena*-phosphorus cations developed here complement the more extensive studies on *catena*-phosphines[3;7-11] and *catena*-phosphorus anions,[3;7-9;54] and lend themselves to a more complete understanding of *catena*-phosphorus chemistry. In this way, this thesis represents a significant contribution towards a systematic development of a fundamentally relevant area of phosphorus chemistry.

8.2 Future Work

In the context of a systematic development, derivatives of 2,3-diphospino-1-phosphonium ions (**N**) are important targets as they are the only unrepresented constitutional isomers of $P_3R_6^+$ (R_3P-P-PR_3^+,[76] and derivatives of **B** are known). Potential routes to these cations include a new reductive coupling route (**Scheme 8.1a**) or phosphine-induced dissociation of cyclotetraphosphorus 1,3-dications of type **D** (**Scheme 8.1b**). Also, the isolation of **L** inspires the search for other 1,2-diphosphonium ions such as **O** and **P**.

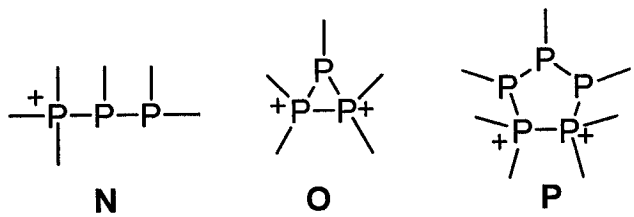

N **O** **P**

a) $[R_3P\text{-}PRCl][OTf] + 2\,R_2PCl + TMSOTf \longrightarrow$ (- TMSCl, - $[R_2PCl_2][OTf]$) **8.1**

b) 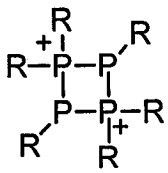 $+ 2\,R_3P \longrightarrow 2$ **8.1**

Scheme 8.1 Potential synthetic routes to 2,3-diphosphino-1-phosphonium ions **8.1**.

Perhaps one of the most promising objectives in this field will be the isolation of *catena*-phosphorus cations which break the current limitations of charge and degree of catenation (number of directly bound phosphorus atoms). To date there have only been reports of *catena*-phosphorus mono- or dications, with higher polycations yet to be isolated. Similarly, only recently have cations with six phosphorus atoms been prepared.[136] In contrast, examples of *catena*-phosphines and *catena*-phosphorus anions involving more than twenty phosphorus atoms are known, the latter of which include examples involving three and four negative charges (discussed in **Chapter 1**).

In analogy to the methods used by Baudler for the synthesis of highly catenated polycyclic phosphines (**Scheme 1.3**),[3;8;9] and Hey-Hawkins for monocyclic *catena*-phosphorus anions (**Scheme 1.4**),[39;53] highly catenated and/or highly charged phosphorus cations may be accessible by the reduction of di- (**8.2**), tri- (**8.3**), and tetrachlorophosphonium ions (**8.4**) in the presence of varying stoichiometric amounts of $RPCl_2$ and/or PCl_3 (**Scheme 8.2**).

One of the challenges expected with this proposed methodology is finding a suitable anion/reducing agent combination. Commonly used reducing agents (RA) such as magnesium, sodium or potassium metal are not likely to be compatible with the triflate anions used throughout this thesis. Therefore bulkier and less coordinating anions[137] (X) may be required. Alternatively, softer reducing agents may work, such as an appropriate phosphine, arsine or stibine (cf. Ph_3P in **Scheme 7.1**). Low oxidation state Group 14 or 13 compounds, such as $SnCl_2$ or GaCl, respectively, also have potential in this regard.

a) w $[R_2PCl_2][X]$ + y $RPCl_2$ + z PCl_3 $\xrightarrow[-(RA)Cl_n]{RA}$ $[P_{w+y+z}R_{2x+y}][X]_w$

8.2

b) w $[RPCl_3][X]$ + y $RPCl_2$ + z PCl_3 $\xrightarrow[-(RA)Cl_n]{RA}$ $[P_{w+y+z}R_{x+y}][X]_w$

8.3

c) w $[PCl_4][X]$ + y $RPCl_2$ + z PCl_3 $\xrightarrow[-(RA)Cl_n]{RA}$ $[P_{w+y+z}R_y][X]_w$

8.4

X = monoanion

RA = reducing agent

Scheme 8.2 Proposed synthetic routes to highly catenated and/or highly charged phosphorus cations.

In these proposed reactions, **8.2**, **8.3**, **8.4**, $RPCl_2$ and PCl_3 are designed to be precursors to sub-units **I** – **V**, respectively, within the product. As a hypothetical example, reactions according to **Scheme 8.2b**, with x = 3, y = 3, and z = 1 could lead to cations of stoichiometry $[P_7R_6]^{3+}$, of which **8.5** is a potential structural motif. Similarly, other potential cations include **8.6** (**Scheme 8.2b** with x = 3, y = 0, and z = 1), **8.7** (**Scheme 8.2b** with x = 4, y = 0, and z = 0), and **8.8** (**Scheme 8.2c** with x = 1, y = 0, and z = 8).

I

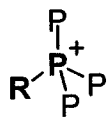

II

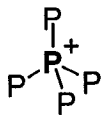

III

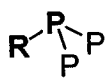

IV

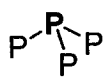

V

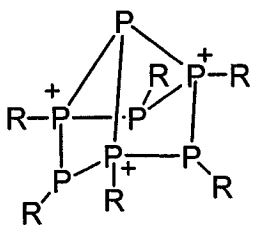

$[P_7R_6]^{3+}$

8.5

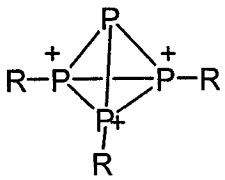

$[P_4R_3]^{3+}$

8.6

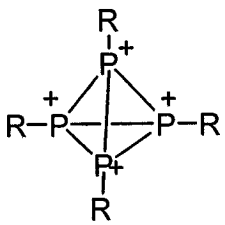

$[P_4R_4]^{4+}$

8.7

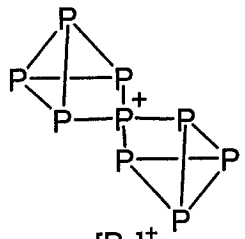

$[P_9]^+$

8.8

As a result of the large number of structural arrangements for products from these reactions, predictions are difficult, and reactions targeting a specific cation are unlikely to proceed as designed. A more practical approach to this synthetic methodology would be to obtain and analyse multinuclear NMR data of reaction mixtures to determine the empirical formula of the dominant product for a given reaction stoichiometry, and then to adjust the reaction stoichiometry to favor the formation of this compound. Based on the preferred ring sizes found in cyclopolyphosphinophosphonium cations, which depend in part on the substituents at phosphorus, it seems reasonable that for most reaction conditions and choice of R group, the reactions in **Scheme 8.2** should lead to a particular cation preferentially.

Chapter 9.0: Experimental

9.1 General Procedures

Small scale reactions were carried out in an Innovative Technology, System One, glove-box with an inert N_2 atmosphere containing less than 10 ppm of oxygen and less than 5 ppm water. These reactions were done in 20 mL glass vials with Teflon-lined caps. Larger scale reactions involved the use of standard Schlenck techniques[138] and an inert Ar atmosphere or methods otherwise specified. All glassware was stored overnight in an oven at 110 °C and pumped into the glove-box while hot, or was flame-dried under vacuum prior to use. Small amounts (< 0.2 mL) of liquid reagents were measured using an Ependorff pipette (10 – 100 μL). Solvents were dried on an MBraun solvent purification system, except $CHCl_3$ which was purchased from Alrich (HPLC grade). All solvents were stored over molecular sieves prior to use. $(^tBuP)_3$,[17] $(^tBuP)_4$,[19] $(CyP)_4$,[18] $(PhP)_4$,[21] $(PhP)_5$,[18] and $(MeP)_5$,[17] were prepared according to literature methods. Me_2PCl and $MePCl_2$ were purchased from Strem and used as received. HOTf (trifluoromethanesulfonic acid), MeOTf (methyltrifluoromethanesulfonate), Ph_3P, HCl (2M in Et_2O) and Me_3P (1 M solution in toluene or hexane) were purchased from Aldrich and used as received. Ph_2PCl, $PhPCl_2$, and TMSOTf were purchased from Aldrich and were purified by vacuum distillation prior to use.

Solution ^1H, ^{13}C, and ^{31}P NMR spectra were collected at the indicated temperature on Bruker AC-250 and Bruker Avance 500 NMR spectrometers. Chemical shifts are reported in ppm relative to an external reference standard at 0 ppm [100% $SiMe_4$ (^1H, ^{13}C), and 85% H_3PO_4 (^{31}P)]. Deuterated solvents were purchased from Aldrich, and used as received (CD_3CN and CD_3NO_2 in ampoules), or stored over molecular sieves for 24 hours prior to use ($CDCl_3$). NMR spectra of reaction mixtures were obtained by transferring an aliquot of the bulk solution to a 5 mm NMR tube. Tubes were then flame-sealed, or capped and tightly covered with parafilm. Most reported ^{31}P NMR parameters for second-order spin systems were derived by iterative simulation of experimental data at fields of 101.3 MHz and 202.6 MHz by use of gNMR.[139] $[(^tBuP)_2P^tBuMe][OTf]$ (**2.2a**[OTf]), $[(CyP)_3PCyH][OTf]$ (**3.7b**[OTf]), $[^nPr_3P\text{-}P^tBu\text{-}P^tBu\text{-}P^tBuMe][OTf]$ (**5.1a**[OTf]), $[CyP)_4PPh_2][OTf]$ (**4.3b**[OTf]), $[Ph_2MeP\text{-}P^tBu\text{-}P^tBu\text{-}P^tBuMe][OTf]$

(**5.1c**[OTf]), [(^{t}BuP)$_2$(PMe$_2$)$_2$][OTf]$_2$ (**5.3**[OTf]), [MeP(^{t}BuP)$_2$P^{t}BuMe][OTf] (**5.7**[OTf]), [Ph$_3$P-PMe-PMe-PPh$_3$][OTf]$_2$ (**7.2b**[OTf]$_2$), and [Me$_3$P-PMe-PMe-PMe$_3$][OTf]$_2$ (**7.4b**[OTf]) were only simulated at 101.3 MHz. Simulations were carried out by Dr. Michael D. Lumsden at the Alantic Region Magnetic Resonance Centre (Dalhousie University). Large $^1J_{PP}$ coupling constants are given a negative value.[140] For cyclic species, coupling constants are conveniently assigned (x, in ^xJ) according to the shortest path (in number of bonds) around the ring. Because of the complex nature of some of the ^{13}C data, which involves many ^{13}C – ^{31}P coupling constants, multiplicity assignments for spectra involving high peak densities are tentative. The phase of ^{13}C signals from DEPTQ135 experiments is indicated with a "+" (for CH and CH$_3$) or "-" (for C and CH$_2$).

Infrared spectra were collected on samples prepared as Nujol mulls on CsI plates using a Bruker Vector FT-IR spectrometer. Peaks are reported in wavenumbers (cm^{-1}) with ranked intensities in parentheses, where a value of one corresponds to the most intense peak in the spectrum. Melting points were obtained on samples sealed in glass capillaries, under dry nitrogen, by use of an Electrothermal apparatus. Chemical analyses were performed by Canadian Microanalytical Services Ltd., Delta, British Columbia, Canada or by Desert Analytics, Tucson, Arizona, USA.

Unless otherwise stated, crystals for single crystal X-ray diffraction studies were obtained by vapor diffusion at -25 °C (glove box freezer) or room temperature by dissolving the sample (0.05 to 0.10 g) with a minimal amount of Solvent A (1-2 mL) in a 5 mL vial which was placed within a capped 20 mL vial containing ~ 5 mL of Solvent B. Solvents are reported for individual samples in the form A/B. After deposition of crystals, the solvent was carefully removed using a pipette and the crystals were coated with paratone oil. Single crystal X-ray diffraction data was collected using a Bruker AXS P4/SMART 1000 diffractometer. All measurements were made with graphite monochromated Mo-Kα radiation (0.71073 Å). The data was reduced (SAINT)[141] and corrected for absorption (SADABS)[142] and were corrected for Lorentz and polarization effects. The structures were solved by direct methods and expanded using Fourier techniques. Full matrix least squares refinement was carried out on F^2 data using the program SHELX97.[143] All crystallographic data collection and refinement was performed

by Dr. Andreas Decken at the University of New Brunswick. Where applicable, CCDC deposition numbers are indicated.

9.2 Preparation and Characterization of Compounds

(CyP)$_3$, 2.1b

Previously prepared by Baudler *et al.* by an alternate method.[20] A 1 M solution of Me_3P in hexane (0.202 mL, 0.202 mmol) was added to a solution of [(CyP)$_3$PCyMe][OTf] (**3.6b**[OTf], 0.104 g, 0.168 mmol) in CH_2Cl_2 (3 mL). After stirring overnight, volatiles were removed *in vacuo* and the resulting mixture was extracted into benzene (3 mL), and filtered through 1 inch of silica (packed into a pipette) to remove ionic materials. Washing the column with another 1.5 mL of benzene and pumping to dryness afforded **4b** with less than 2 % of $(CyP)_4$ as impurity.

Yield: 0.025 g (0.073 mmol, 43 %);

$^{31}P\{^1H\}$ NMR (101.3 MHz, CH_2Cl_2, 298 K): A_2B spin system centered at -140 ppm.[20]

[(^{t}BuP)$_2$P^{t}BuMe][OTf], 2.2a[OTf]

MeOTf (0.080 mL, 0.71 mmol) was added dropwise to a solution of (^{t}BuP)$_3$ (0.096 g, 0.36 mmol) in fluorobenzene (4 mL). The reaction mixture was filtered after 15 minutes. Slow diffusion of hexane vapors into the filtrate at -25 °C gave colorless crystals suitable for X-ray diffraction. Crystals not submitted for X-ray analysis were washed with hexane (2 x 1 mL), and dried in vacuo.

Yield: 0.14 g (0.32 mmol, 87 %);

M.p. 121-125 °C;

Elemental analysis (%) calcd for $C_{14}H_{30}F_3O_3P_3S$: C 39.3, H 7.1; found: C 39.5, H 7.0;

$^{31}P\{^1H\}$ NMR (101.3 MHz, $CDCl_3$, 298 K): AMX spin system, δA = -110.3 ppm, δM = -50.8 ppm, δX = -20.4 ppm, $^1J_{AM}$ = -123 Hz, $^1J_{AX}$ = -334 Hz, $^1J_{MX}$ = -317 Hz;

^1H NMR (500.1 MHz, $CDCl_3$, 298 K): δ = 2.36 ppm (dd, J_{PH} = 13 Hz, J_{PH} = 8 Hz, 3H), 1.62 ppm (d, $^3J_{PH}$ = 22 Hz, 9H), 1.43 ppm (d, $^3J_{PH}$ = 17 Hz, 9H), 1.35 ppm (d, $^3J_{PH}$ = 17 Hz, 9H);

^{13}C NMR (125.8 MHz, $CDCl_3$, 298 K): δ = 39.6 ppm (ddd, J_{PC} = 3 Hz, J_{PC} = 9 Hz, J_{PC} = 13 Hz), 35.0 ppm (ddd, J_{PC} = 7 Hz, J_{PC} = 13 Hz, J_{PC} = 51 Hz), 34.1 ppm (ddd, J_{PC} = 5 Hz, J_{PC} = 13 Hz, J_{PC} = 45 Hz), 31.8 ppm (ddd, J_{PC} = 4 Hz, J_{PC} = 6 Hz, J_{PC} = 17 Hz), 30.6 ppm (ddd, J_{PC} = 3 Hz, J_{PC} = 5 Hz, J_{PC} = 17 Hz), 28.8 ppm (m), 7.9 ppm (m);
FT-IR (nujol, ranked intensties): ν = 1399 (9), 1260 (1), 1151 (2), 1030 (4), 904 (5), 800 (10), 751 (8), 638 (3), 572 (7), 516 (6) cm^{-1};
Crystal Data: $C_{14}H_{30}F_3O_3P_3S$; colorless, plate, crystal size 0.40 x 0.40 x 0.10 mm; monoclinic, space group $P2_1/n$, a = 13.6318(9) Å, b = 10.5918(7) Å, c = 15.487(1) Å, β = 104.084(1)°, V = 2168.9(2) $Å^3$, Z = 4, μ = 0. 405 mm^{-1}; $2\theta_{max}$ = 53.8°, collected (independent) reflections = 14573 (4869), R_{int} = 0.0213; 337 refined parameters, R_1 = 0.0487, wR_2 = 0.1056 for all data, max/min residual electron density = 0.646/-0.476 $eÅ^{-3}$;
CCDC- 271727

Larger quantities of spectroscopically pure, crystalline, **2.2a[OTf]** have been prepared by the following method: MeOTf (0.42 mL) was added to a solution of (^{t}BuP)$_3$ (0.500 g) in CH_2Cl_2 (8 mL). After stirring 10 minutes, hexane (15 mL) was added and the resulting mixture was put in the freezer (-25 °C) overnight. Decanting solvents, washing the precipitate with hexane (2 x 1.5 mL) and drying in vacuoo afforded 0.77 g (95 %) of **2.2a[OTf]**.

[(CyP)$_2$PCyMe][OTf], 2.2b[OTf]

MeOTf (0.009 mL, 0.079) was added to (CyP)$_3$ (0.025 g, 0.073 mmol) in CH_2Cl_2 (1.5 mL). After stirring for 1.5 hours, $^{31}P\{^1H\}$ NMR of the colorless solution shows **2.2b**[OTf], along with approximately equal amounts of [(CyP)$_3$PCyMe][OTf] (**3.6b**[OTf]), and some minor unassigned multiplets at -10 ppm and 55 ppm.
$^{31}P\{^1H\}$ NMR (101.3 MHz, $CDCl_3$, 298 K): AMX spin system, δA = -156 ppm, δM = -129 ppm, δX = -46 ppm, $^1J_{AM}$ = -97 Hz, $^1J_{AX}$ = -292 Hz, $^1J_{MX}$ = -292 Hz.

H^{t}BuP-P^{t}Bu-P^{t}BuCl, 2.3

Previously observed by Baudler *et al.* by an alternate method.[19] A 2 M solution of HCl in Et_2O (0.38 mL, 0.72 mmol) was added to a solution of (^{t}BuP)$_3$ (0.20 g, 0.76 mmol) in CH_2Cl_2 (5 mL) at -80 °C. The mixture was allowed to warm slowly to room temperature and was analyzed by $^{31}P\{^1H\}$ and ^{31}P NMR spectroscopy, demonstrating virtually quantitative formation of **2.3**.[19]

[(^{t}BuP)$_3$P^{t}BuMe][OTf], 3.6a[OTf]

MeOTf (0.090 mL, 0.79 mmol) was added to a solution of (^{t}BuP)$_4$ (0.14 g, 0.40 mmol) in fluorobenzene (3 mL). Stirring was stopped after 1 hour, and hexane was added dropwise, with periodic agitation, until the point where it seemed the precipitate would not likely go back into solution if more hexane was added. This saturated fluorobenzene/hexane solution was put in the freezer (-25 °C) for 40 days, giving colorless crystals suitable for X-ray diffraction. These crystals were isolated rapidly by decanting solvents, as they were found to redissolve upon warming. Crystals not submitted for X-ray analysis were washed with hexane (2 x 1 mL), and dried *in vacuuo*.
Yield: 0.10 g (0.20 mmol, 50 %);
Elemental analysis (%) calcd for $C_{14}H_{30}F_3O_3P_3S$: C 39.3, H 7.1; found: C 39.5, H 7.0;
M.p. 147-152 °C;
$^{31}P\{^1H\}$ NMR (101.3 MHz, $CDCl_3$, 298 K): AB_2X spin system, δA = -43 ppm, δB = -39 ppm, δX = 18 ppm, $^1J_{AB}$ = -152 Hz, $^1J_{BX}$ = -275 Hz, $^2J_{AX}$ = 8.8 Hz; See also **Table 3.1**;
^1H NMR (500.1 MHz, $CDCl_3$, 298 K): δ = 2.62 ppm (d, $^2J_{PH}$ = 12 Hz, 3H), 1.43 ppm (2 overlapping doublets, 18H), 1.32 ppm (d, $^3J_{PH}$ = 14 Hz, 9H);
^{13}C NMR (125.8 MHz, DEPTQ135, $CDCl_3$, 298 K): δ = 30.3 ppm (m, +), 28.8 ppm (m, +), 23.5 ppm (s, +), 5.6 ppm (d, $^1J_{PC}$ = 10 Hz, +); Low intensity multiplets of negative phase, which likely correspond to quaternary ^{13}C signals were observed at 36.1 and 31.7 ppm;
FT-IR (nujol, ranked intensties): ν = 1282 (3), 1250 (4), 1225 (8), 1154 (5), 1030 (2), 844 (11), 801 (10), 756 (12), 637 (1), 572 (7), 517 (6), 394 (9) cm^{-1};

Crystal Data: $C_{18}H_{39}F_3O_3P_4S$; colorless, plate, crystal size 0.30 x 0.10 x 0.01 mm; orthorhombic, space group *Pna2₁*, a = 17.498(9) Å, b = 13.694(7) Å, c = 11.349(6) Å, V = 2719(2) Å^3, Z = 4, μ = 0.391 mm^{-1}; $2\theta_{max}$ = 54.1°, collected (independent) reflections = 17506 (5729), R_{int} = 0.0677; 275 refined parameters, R_1 = 0.1024, wR_2 = 0.0966 for all data, max/min residual electron density = 0.502/-0.292 eÅ^{-3}.

CCDC-622978

[(CyP)$_3$PCyMe][OTf], 3.6b[OTf]

MeOTf (0.095 mL, 0.84 mmol) was added dropwise to a mixture of $(CyP)_4$ (0.25 g, 0.55 mmol) in CH_2Cl_2 (5 mL). The reaction mixture was filtered after 90 minutes and removal of the solvent *in vacuo* gave a white solid that was recrystallized over three days at –25 °C by vapor diffusion with fluorobenzene/hexane.

Yield: 0.15 g (0.23 mmol, 43 %);

M.p. 175-177 °C;

Elemental analysis (%) calcd for $C_{26}H_{47}F_3O_3P_4S$: C 50.3, H 7.6; found: C 50.4, H 7.3;

$^{31}P\{^1H\}$ NMR (202.6 MHz, $CDCl_3$, 298 K): A_2MX spin system, δA = -70 ppm, δM = -56 ppm, δX = 10 ppm, $^1J_{AM}$ = -122 Hz, $^1J_{AX}$ = -230 Hz, $^2J_{MX}$ = -17 Hz; See also **Table 3.1**;

^1H NMR (500.1 MHz, $CDCl_3$, 298 K): δ = 2.59 ppm (m, 1H) 2.41 (m, 2H), 2.40 ppm (d, $^2J_{PH}$ = 12 Hz, 3H), 2.05 ppm (m, 2H), 2.0 –1.7 ppm (m, 19H), 1.5 – 1.1 ppm (m, 20H);

^{13}C NMR (125.8 MHz, DEPTQ135, $CDCl_3$, 298 K): 38.8 ppm (m, +), 37.3 ppm (m, +), 35.0 ppm (m, +), 32.3 ppm (m, -), 30.0 ppm (m, -), 28.4 ppm (m, -), 26.7 ppm (s, -), 26.6 ppm (m, -), 26.3 ppm (m, -), 25.9 (m, -), 25.6 ppm (s, -), 25.5 ppm (s, -), 25.4 ppm (s, -), 25.1 (s, -), 3.6 (d, $^1J_{PC}$ 15 Hz, +);

FT-IR (nujol, ranked intensties): ν = 1284 (4), 1246 (1), 1158 (5), 1083 (3), 926 (9), 883 (8), 754 (10), 636 (2), 572 (7), 527 (6) cm^{-1};

Crystals suitable for X-ray diffraction were obtained by vapor diffusion with fluorobenzene/hexane at room temperature;

Crystal Data: $C_{26}H_{47}F_3O_3P_4S$; colorless parallelepiped, crystal size 0.275 x 0.20 x 0.175 mm; Triclinic, space group *P-1*, a = 11.4946(7) Å, b = 11.5640(7) Å, c = 14.0822(9) Å, α = 110.984(1)°, β = 102.476(1)°, γ = 106.868(1)°, V = 1561.62(17) Å^3, Z = 2, μ = 0.352

mm^{-1}; $2\theta_{max}$ = 52.2°, collected (independent) reflections = 10965 (6795), R_{int} = 0.0195; 522 refined parameters, R_1 = 0.0475, wR_2 = 0.0964 for all data, max/min residual electron density = 0.491/-0.247 $eÅ^{-3}$.

CCDC- 271728

[(^{t}BuP)$_3$P^{t}BuH][OTf], 3.7a[OTf]

HOTf (0.014 mL, 0.16 mmol) was added to a solution of (^{t}BuP)$_4$ (0.046 g, 0.14 mmol) in CH_2Cl_2 (2 mL). After stirring 1 hour, the reaction mixture was pumped to dryness, and the resulting precipitate was recrystallized over 10 days at room temperature by vapor diffusion with fluourbenzene/Et_2O. Crystals not submitted for X-ray diffraction were washed with hexane (2 x 1 mL), and dried *in vacuo*.

Yield: 0.045 g (0.090 mmol, 64%);

M.p. 106 – 110 °C;

$^{31}P\{^1H\}$ NMR (101.3 MHz, CH_2Cl_2, 200 K): A_2BX spin system; δA = -57 ppm, δB = -55 ppm, δX = -32 ppm, $^1J_{AB}$ = -156 Hz, $^1J_{AX}$ = -260 Hz, $^2J_{BX}$ = 12 Hz; See also **Table 3.1**;

$^{31}P\{^1H\}$ NMR (202.5 MHz, $CDCl_3$, 298 K): -29 ppm (m), -52 (m);

^1H NMR (500.1 MHz, $CDCl_3$, 298 K): 7.84 ppm (d, $^1J_{PH}$ = 452 Hz), 1.40 (broad s); peaks are broad and integrations are unreliable at room temperature;

^{13}C NMR (125.8 MHz, DEPTQ135, $CDCl_3$, 298 K): 28.5 ppm (broad s, +), 27.5 ppm (broad s, +), 24.0 ppm (broad s, +);

FT-IR (nujol, ranked intensties): ν = 1282 (3), 1250 (4), 1225 (8), 1154 (5), 1030 (2), 844 (11), 801 (10), 756 (12), 637 (1), 572 (7), 517 (6), 394 (9) cm^{-1};

Crystal Data: $C_{17}H_{37}F_3O_3P_4S$; colorless, irregular, crystal size 0.425 x 0.35 x 0.125 mm; Monoclinic, space group $P2_1/n$, a = 13.773(10) Å, b = 12.781(9) Å, c = 15.071(10) Å, β = 98.354(12)°, V = 2625(3) $Å^3$, Z = 4, μ = 0.403 mm^{-1}; $2\theta_{max}$ = 53.5°, collected (independent) reflections = 17562 (5889), R_{int} = 0.0447; 401 refined parameters, R_1 = 0.0760, wR_2 = 0.0962 for all data, max/min residual electron density = 0.361/-0.285 $eÅ^{-3}$;

CCDC-622977

3.7a[OTf] was also observed by $^{31}P\{^{1}H\}$ NMR spectroscopy as the exclusive product from the addition of HOTf (0.047 mL, 0.53 mmol) to (^{t}BuP)$_3$ (0.128 g, 0.484 mmol) in CH_2Cl_2 (5 mL).

[(CyP)$_3$PCyH][OTf], 3.7b[OTf]

HOTf (0.025 mL, 0.23 mmol) was added to mixture of (CyP)$_4$ (0.100 g, 0.22 mmol) in $CDCl_3$ (3 mL). Upon stirring for 2 minutes all (CyP)$_4$ was dissolved and after another 20 minutes hexane (5 mL) was added. The resulting solution was then pumped to dryness.

Yield: 0.107 g (0.176 mmol, 80%);

D.p. 73 – 75 °C;

$^{31}P\{^{1}H\}$ NMR (101.3 MHz, CH_2Cl_2, 200 K): A_2MX spin system; δA = -74 ppm, δM = -64 ppm, δX = -23 ppm, $^{1}J_{AM}$ = -126 Hz, $^{1}J_{AX}$ = -233 Hz, $^{2}J_{MX}$ = 16 Hz; See also **Table 3.1**;

$^{31}P\{^{1}H\}$ NMR (202.5 MHz, $CDCl_3$, 298 K): A_2MX spin system; δA = -71 ppm, δM = -64 ppm, δX = -27 ppm;

^{31}P NMR (202.5 MHz, $CDCl_3$, 298 K): A_2MXZ spin system (Z = ^{1}H); δA = -71 ppm, δM = -64 ppm, δX = -27 ppm, $^{1}J_{XZ}$ = $^{1}J_{PH}$ = 461 Hz; $^{1}J_{PH}$ was determined manually.

^{1}H NMR (500.1 MHz, $CDCl_3$, 298 K): 7.71 ppm (d, $^{1}J_{PH}$ = 464 Hz), 2.63 ppm (m), 1.88 ppm (m), 1.37 (m); peaks are broad and integrations are unreliable at room temperature;

^{13}C NMR (125.8 MHz, DEPTQ135, $CDCl_3$, 298 K): 37.5 ppm (broad, +), 34.5 ppm (broad, +), 30.6 ppm (broad, -), 29.3 ppm (broad, -), 27.1 ppm (broad, -), 26.2 ppm (broad, -), 25.4 ppm (broad, -);

FT-IR (nujol, ranked intensties): ν = 1264 (3), 1185 (1), 1020 (8), 996 (6), 849 (9), 814 (10), 631 (2), 551 (7), 511 (5), 440 (4) cm^{-1}.

[(^{t}BuP)$_3$PMe$_2$][OTf], 3.8[OTf]

A solution of PMe_2Cl (0.044 mL, 0.55 mmol) and TMSOTf (0.10 mL, 0.67 mmol) in CH_2Cl_2 (3 mL) was added dropwise to a solution of (^{t}BuP)$_3$ (0.098g, 0.37 mmol) in CH_2Cl_2 (3 mL). After stirring for 45 minutes, the solvent was removed *in vacuo*

and the white solid was washed with hexane (2 x 4 mL). The product was recrystallized over 5 days by vapor diffusion with fluorobenzene/hexane, giving X-ray quality crystals. Crystals not submitted for X-ray analysis were washed with hexane (2 x 1 mL), and dried *in vacuuo*.

Yield: 0.095 g (0.20 mmol, 54 %);

M.p. 112-114 °C;

Elemental analysis (%) calcd for $C_{15}H_{33}F_3O_3P_4S$: C 38.0, H 7.0; found: C 38.5, H 6.9;

$^{31}P\{^1H\}$ NMR (101.3 MHz, $CDCl_3$, 298 K): AB_2X spin system, δA = -28 ppm, δB = -24 ppm, δX = -2 ppm, $^1J_{AB}$ = -143 Hz, $^1J_{BX}$ = -251 Hz, $^2J_{AX}$ = 28 Hz; See also **Table 3.1**;

^1H NMR (500.1 MHz, $CDCl_3$, 298 K): 2.66 ppm (d, $^2J_{PH}$ = 14 Hz, 3H), 2.37 ppm (dt, J_{PH} = 13 Hz, J_{PH} = 8 Hz, 3H), 1.45 ppm (m, 18H), 1.34 ppm (d, $^3J_{PH}$ = 14 Hz, 9H);

^{13}C NMR (125.8 MHz, $CDCl_3$, 298 K): 36.2 ppm (m), 30.8 ppm (m) 30.4 (m), 29.2 ppm (dt, J_{PC} = 15 Hz, J_{PC} = 5 Hz), 20.3 ppm (m), 11.2 ppm (d, $^1J_{PC}$ 15 Hz);

FT-IR (nujol, ranked intensties): ν = 1304 (6), 1267 (2), 1224 (7), 1155 (3), 1032 (4), 957 (8), 914 (9), 638 (1), 573 (10), 517 (5) cm^{-1};

Crystal Data: $C_{15}H_{33}F_3O_3P_4S$; colorless parallelepiped, crystal size 0.40 x 0.275 x 0.25 mm; Tetragonal, space group $I4_1/a$, a = 25.6452(11) Å, b = 25.6452(11) Å, c = 14.7549(8) Å, V = 9703.9(8) $Å^3$, Z = 16, μ = 0.432 mm^{-1}; $2\theta_{max}$ = 54.7°, collected (independent) reflections = 33323 (5547), R_{int} = 0.0293; 367 refined parameters, R_1 = 0.0445, wR_2 = 0.0809 for all data, max/min residual electron density = 0.414/-0.237 $eÅ^{-3}$.

CCDC- 271729

Reactions of Cyclotriphosphinophosphonium Triflate and Me_3P

General procedure: To 2 mL of a 0.046 M solution of cyclotriphosphinophosphonium triflate in CH_2Cl_2 was added a 1 M hexane solution of Me_3P (0.101 mL, 0.101 mmol), dropwise. The reaction mixtures were studied by $^{31}P\{^1H\}$ NMR. Specific reactions and products are detailed in **Chapter 3.5.**

[(PhP)$_4$PPhMe][OTf], 4.2a[OTf]

MeOTf (0.038 mL, 0.33 mmol), was added to a solution of $(PhP)_5$ (0.100 g, 0.19 mmol) in benzene (3 mL). After stirring 5 minutes, hexane (2 mL) was added giving an oily precipitate, which was left at room temperature to settle overnight. The solvents were decanted from the settled precipitate, which was then crystallized as **4.2a**[OTf]•1.5 C_6H_6 over 24 hours by vapor diffusion with $CHCl_3/Et_2O$ at room temperature. Crystals not sent for X-ray analysis were washed with Et_2O (2 x 1 mL) and dried *in vacuo*. As indicated by ^{1}H NMR, the benzene is only partially removed by vacuum.

Yield: 0.107 g, (0.139 mmol, 73% ; based on **4.2a**[OTf]•0.83 C_6H_6 as determined by ^{1}H NMR integrations);

D.p. 97 – 107 °C;

^{31}P{^{1}H} NMR (101.3 MHz, $CDCl_3$, 298 K): ABCDX spin system; δA = -35.7 ppm, δB = -33.7 ppm, δC = -31.8 ppm, δD = -24.6 ppm, δX = 22.2 ppm, $^1J_{AB}$ = -162 Hz, $^1J_{AX}$ = -328 Hz, $^1J_{BC}$ = -166 Hz, $^1J_{CD}$ = -193 Hz, $^1J_{DX}$ = -315 Hz, $^2J_{AC}$ = 71 Hz, $^2J_{AD}$ = -14 Hz, $^2J_{BD}$ = 58 Hz, $^2J_{BX}$ = 30 Hz, $^2J_{CX}$ = 17 Hz; See also **Table 4.1**;

^{1}H NMR (500.1 MHz, $CDCl_3$, 298 K): δ = 7.96 ppm ($^3J_{HH}$ = 7 Hz, $^3J_{HH}$ = 7 Hz, 2H), 7.88 ppm (m, 2H), 7.72 ppm (m, 2H), 7.60 – 7.40 ppm (m, 17H), 7.29 ppm (m, 2H), 2.23 ppm (dd, J_{PH} = 12 Hz, J_{PH} = 7.5 Hz, 3H);

^{13}C NMR (125.8 MHz, DEPTQ135, $CDCl_3$, 298 K): δ = 135.5 ppm (m, +), 134.9 ppm (m, +), 134.4 – 133.8 (m, +), 132.9 (m, +), 131.9 (s, +), 131.5 ppm (s, +), 131.3 ppm (s, +), 130.4 (m, +), 130.0 ppm (s, +), 129.9 (s, +), 129.8 ppm (s, +), 129.7 (m, +), 9.4 ppm (m, +);

FT-IR (nujol, ranked intensities): 1261 (1), 1219 (8), 1146 (7), 1029 (6), 996 (12), 903 (13), 805 (9), 752 (4), 740 (5), 689 (2), 635 (3), 570 (11), 515 (10), 456 (14) cm^{-1};

4.2a[OTf] was also observed by ^{31}P{^{1}H} NMR spectroscopy as the exclusive product from the addition of MeOTf (0.007 mL, 0.064 mmol) to $(PhP)_4$ (0.014 g, 0.032 mmol) in CH_2Cl_2 (1 mL).

[(CyP)$_4$PMe$_2$][OTf], 4.3a[OTf]

TMSOTf (0.075 mL, 0.42 mmol) was added to a solution of Me_2PCl (0.026 mL, 0.33 mmol) in CH_2Cl_2 (3 mL). This solution was then added to a mixture of $(PCy)_4$ (0.126 g, 0.28 mmol) in CH_2Cl_2 (3 mL) and was stirred for 4 days. After filtering, the volatiles were removed *in vacuo*. Washing with hexane (2 x 3 mL portions) afforded a white solid. Recrystallization by vapor diffusion with fluorobenzene/hexane at room temperature afforded X-ray quality crystals. Crystals not submitted for X-ray analysis were washed with hexane (2 x 1 mL), and dried *in vacuo*.

Yield: 0.048 g (0.072 mmol, 26%);

M.p. 159 – 161 °C;

$^{31}P\{^1H\}$ NMR (101.3 MHz, $CDCl_3$, 298 K): AA'BB'X spin system; δA = -14 ppm, δB = -8 ppm, δX = 42 ppm, $^1J_{AA'}$ = -255 Hz, $^1J_{AB} = {}^1J_{A'B'}$ = -264 Hz, $^1J_{BX} = {}^1J_{B'X}$ = -332 Hz, $^2J_{AX} = {}^2J_{A'X}$ = 9 Hz, $^2J_{AB'} = {}^2J_{A'B}$ = 0 Hz, $^2J_{BB'}$ = -21 Hz; See also **Table 4.2**;

^1H NMR (500.1 MHz, $CDCl_3$, 298 K): 2.35 ppm (m, 8H), 2.15 ppm (m, 2H), 2.00 ppm (m, 6H), 1.87 ppm (m, 10H), 1.75 ppm (m, 4H), 1.46 ppm (m, 8H), 1.30 ppm (m, 12H);

^{13}C NMR (125.8 MHz, DEPTQ135, $CDCl_3$, 298 K): 36.3 ppm (m, +), 34.5 ppm (m, +), 33.6 ppm (m, -), 33.0 ppm (m, -), 32.5 ppm (m, -), 32.2 ppm (m, -), 27.0 ppm (m, -), 26.8 ppm (m, -), 26.5 ppm (m, -), 25.6 ppm (s, -), 25.3 ppm (s, -), 12.8 ppm (m, +);

FT-IR (nujol, ranked intensties): ν = 1309 (11), 1256 (1), 1220 (5), 1147 (4), 1031 (3), 958 (8), 906 (9), 803 (10), 635 (2), 571 (7), 516 (6) cm^{-1};

Crystal Data: $C_{27}H_{50}F_3O_3P_5S$; colorless parallelepiped, crystal size 0.40 x 0.275 x 0.25 mm; Monoclinic, space group $P2_1/c$, a = 20.0981(15) Å, b = 34.842(3) Å, c = 9.6712(7) Å, β = 94.697(1)°, V = 6749.7(9) $Å^3$, Z = 8, μ = 0.376 mm^{-1}; $2\theta_{max}$ = 53.5°, collected (independent) reflections = 45853 (15082), R_{int} = 0.0374; 707 refined parameters, R_1 = 0.0848, wR_2 = 0.1389 for all data, max/min residual electron density = 0.997/-0.416 $eÅ^{-3}$.

[(CyP)$_4$PPh$_2$][OTf], 4.3b[OTf]

A solution of TMSOTf (0.074 mL, 0.41 mmol) and Ph_2PCl (0.066 mL, 0.37 mmol) in CH_2Cl_2 (2 mL) was added to $(PCy)_4$ (0.084 g, 0.18 mmol) in CH_2Cl_2 (2 mL). Stirring vigorously for 20 minutes afforded a solution, which was analyzed by $^{31}P\{^1H\}$

NMR spectroscopy, showing mostly **4.3b**[OTf]. Small amounts of what is assigned to $[(PCy)_3(PPh_2)][OTf]$ (**4.4**[OTf], AB_2X spin system: δA = -54 ppm, δB = -44 ppm, δX = -2 ppm, $^1J_{AB}$ = -123 Hz, $^1J_{BX}$ = -233 Hz, $^2J_{AX}$ = 14 Hz) were present along with excess Ph_2PCl (82 ppm), and a minor unidentified peak at 46 ppm. Relative amounts of **4.3b**:**4.4** were 89:11 (from $^{31}P\{^1H\}$ simulation).

$^{31}P\{^1H\}$ NMR (101.3 MHz, CH_2Cl_2, 298 K): AA'BB'X spin system; δA = -15 ppm, δB = -2 ppm, δX = 52 ppm, $^1J_{AA'}$ = -247 Hz, $^1J_{AB} = {}^1J_{A'B'}$ = -262 Hz, $^1J_{BX} = {}^1J_{B'X}$ = -352 Hz, $^2J_{AX} = {}^2J_{A'X}$ = 2 Hz, $^2J_{AB'} = {}^2J_{A'B}$ = 0 Hz, $^2J_{BB'}$ = -21 Hz; See also **Table 4.2**;

[(PhP)$_4$PPh$_2$][OTf], 4.3c[OTf]

A solution of Ph_2PCl (0.045 mL, 0.25 mmol) and TMSOTf (0.060 mL, 0.30 mmol) in CH_2Cl_2 (2 mL), was added to $(PhP)_5$ (0.100 g, 0.185 mmol) in CH_2Cl_2 (2 mL). The solvent was removed in vacuo and the solid washed with hexane (2 x 4 mL);

Yield: 0.123 g (0.16 mmol, 87 %).

D.p. 65-75 °C;

Elemental analysis (%) calcd for $C_{37}H_{30}F_3O_3P_5S$: C 58.0, H 3.9, P 20.2; found: C 57.4, H 3.9, P 20.4;

$^{31}P\{^1H\}$ NMR (101.3 MHz, $CDCl_3$, 298 K): AA'BB'X spin system; δA = -42 ppm, δB = -36 ppm, δX = 22 ppm, $^1J_{AA'}$ = -142 Hz, $^1J_{AB} = {}^1J_{A'B'}$ = -160 Hz, $^1J_{BX} = {}^1J_{B'X}$ = -325 Hz, $^2J_{AX} = {}^2J_{A'X}$ = 28 Hz, $^2J_{AB'} = {}^2J_{A'B}$ = 79 Hz, $^2J_{BB'}$ = -14 Hz; See also **Table 4.2**;

^1H NMR (500.1 MHz, $CDCl_3$, 298 K): δ = 7.92 ppm (m, 4H), 7.69 ppm (m, 2H), 7.47 ppm (m, 16H), 7.28 ppm (m, 8H);

^{13}C NMR (125.8 MHz, DEPTQ135, $CDCl_3$, 298 K): δ = 135.9 ppm (m, +), 135.0 ppm (s, +), 134.1 ppm (m, +), 132.5 ppm (s, +), 131.7 ppm (s, +), 130.2 ppm(s, +), 130.0 ppm (s, +), 129.9 ppm (m, +);

FT-IR (nujol, ranked intensities): 1312 (11), 1263 (1), 1146 (6), 1093 (8), 1029 (2), 997 (9), 843 (7), 740 (3), 687 (5), 635 (4), 570 (12), 517 (10) cm^{-1};

Crystals for X-ray diffraction were grown by vapor diffusion with CH_2Cl_2/Et_2O;

Crystal Data: $C_{37}H_{30}F_3O_3P_5S$; colorless rod, crystal size 0.60 x 0.20 x 0.10 mm; Monoclinic, space group $P2_1/c$, a = 10.6004(6) Å, b = 16.7110(8) Å, c = 20.601(1) Å, β =

92.255(1)°, V = 3550.8(3) Å^3, Z = 4, μ = 0.369 mm^{-1}; $2\theta_{max}$ = 53.4°, collected (independent) reflections = 23629 (7915), R_{int} = 0.0232; 562 refined parameters, R_1 = 0.0502, wR_2 = 0.0930 for all data, max/min residual electron density = 0.432/-0.421 eÅ^{-3}; **CCDC-257691**

4.3c[OTf] was also observed by $^{31}P\{^1H\}$ NMR spectroscopy as the exclusive product in from the addition of a solution of Ph_2PCl (0.019 mL, 0.106 mmol) and TMSOTf (0.023 mL, 0.127 mmol) in CH_2Cl_2 (3 mL) to solid $(PhP)_4$ (0.045 g, 0.104 mmol).

[(PhP)$_4$PMe$_2$][OTf], 4.3d[OTf]

Me_2PCl (0.014 mL, 0.185 mmol) was added to TMSOTf (0.040 mL, 0.22 mmol) in CH_2Cl_2 (2 mL). This solution was added to solid $(PhP)_5$ (0.050 g, 0.093 mmol). Filtration and slow diffusion of ether vapor into the solution at –25 °C gave a precipitate;
Yield 0.027 g (0.042 mmol, 45 %);
D.p. 142 – 145 °C;
Elemental analysis (%) calcd for $C_{27}H_{26}F_3O_3P_5S$: C 50.5, H 4.1; found: C 49.4, H 3.6;
$^{31}P\{^1H\}$ NMR (101.3 MHz, $CDCl_3$, 298 K): AA'BB'X spin system; δA = -32 ppm, δB = -26 ppm, δX = 27 ppm, $^1J_{BB'}$ = -186 Hz, $^1J_{AB} = {}^1J_{A'B'}$ = -192 Hz, $^1J_{AX} = {}^1J_{A'X}$ = -315 Hz, $^2J_{BX} = {}^2J_{B'X}$ = 24 Hz, $^2J_{AB'} = {}^2J_{A'B}$ = 50 Hz, $^2J_{AA'}$ = -15 Hz; See also **Table 4.2**;
^1H NMR (ppm, 500.1 MHz, $CDCl_3$, 298 K): δ = 7.86 ppm (m, 8H), 7.63 ppm (m, 2H) 7.55 ppm (m, 4H), 7.49 ppm (m, 6H), 1.86 ppm (m, 6H);
^{13}C NMR (125.8 MHz, DEPTQ135, $CDCl_3$, 298 K): δ = 135.3 ppm (m, +), 133.8 ppm (m, +), 132.5 ppm (s, +), 131.1 ppm (s, +), 130.3 ppm (s, +), 129.8 ppm (s, +), 10.4 ppm (m, +);
FT-IR (nujol, ranked intensities): 1304 (8), 1288 (1), 1247 (2), 1150 (7), 1032 (3), 958 (10), 918 (9), 733 (4), 691 (5), 638 (6), 572 (13), 516 (12), 465 (11) cm^{-1};
Crystals suitable for X-ray diffraction were obtained from the addition of Et_2O (1.5 mL) to a solution of 0.26 g of **4.3d**[OTf] in 1.5 mL CH_2Cl_2, upon standing at room temperature for 5 days (Yield 0.19 g);

Crystal Data: $C_{27}H_{26}F_3O_3P_5S$; colorless, irregular, crystal size 0.375 x 0.35 x 0.15 mm; Triclinic, space group *P-1*, a = 9.9468(12) Å, b = 12.7582(15) Å, c = 12.9535(15) Å, α = 109.358(2)°, β = 97.345(2)°, γ = 104.076(2)°, V = 1464.8(3) Å^3, Z = 2, μ = 0.432 mm^{-1}; $2\theta_{max}$ = 54.2°, collected (independent) reflections = 9520 (9520); 363 refined parameters, R_1 = 0.0581, wR_2 = 0.0647 for all data, max/min residual electron density = 0.533/-0.499 eÅ^{-3};

4.3d[OTf] was also observed by $^{31}P\{^1H\}$ NMR spectroscopy as the exclusive product in from the addition of a solution of Me_2PCl (0.016 mL, 0.202 mmol) and TMSOTf (0.046 mL, 0.254 mmol) in CH_2Cl_2 (4 mL) to solid $(PhP)_4$ (0.087 g, 0.202 mmol).

[^{n}Pr$_3$P-P^{t}Bu-P^{t}Bu-P^{t}BuMe][OTf], 5.1a[OTf]

^{n}Pr$_3$P (0.273 mL, ~0.14 mmol) was added to a solution of [(^{t}BuP)$_3$Me][OTf] (**2.2a**[OTf], 0.039 g, 0.091 mmol) in CH_2Cl_2 (1.5 mL). The reaction was complete within 5 minutes, and the mixture was analyzed by low temperature $^{31}P\{^1H\}$ NMR spectroscopy.

$^{31}P\{^1H\}$ NMR (101.3 MHz, CH_2Cl_2, 193 K): AMNX spin system; δA = -34 ppm, δM = -19 ppm, δN = -11 ppm, δX = 27 ppm, $^1J_{AM}$ = -345 Hz, $^1J_{AN}$ = -403 Hz, $^1J_{MX}$ = -324 Hz, $^2J_{AX}$ = 75 Hz, $^2J_{MN}$ = -5 Hz, $^3J_{NX}$ = -2 Hz; See also **Table 5.2**; The spectrum also contains excess ^{n}Pr$_3$P (δ = -32 ppm), and peaks of very low intensity that could correspond to another diastereomer of **5.1a**[OTf].

[Me$_3$P-P^{t}Bu-P^{t}Bu-P^{t}BuMe][OTf], 5.1b[OTf]

Me_3P (0.138 mL, 1 M in hexane, 0.138 mmol) was added to a solution of [(^{t}BuP)$_3$Me][OTf] (**2.2a**[OTf], 0.039 g, 0.091 mmol) in CH_2Cl_2 (1.5 mL). The reaction was complete within 5 minutes, and the mixture was analyzed by low temperature $^{31}P\{^1H\}$ NMR spectroscopy.

$^{31}P\{^1H\}$ NMR (101.3 MHz, CH_2Cl_2, 193 K): A 50:50 mixture of two AMNX spin systems; *Diastereomer 1*: δA = -35 ppm, δM = -14 ppm, δN = -13 ppm, δX = 17 ppm,

$^1J_{AM}$ = -331 Hz, $^1J_{AN}$ = -399 Hz, $^1J_{MX}$ = -315 Hz, $^2J_{AX}$ = 88 Hz, $^2J_{MN}$ = -8 Hz, $^3J_{NX}$ = -1 Hz; *Diastereomer 2*: δA = -26 ppm, δM = -7 ppm, δN = 0 ppm, δX = 18 ppm, $^1J_{AM}$ = -363 Hz, $^1J_{AN}$ = -365 Hz, $^1J_{NX}$ = -397 Hz, $^2J_{AX}$ = -9 Hz, $^2J_{MN}$ = -11 Hz, $^3J_{MX}$ = 46 Hz; See also **Table 5.2**; Excess Me_3P (δ = -60 ppm) was also observed.

[PhMe$_2$P-P^{t}Bu-P^{t}Bu-P^{t}BuMe][OTf], 5.1c[OTf]

(Ph)(Me)$_2$P (0.019 mL, 0.136 mmol) was added to a solution of [(^{t}BuP)$_3$Me][OTf] (**2.2a**[OTf], 0.039 g, 0.091 mmol) in CH_2Cl_2 (1.5 mL). The solvent was removed to give a colorless oil, which was washed with hexane (1.5 mL). Et_2O (1.5 mL) was added, and the mixture was stored at -25 °C until a white solid formed. This solid was redissolved in $CDCl_3$, and analyzed by low temperature $^{31}P\{^1H\}$ NMR spectroscopy.
$^{31}P\{^1H\}$ NMR (101.3 MHz, $CDCl_3$, 213 K): A 50:50 mixture of two AMNX spin systems; *Diastereomer 1*: δA = -34 ppm, δM = -11 ppm, δN = -7 ppm, δX = 18 ppm, $^1J_{AM}$ = -401 Hz, $^1J_{AN}$ = -335 Hz, $^1J_{NX}$ = -318 Hz, $^2J_{AX}$ = 92 Hz, $^2J_{MN}$ = 1 Hz, $^3J_{MX}$ = -1 Hz; *Diastereomer 2*: δA = -24 ppm, δM = -5 ppm, δN = 4 ppm, δX = 18 ppm, $^1J_{AM}$ = -361 Hz, $^1J_{AN}$ = -362 Hz, $^1J_{NX}$ = -407 Hz, $^2J_{AX}$ = -8 Hz, $^2J_{MN}$ = -11 Hz, $^3J_{MX}$ = 44 Hz; See also **Table 5.2**.

[(^{t}BuP)$_2$(PMe$_2$)$_2$][OTf]$_2$, 5.3[OTf]$_2$

Me_2PCl (0.088 mL, 1.11 mmol) was added to a solution of [(^{t}BuP)$_3$Me][OTf] (**2.2a**[OTf], 0.234 g, 0.546 mmol) in CH_2Cl_2 (4 mL). After stirring 30 minutes, TMSOTf (0.22 mL, 1.22 mmol) was added to the reaction mixture. After another 30 minutes, Et_2O (15 mL) was added, giving a cloudy mixture which was stored at -25 °C overnight. Solvents were decanted, and CH_2Cl_2 (1 mL) was added to the remaining solid giving a solution from which a precipitate formed within 1 minute. Et_2O (8 mL) was added to further precipitation, and the precipitate was allowed to settle at -25 °C for 20 minutes before decanting solvents and dissolving the precipitate in CH_3CN (4 mL). This solution was crystallized in two equal portions by vapor diffusion with CH_3CN/Et_2O (6 days at -25 °C, and 1 day at room temperature) affording crystals suitable for X-ray diffraction.

Crystals not submitted for X-ray analysis were washed with Et_2O (3 x 1 mL), and dried *in vacuo*.

Yield: 0.082 g, (0.137 mmol, 25%);

D.p. 155 – 165 °C;

$^{31}P\{^1H\}$ NMR (101.3 MHz, CH_2Cl_2, 298 K): AA'BB' spin system; δA = 4 ppm, δB = 31 ppm, $^1J_{AA'}$ = -169 Hz, $^1J_{AB} = {}^1J_{A'B'}$ = -284 Hz, $^1J_{BB'}$ = -40 Hz, $^2J_{A'B} = {}^2J_{AB'}$ = 5 Hz;

^1H NMR (500.1 MHz, CD_3CN, 298 K): δ = 2.82 ppm (m, 6H), 2.73 ppm (m, 6H), 1.54 ppm (m, 18H);

^{13}C NMR (125.8 MHz, DEPTQ135, CD_3CN, 298 K): δ = 29.5 ppm (m, +), 13.5 ppm (m, +), 9.7 (m, +);

FT-IR (nujol, ranked intensities): 1259 (1), 1155 (3), 1031 (4), 983 (8), 930 (8), 898 (9), 758 (10), 638 (2), 573 (6), 517 (5) cm^{-1};

Crystal Data: $C_{14}H_{30}F_6O_6P_4S_2$; colorless, irregular plate, crystal size 0.40 x 0.30 x 0.025 mm; Monoclinic, space group $P2_1/c$, a = 11.385(6) Å, b = 14.133(7) Å, c = 17.412(8) Å, β = 100.007(8)°, V = 2759(2) $Å^3$, Z = 4, μ = 0.491 mm^{-1}; $2\theta_{max}$ = 53.5°, collected (independent) reflections = 18437 (6162), R_{int} = 0.0370; 299 refined parameters, R_1 = 0.0685, wR_2 = 0.0882 for all data, max/min residual electron density = 0.481/-0.343 $eÅ^{-3}$.

[MeP(tBuP)$_2$PtBuMe][OTf], 5.7[OTf]$_2$

$MePCl_2$ (0.045 mL, 0.501 mmol) was added to a solution of [(^{t}BuP)$_3$Me][OTf] (**2.2a**[OTf], 0.174 g, 0.406 mmol) in CH_2Cl_2 (3 mL). After stirring for 15 minutes, the volume of the reaction mixture was reduced to 1.5 mL and Et_2O (10 mL) was added giving a white precipitate. After storing at -25 °C for 45 minutes, solvents were decanted from the precipitate which was recrystallized by vapor diffusion with CH_2Cl_2/Et_2O (4 days at -25 °C followed by 1 day at room temperature), giving crystals that were washed with Et_2O (3 x 1 mL) and dried *in vacuo*.

Yield: 0.063 g, (0.133 mmol);

D.p. 90 - 133 °C;

$^{31}P\{^1H\}$ NMR (101.3 MHz, $CDCl_3$, 298 K): AMNX spin system; δA = -95 ppm, δM = -31 ppm, δN = -26 ppm, δX = 22 ppm, $^1J_{AN}$ = -123 Hz, $^1J_{AX}$ = -221 Hz, $^1J_{MN}$ = -145 Hz, $^1J_{MX}$ = -283 Hz, $^2J_{AM}$ = 41 Hz $^2J_{NX}$ = 19 Hz;

^1H NMR (500.1 MHz, $CDCl_3$, 298 K): δ = 2.47 ppm (d, $^2J_{PH}$ = 13 Hz, 3H), 1.80 ppm (m, 3H), 1.42 ppm (m, 18H), 1.31 (d, $^3J_{PH}$ = 15 Hz, 9H);

^{13}C NMR (125.8 MHz, DEPTQ135, $CDCl_3$, 298 K): δ = 30.5 ppm (m, +), 28.4 ppm (m, +), 24.3 ppm (s, +), 8.9 ppm (t, J_{PC} = 32 Hz, +), 3.8 ppm (d, J_{PC} = 12 Hz, +);

FT-IR (nujol, ranked intensities): 1408 (10), 1303 (11), 1265 (1), 1223 (7), 1154 (3), 1031 (4), 895 (5), 803 (6), 638 (2), 572 (9), 517 (8) cm^{-1}.

[Me_2P-PMe_2-PMe_2][OTf], 6.2a[OTf]

To a solution prepared by the addition of Me_2PCl (0.029 mL, 0.37 mmol) to TMSOTf (0.080 mL, 0.44 mmol) in CH_2Cl_2 (6 mL), was added Me_2PPMe_2 (0.054 mL, 0.37 mmol). Cystallization by vapor diffusion of ether into the reaction mixture over 4 days at -25 °C afforded X-ray quality crystals.

Yield: 0.076 g (0.23 mmol, 62 %);

D.p. 44 – 65 °C;

Elemental analysis (%) calcd for $C_7H_{18}F_3O_3P_3S$: C 25.3, H 5.5; found: C 25.2, H 5.2;

$^{31}P\{^1H\}$ NMR (101.3 MHz, $CDCl_3$, 220 K): A_2B spin system; δA = -62 ppm, δB = 12 ppm, $^1J_{AB}$ = -298 Hz;

^1H NMR (250.1 MHz, $CDCl_3$, 220 K): δ = 1.98 ppm (d, $^2J_{PH}$ = 13 Hz, 6H), 1.54 ppm (d, $^2J_{PH}$ = 18 Hz, 12H);

FT-IR (nujol, ranked intensities): 1314 (8), 1302 (7), 1260 (1), 1224 (3), 1154 (4), 1031 (2), 977 (11), 934 (12), 892 (6), 638 (5), 573 (10), 517 (9) cm^{-1};

Crystal Data: $C_7H_{18}F_3O_3P_3S$; colorless, irregular, crystal size 0.60 x 0.15 x 0.15 mm; Monoclinic, space group $P2_1/c$, a = 11.9395(8) Å, b = 11.3475(7) Å, c = 12.3165(8) Å, β = 115.818(1)°, V = 1502.1(2) $Å^3$, Z = 4, μ = 0.561 mm^{-1}; $2\theta_{max}$ = 53.5°, collected (independent) reflections = 10152 (3362), R_{int} = 0.0210; 226 refined parameters, R_1 = 0.0443, wR_2 = 0.0854 for all data, max/min residual electron density = 0.543/-0.455 $eÅ^{-3}$.

CCDC- 257962

[Ph_2P-PPh_2-PPh_2][OTf], 6.2b[OTf]

To a solution of Ph_2PCl (0.050 mL, 0.28 mmol) and TMSOTf (0.060 mL, 0.33 mmol) in fluorobenzene (1 mL) was added Ph_2PPPh_2 (0.104 g,0.28 mmol) in fluorobenzene (1 mL). Slow diffusion of ether into the filtered reaction mixture at -28 °C afforded a white solid which was washed with ether (2 x 3 mL).

Yield: 0.127 g (0.18 mmol, 64 %);

M.p. 138 - 142 °C;

Elemental analysis (%) calcd for $C_{37}H_{30}F_3O_3P_3S$: C 63.1, H 4.3; found: C 62.2, H 4.2;

$^{31}P\{^1H\}$ NMR (101.3 MHz, CH_2Cl_2, 193 K): A_2B spin system; δA = -22 ppm, δB = 18 ppm, $^1J_{AB}$ = -351 Hz

FT-IR (nujol, ranked intensities): 1264 (1), 1223 (2), 1149 (7), 1090 (11), 1030 (6), 742 (4), 691 (3), 636 (5), 570 (10), 515 (9), 450 (8) cm^{-1}.

[Me_2P-PMe_2-PPh_2][OTf], 6.2c[OTf]

To a solution of Ph_2PCl (0.033 mL, 0.19 mmol) and TMSOTf (0.040 mL, 0.22 mmol) in CH_2Cl_2 (3 mL) was added Me_2PPMe_2 (0.027 mL, 0.19 mmol). The resulting mixture was analyzed by low temperature $^{31}P\{^1H\}$ NMR spectroscopy.

$^{31}P\{^1H\}$ NMR (101.3 MHz, CH_2Cl_2, 193 K): AMX spin system; δA = -52 ppm, δM = -28 ppm, δX = 8 ppm, $^1J_{AX}$ = -331 Hz, $^1J_{MX}$ = -296 Hz, $^2J_{AM}$ = 13 Hz; **6.2a**[OTf], and Ph_2PPPh_2 (-19 ppm) were also observed in the mixture.

[Ph_2P-PMe_2-PPh_2][OTf], 6.2e[OTf]

A solution of Me_2PCl (0.029 mL, 0.37mmol) and TMSOTf (0.080 mL, 0.44 mmol) in CH_2Cl_2 (6 mL) was added to solid Ph_2PPPh_2 (0.137 g, 0.37 mmol). The mixture was pumped to dryness and the resulting oil was taken up in $CDCl_3$ and analyzed by low temperature $^{31}P\{^1H\}$ NMR spectroscopy.

$^{31}P\{^1H\}$ NMR (101.3 MHz, $CDCl_3$, 193 K): A_2B spin system; δA = -20 ppm, δB = 5 ppm, $^1J_{AB}$ = -337 Hz.

[Ph_3P-PPhCl][OTf], 7.1a[OTf]

$PhPCl_2$ (0.040 mL, 0.29 mmol) was added to a solution of Ph_3P (0.077 g, 0.29 mmol) in CH_2Cl_2 (2 mL) with stirring, followed immediately by the addition of TMSOTf (0.059 mL, 0.33 mmol). After 30 minutes, Et_2O (10 mL) was added, resulting in a white precipitate. After storing the mixture at -23 °C overnight, the solvents were decanted, and the precipitate was washed with Et_2O (2 x 2 mL). Recrystallization over 9 days by vapor diffusion with CH_2Cl_2/Et_2O at -23 °C afforded colorless crystals suitable for X-ray diffraction. Crystals not submitted for X-ray analysis were washed with Et_2O (2 x 1 mL) and dried *in vacuo*.

Yield: 0.12 g (0.23 mmol, 77%).

D.p. 114-123 °C;

$^{31}P\{^1H\}$ NMR (101.3 MHz, CH_2Cl_2, 298 K): 22 ppm (s), 55 ppm (s);

$^{31}P\{^1H\}$ NMR (101.3 MHz, CH_2Cl_2, 213 K): AB spin system, δA = 22 ppm, δB = 49 ppm, $^1J_{AB} = {}^1J_{PP}$ = 333 Hz;

FT-IR (nujol, ranked intensities): 1283 (8), 1259 (5), 1222 (13), 1149 (7), 1101 (9), 1030 (6), 995 (14), 741 (3), 687 (4), 634 (2), 570 (11), 545 (12), 510 (1), 478 (15), 305 (10) cm^{-1};

Crystal Data: $C_{25}H_{20}ClF_3O_3P_2S$; colorless, plate, crystal size 0.40 x 0.125 x 0.025 mm; Monoclinic, space group *Pn*, a = 10.0707(16) Å, b = 8.8891(15) Å, c = 14.166(2) Å, β = 104.192(3)°, V = 1229.5(3) $Å^3$, Z = 2, μ = 0.420 mm^{-1}; $2\theta_{max}$ = 53.5°, collected (independent) reflections = 8149 (4027), R_{int} = 0.0256; 396 refined parameters, R_1 = 0.0311, wR_2 = 0.0630 for all data, max/min residual electron density = 0.309/-0.176 $eÅ^{-3}$.

CCDC-605574

[Ph_3P-PPh-PPh-PPh_3][OTf]$_2$, 7.2a[OTf]$_2$

$PhPCl_2$ (1.2 mL, 8.8 mmol) and TMSOTf (3.5 mL, 19.3 mmol) were added to Ph_3P (4.62 g, 17.6 mmol) in CH_2Cl_2 (90 mL). After stirring 48 hours, conversion to **7.2a**[OTf]$_2$ was virtually complete (^{31}P NMR). The solvent volume was reduced to 30

mL, and Et_2O was added slowly with stirring until the solution became slightly cloudy (~ 10 mL Et_2O), resulting in the precipitation of a white solid. Filtration and recrystallization of the solid by slow evaporation of a CH_2Cl_2 solution, and washing with small portions of CH_2Cl_2 afforded crystalline **7.2a**$[OTf]_2$ with ~ 2 % $[Ph_3PCl][OTf]$ (^{31}P, δ = 66 ppm) as impurity; crude yield = 3.8 g. This material contained single crystals suitable for X-ray diffraction.

Pure material can be obtained by further recrystallization. Thus 1.0 g of crude **7.2a**$[OTf]_2$ was dissolved in boiling chloroform (27 mL), and the cooled solution left undisturbed at room temperature for 3 days. Decanting the solvent, washing the crystals with $CHCl_3$ (2 x 5 mL), and isolation afforded pure **7.2a**$[OTf]_2$.

Yield: 0.67 g (0.64 mmol, 56% based on $PhPCl_2$).

D.p. 216-222 °C.

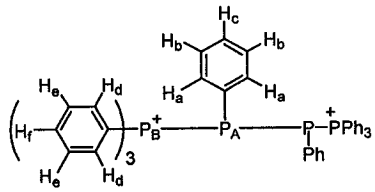

$^{31}P\{^1H\}$ NMR (101.3 MHz, CH_2Cl_2, 298 K): *Major diastereomer* (81% by ^1H NMR integration): AA'BB' spin system, δA = -33 ppm, δB = 24 ppm, $^1J_{AA'}$ = -124 Hz, $^1J_{AB}$ = $^1J_{A'B'}$ = -343 Hz, $^2J_{AB'}$ = $^2J_{A'B}$ = 69 Hz, $^3J_{BB'}$ = 51 Hz; *Minor diastereomer* (19% by ^1H NMR integration): not simulated, approx. shifts: δA = -42 ppm, δB = 22 ppm.

^1H NMR (500.1 MHz, CD_3CN, 298 K): *Major diastereomer* (81%): δ = 7.79 ppm (t, J_{HfHe} = 7 Hz, H_f, 6H), 7.58 ppm (m, H_e, 12H), 7.48 ppm (m, H_d, 12H), 7.39 ppm (t, J_{HcHb} = 7 Hz, H_c, 2H), 7.31 ppm (m, H_a, 4H), 7.12 ppm (dd, J_{HcHb} = 7 Hz, J_{HaHb} = 7 Hz, H_b, 4H,); *Minor diastereomer* (19 %): δ = 7.89 ppm (m, H_f, 6H), 7.68 ppm (m, $H_{c\text{-}e}$, 26H), 7.06 ppm (dd, J_{HcHb} = 7 Hz, J_{HaHb} = 7 Hz, H_b, 4H), 6.70 ppm (m, H_a, 4H,);

$^1H\{^{31}P\}$ NMR (500.1 MHz, CD_3CN, 298 K): *Major diastereomer* (81%): δ = 7.79 ppm (t, J_{HfHe} = 7 Hz, H_f, 6H), 7.58 ppm (dd, J_{HdHe} = 7 Hz, J_{HeHf} = 7 Hz, H_e, 12H), 7.48 ppm (d, J_{HdHe} = 7 Hz, H_d, 12H), 7.39 ppm (t, J_{HcHb} = 7 Hz, H_c, 2H), 7.31 ppm (d, J_{HaHb} = 8 Hz, H_a, 4H), 7.12 ppm (dd, J_{HcHb} = 7 Hz, J_{HaHb} = 7 Hz, H_b, 4H); *Minor diastereomer* (19 %): δ = 7.89 ppm (m, H_f, 6H), 7.68 ppm (m, $H_{c\text{-}e}$, 26H), 7.06 ppm (dd, J_{HcHb} = 7 Hz, J_{HaHb} = 7 Hz, H_b, 4H), 6.70 ppm (d, J_{HaHb} = 7 Hz, H_a, 4H);

^{13}C NMR (125.8 MHz, DEPTQ135, CD_3CN, 298 K): Isomer assignments confirmed by correlation to proton signals (HSQC experiment); *Major diastereomer*: δ =138.0 ppm (m, +, C_a), 135.5 ppm (s, +, C_f), 134.4 ppm (m, +, C_d), 133.8 ppm (s, +, C_c), 130.5 ppm (m, +, C_e), 130.2 ppm (m, +, C_b); *Minor diastereomer*: δ = 138.5 ppm (broad, +, C_a), 135.8 ppm (s, +, C_f), 133.9 ppm (s, +, ?), 130.9 ppm (m, +, $C_{c\text{-}e}$) 129.8 ppm (m, +, C_b), other two peaks for $C_{c\text{-}e}$ were not assignable;

^{31}P CP/MAS NMR (162.0 MHz, 4 mm rotor, ice cooled carrier gas): *Major diastereomer* δ = 24 ppm, -40 ppm; *Minor diastereomer* δ = 19 ppm, -31 ppm;

FT-IR (nujol, ranked intensities): 1582 (16), 1437 (12), 1264 (1), 1223 (8), 1152 (4), 1099 (7), 1030 (3), 997 (13), 741 (6), 690 (5), 636 (2), 572 (15), 531 (9), 513 (10), 497 (11), 470 (14) cm^{-1};

Crystal Data: $C_{50}H_{40}F_6O_6P_4S_2$; colorless, plate, crystal size 0.45 x 0.275 x 0.075 mm; Monoclinic, space group $P2_1/n$, a = 10.942(4) Å, b = 20.769(7) Å, c = 11.462(4) Å, β = 113.120(6)°, V = 2395.7(15) $Å^3$, Z = 2, μ = 0.318 mm^{-1}; $2\theta_{max}$ = 53.5°, collected (independent) reflections = 16121 (5349), R_{int} = 0.0239; 387 refined parameters, R_1 = 0.0635, wR_2 = 0.1450 for all data, max/min residual electron density = 1.913/-0.409 $eÅ^{-3}$.

CCDC-605575

[Ph$_3$P-PMe-PMe-PPh$_3$][OTf]$_2$, 7.2b[OTf]$_2$

In a glove box, $MePCl_2$ (0.079 mL, 0.885 mmol) and TMSOTf (0.266 mL, 1.47 mmol) were added to a solution of Ph_3P (0.35 g, 1.34 mmol) in $CHCl_3$ (9 mL) contained in a 50 mL 1-necked bulb with a Teflon stopper. The mixture was degassed by three freeze-pump-thaw cycles and subsequently heated to reflux within the closed system by use of an oil bath (~ 60 °C). After 4 days the reaction was virtually complete (^{31}P NMR), and a white precipitate was present. This solid was collected by filtration in a glove box, washed with $CHCl_3$ (1.5 mL) and dried *in vacuo*.

Yield: 0.224 g (0.245 mmol, 55%).

D.p. 225-237 °C.

^{31}P{^{1}H} NMR (101.3 MHz, CH_2Cl_2, 298 K): AA'BB' spin system, δA = -71 ppm, δB = 26 ppm, $^1J_{AA'}$ = -278 Hz, $^1J_{AB}$ = $^1J_{A'B'}$ = -282 Hz, $^2J_{AB'}$ = $^2J_{A'B}$ = 78 Hz, $^3J_{BB'}$ = 62 Hz;

$^{31}P\{^1H\}$ NMR (101.3 MHz, CD_3CN, 298 K): not simulated, approximate shifts: δA = -67 ppm, δB = 32 ppm;

^1H NMR (500.1 MHz, CD_3CN, 298 K): δ = 7.97 ppm (t, $^3J_{HH}$ = 7.5 Hz, 6H), 7.90 ppm (m, 12H), 7.81 ppm (m, 12H), 0.76 ppm (m, 6H);

^1H NMR (500.1 MHz, CD_3NO_2, 298 K): δ = 8.03 ppm (m, 18H), 7.88 ppm (m, 12H), 0.95 ppm (m, 6H);

^{13}C NMR (125.8 MHz, DEPTQ135, CD_3NO_2, 298 K): δ = 136.0 ppm (s, +), 134.0 ppm (s, +), 131.1 ppm (m, +), 117.1 ppm (m, -), 0.0 ppm (m, +);

FT-IR (nujol, ranked intensities): 1439 (10), 1262 (1), 1223 (12), 1152 (7), 1103 (10), 1030 (4), 995 (14), 879 (15), 755 (9), 721 (8), 692 (5), 637 (2), 572 (13), 543 (6), 511 (3), 306 (16) cm^{-1};

Crystals suitable for X-ray diffraction were grown by vapor diffusion with CH_3CN/Et_2O.

Crystal Data: $C_{40}H_{36}F_6O_6P_4S_2$; colorless, rod, crystal size 0.45 x 0.10 x 0.10 mm; Monoclinic, space group $P2_1/c$, a = 8.761(5) Å, b = 27.114(17) Å, c = 17.578(11) Å, β = 96.807(11)°, V = 4146(4) $Å^3$, Z = 4, μ = 0.356 mm^{-1}; $2\theta_{max}$ = 53.6°, collected (independent) reflections = 27998 (9274), R_{int} = 0.0583; 525 refined parameters, R_1 = 0.1051, wR_2 = 0.1070 for all data, max/min residual electron density = 0.457/-0.359 $eÅ^{-3}$.

[Me$_3$P-PPh-PPh-PMe$_3$][OTf]$_2$, 7.4a[OTf]$_2$

Me_3P (0.66 mL, 1 M in toluene, 0.66 mmol) was added dropwise to a stirred solution of $[Ph_3P\text{-}PPh\text{-}PPh\text{-}PPh_3][OTf]_2$, (**7.2a**$[OTf]_2$, 0.36 g, 0.346 mmol) in CH_2Cl_2 (9 mL). After stirring overnight, the precipitate was collected by filtration, and washed with CH_2Cl_2 (1 mL). Recrystallization over 4 days at -25 °C by vapor diffusion with CH_3CN/Et_2O gave crystals suitable for X-ray diffraction. Crystals not submitted for X-ray analysis were washed Et_2O (2 x 1 mL) and dried *in vacuo*.

Yield = 0.187 g (0.281 mmol, 81%);

M.p. 220-224 °C;

Elemental analysis (%) calcd for $C_{20}H_{28}F_6O_6P_4S_2$: C 36.0, H 4.2; found: C 35.5, H 4.4;

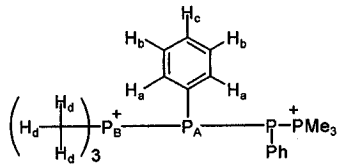

$^{31}P\{^{1}H\}$ NMR (101.3 MHz, CD_3CN, 298 K): *Major diastereomer* (86% by ^{1}H NMR integration): AA'BB' spin system, δA = -52 ppm, δB = 25 ppm, $^{1}J_{AA'}$ = -105 Hz, $^{1}J_{AB}$ = $^{1}J_{A'B'}$ = -305 Hz, $^{2}J_{AB'}$ = $^{2}J_{A'B}$ = 66 Hz, $^{3}J_{BB'}$ = 56 Hz; *Minor diastereomer* (14% by ^{1}H NMR integration): not simulated, approx. shifts: δA = -56 ppm, δB = 23 ppm.

^{1}H NMR (500.1 MHz, CD_3CN, 298 K): *Major isomer* (86%): 8.05 ppm (m, H_a, 4H), 7.84 ppm (t, J_{HbHc} = 7 Hz, H_c, 2H), 7.74 ppm (dd, J_{HaHb} = 7 Hz, J_{HbHc} = 7 Hz, H_b, 4H), 1.70 ppm (m, H_d, 18H); *Minor isomer* (14%): 7.59 ppm (t, J_{HbHc} = 7 Hz, H_c, 2H), 7.40 ppm (m, $H_{a,b}$, 8H), 2.04 ppm (m, H_d, 18H);

$^{1}H\{^{31}P\}$ NMR (ppm, 500.1 MHz, CD_3CN, 298 K): *Major isomer* (86%): 8.05 ppm (d, J_{HaHb} = 7 Hz, H_a, 4H), 7.84 ppm (t, J_{HbHc} = 7 Hz, H_c, 2H), 7.74 ppm (dd, J_{HaHb} = 7 Hz, J_{HbHc} = 7 Hz, H_b, 4H), 1.70 ppm (s, H_d, 18H); *Minor isomer* (14%): 7.59 ppm (t, J_{HbHc} = 7 Hz, H_c, 2H), 7.40 ppm (m, $H_{a,b}$, 8H), 2.04 ppm (s, H_d, 18H);

^{13}C NMR (125.8 MHz, DEPTQ135, CD_3CN, 298 K): Isomer assignments confirmed by correlation to proton signals (HSQC experiment); *Major diastereomer*: δ =137.2 ppm (m, +, C_a), 134.5 ppm (s, +, H_c), 131.2 ppm (s, +, C_b), 8.8 ppm (m, +, H_d); *Minor diastereomer*: δ = 138.0 ppm (m, +, $C_{a,b}$), 133.3 ppm (s, +, C_c), 130.1 ppm (s, +, $C_{a,b}$), 9.0 ppm (m, +, C_d);

FT-IR (nujol, ranked intensities): 1440 (16), 1300 (8), 1275 (2), 1254 (1), 1224 (9), 1172 (15), 1158 (7), 1140 (6), 1030 (4), 961 (5), 743 (10), 697 (12), 637 (3), 573 (13), 517 (11), 484 (14) cm^{-1};

Crystal Data: $C_{20}H_{28}F_6O_6P_4S_2$; colorless, irregular, crystal size 0.60 x 0.40 x 0.20 mm; Monoclinic, space group $P2_1/c$, a = 8.9520(14) Å, b = 16.597(3) Å, c = 10.0504(16) Å, β = 101.328(3)°, V = 1464.1(4) $Å^3$, Z = 2, μ = 0.472 mm^{-1}; $2\theta_{max}$ = 53.2°, collected (independent) reflections = 9319 (3253), R_{int} = 0.0477; 228 refined parameters, R_1 = 0.0554, wR_2 = 0.1393 for all data, max/min residual electron density = 1.226/-0.466 $eÅ^{-3}$.

CCDC-605576

[Me$_3$P-PMe-PMe-PMe$_3$][OTf]$_2$, 7.4b[OTf]$_2$

Me_3P (0.235 mL, 1 M in toluene, 0.235 mmol) was added dropwise to a stirred mixture of [Ph_3P-PMe-PMe-PPh_3][OTf]$_2$, (**7.2b**[OTf]$_2$, 0.106 g, 0.116 mmol) in CH_2Cl_2 (3 mL). After stirring for 30 minutes, the white precipitate was collected by filtration, and washed with CH_2Cl_2 (1 mL). Recrystallization over 1 day, by vapor diffusion with CD_3CN/Et_2O at -25 °C gave crystals suitable for X-ray diffraction. Crystals not submitted for X-ray analysis were washed with Et_2O (2 x 1mL), and dried *in vacuo*.

Yield: 0.032 g (0.059 mmol, 51%).

M.p. 221-224 °C

$^{31}P\{^1H\}$ NMR (101.3 MHz, CD_3CN, 298 K): AA'BB' spin system, δA = -73 ppm, δB = 26 ppm, $^1J_{AA'}$ = -238 Hz, $^1J_{AB} = {}^1J_{A'B'}$ = -269 Hz, $^2J_{AB'} = {}^2J_{A'B}$ = 80 Hz, $^3J_{BB'}$ = 58 Hz;

^1H NMR (500.1 MHz, CD_3NO_2, 298 K): δ = 2.21 ppm (m, 18H), 1.93 ppm (m, 6H);

^{13}C NMR (125.8 MHz, DEPTQ135, CD_3NO_2, 298 K): δ = 7.78 ppm (m, +), -0.4 ppm (m, +);

FT-IR (nujol, ranked intensities): 1426 (14), 1260 (1), 1301 (13), 1225 (10), 1152 (5), 1029 (3), 966 (4), 901 (8), 861 (9), 809 (17), 768 (16), 758 (15), 680 (11), 636 (2), 573 (7), 517 (6) cm^{-1};

Crystal Data: $C_{10}H_{24}F_6O_6P_4S_2$; colorless, irregular, crystal size 0.50 x 0.25 x 0.20 mm; Monoclinic, space group $P2_1/c$, a = 12.431(2) Å, b = 13.520(3) Å, c = 13.883(3) Å, β = 94.872(3)°, V = 2324.7(7) $Å^3$, Z = 4, μ = 0.574 mm^{-1}; $2\theta_{max}$ = 54.6°, collected (independent) reflections = 15518 (5164), R_{int} = 0.0380; 261 refined parameters, R_1 = 0.0864, wR_2 = 0.2112 for all data, max/min residual electron density = 0.806/-0.461 $eÅ^{-3}$.

References

(1) "catenation." Encyclopædia Britannica. 2006. Encyclopædia Britannica Premium Service. 27 June 2006 <http://www.britannica.com/eb/article?tocId=9020792>.

(2) Dillon, K. B.; Mathey, F.; Nixon, J. F. *Phosphorus: The Carbon Copy*; John Wiley & Sons: 1998.

(3) Baudler, M. *Angew.Chem.Int.Ed.Engl.* **1982**, *21*, 492-512.

(4) Mathey, F. *Angew.Chem.Int.Ed.* **2003**, *42*, 1578-1604.

(5) Pfitzner, A.; Bräu, M. F.; Zweck, J.; Brunklaus, G.; Eckert, H. *Angew.Chem.Int.Ed.* **2004**, ***43***, 4228-4231.

(6) Housecroft, C. E.; Sharpe, A. G. *Inorganic Chemitry*; Pearson Education Limited: 2001.

(7) Baudler, M.; Glinka, K. *Chem.Rev.* **1994**, *94*, 1273-1297.

(8) Baudler, M.; Glinka, K. *Chem.Rev.* **1993**, *93*, 1623-1667.

(9) Baudler, M. *Angew.Chem.Int.Ed.Engl.* **1987**, *26*, 419-441.

(10) Haiduc, I. *The Chemistry of Inorganic Ring Systems*; Wiley-Interscience: 1970; pp 82-102.

(11) Kosolapoff, G. M.; Maier, L. *Organic Phosphorus Compounds*; Wiley-Interscience: 1972; pp 289-331.

(12) Fritz, G.; Matern, E.; Krautscheid, H.; Ahlrichs, R.; Olkowska, J. W.; Pikies, J. *Z.Anorg.Allg.Chem.* **1999**, *625*, 1604-1607.

(13) Scheer, M.; Gremler, St.; Herrmann, E.; Dargatz, M.; Schädler, H.-D. *Z.Anorg.Allg.Chem.* **1993**, *619*, 1047-1052.

(14) Yoshifuji, M.; Shima, I.; Inamoto, N.; Hirotsu, K.; Higuchi, T. *J.Am.Chem.Soc.* **1981**, *103*, 4587-4589.

(15) Twamley, B.; Sofield, C. D.; Olmstead, M. M.; Power, P. P. *J.Am.Chem.Soc.* **1999**, *121*, 3357-3367.

(16) Smith, R. C.; Ren, T.; Protasiewicz, J. D. *Eur.J.Inorg.Chem.* **2002**, 2779-2783.

(17) Baudler, M.; Glinka, K. *Inorg.Synth.* **1989**, *25*, 1-5.

(18) Henderson, W. A.; Epstein, M.; Seichter, F. S. *J.Am.Chem.Soc.* **1963**, *85*, 2462-2466.

(19) Baudler, M.; Hellmann, J. *Z.Anorg.Allg.Chem.* **1981**, *480*, 129-141.

(20) Baudler, M.; Pinner, C.; Gruner, C.; Hellmann, J.; Schwamborn, M.; Kloth, B. *Z.Naturforsch.* **1977**, *32b*, 1244-1251.

(21) Breen, T. L.; Stephan, D. W. *Organometallics* **1997**, *16*, 365-369.

(22) Baudler, M.; Carlsohn, B.; Böhm, W.; Reuschenbach, G. *Z.Naturforsch.* **1976**, *31b*, 558-564.

(23) Daly, J. J. *J.Chem.Soc.* **1965**, 4789-4799.

(24) Köhler, H.; Michaelis, A. *Ber.Dtsch.Chem.Ges.* **1877**, *10*, 807-814.

(25) Kuchen, W.; Buchwald, H. *Chem.Ber.* **1958**, *91*, 2296-2304.

(26) Daly, J. J.; Maier, L. *Nature* **1964**, *203*, 1167-1168.

(27) Daly, J. J. *J.Chem.Soc.,Suppl.* **1964**, 6147-6166.

(28) Hoffman, P. R.; Caulton, K. G. *Inorg.Chem.* **1975**, *14*, 1997-1999.

(29) Etkin, N.; Fermin, M. C.; Stephan, D. W. *J.Am.Chem.Soc.* **1997**, *119*, 2954-2955.

(30) Baudler, M.; Aktalay, Y.; Arndt, V.; Tebbe, K.-F.; Fehér, M. *Angew.Chem.Int.Ed.Engl.* **1983**, *22*, 1002-1003.

(31) Baudler, M.; Jachow, H.; Tebbe, K.-F. *Z.Anorg.Allg.Chem.* **1992**, *614*, 17-20.

(32) Baudler, M.; Jachow, H.; Lieser, B.; Tebbe, K.-F.; Fehér, M. *Angew.Chem.Int.Ed.Engl.* **1989**, *28*, 1231-1232.

(33) Dillon, K. B.; Mathey, F.; Nixon, J. F. *Phosphorus: The Carbon Copy*; John Wiley & Sons: 1997; pp *Phosphorus: The Carbon Copy*, John Wiley & Sons.

(34) Fluck, E.; Issleib, K. *Z.Anorg.Allg.Chem.* **1965**, *339*, 274-280.

(35) Issleib, K.; Krech, K. *Chem.Ber.* **1966**, *99*, 1310-1315.

(36) Issleib, K.; Hoffmann, M. *Chem.Ber.* **1966**, *99*, 1320-1324.

(37) Issleib, K.; Krech, K. *Chem.Ber.* **1965**, *98*, 2545-2550.

(38) Geier, J.; Rüegger, H.; Wörle, M.; Grützmacher, H. *Angew.Chem.Int.Ed.* **2003**, *42*, 3951-3954.

(39) Wolf, R.; Schisler, A.; Lönnecke, P.; Jones, C.; Hey-Hawkins, E. *Eur.J.Inorg.Chem.* **2004**, 3277-3286.

(40) West, R. *Science* **2004**, *305*, 1724-1725.

(41) Wiberg, N.; Wörner, A.; Lerner, H.-W.; Karaghiosoff, K.; Fenske, D.; Baum, G.; Dransfeld, A.; Schleyer, P. v. R. *Eur.J.Inorg.Chem.* **1998**, 833-841.

(42) Lerner, H.-W.; Bolte, M.; Karaghiosoff, K.; Wagner, M. *Organometallics* **2004**, *23*, 6073-6076.

(43) Wiberg, N.; Wörner, A.; Karaghiosoff, K.; Fenske, D. *Chem.Ber./Recueil* **1997**, *130*, 135-140.

(44) Abicht, H.-P.; Hönle, W.; von Schnering, H. G. *Z.Anorg.Allg.Chem.* **1984**, *519*, 7-23.

(45) Schmettow, W.; Lipka, A.; von Schnering, H. G. *Angew.Chem.Int.Ed.Engl.* **1974**, *13*, 345.

(46) von Schnering, H. G.; Meyer, T.; Hönle, W.; Schmettow, W.; Hinze, U.; Bauhofer, W.; Kliche, G. *Z.Anorg.Allg.Chem.* **1987**, *553*, 261-279.

(47) Kraus, F.; Aschenbrenner, J.; Korber, N. *Angew.Chem.Int.Ed.* **2003**, *42*, 4030-4033.

(48) Baudler, M.; Düster, D.; Ouzounis, D. *Z.Anorg.Allg.Chem.* **1987**, *544*, 87-94.

(49) Baudler, M.; Ouzounis, D. *Z.Naturforsch.* **1989**, *44b*, 381-382.

(50) Baudler, M.; Etzbach, T. *Chem.Ber.* **1991**, *124*, 1159-1160.

(51) Baudler, M.; Akpapoglou, S.; Ouzounis, D.; Wasgestian, F.; Meinigke, B.; Budzikiewicz, H.; Münster, H. *Angew.Chem.Int.Ed.Engl.* **1988**, *27*, 280-281.

(52) Kraus, F.; Korber, N. *Chem.Eur.J.* **2005**, *11*, 5945-5959.

(53) Schisler, A.; Lonnecke, P.; Huniar, U.; Ahlrichs, R.; Hey-Hawkins, E. *Angew.Chem.Int.Ed.* **2001**, *40*, 4217-4219.

(54) von Schnering, H. G.; Hönle, W. *Chem.Rev.* **1988**, *88*, 243-273.

(55) Hönle, W.; von Schnering, H. G.; Schmidpeter, A.; Burget, G. *Angew.Chem.Int.Ed.Engl.* **1984**, *23*, 817-818.

(56) Korber, N.; Daniels, J.; von Schnering, H. G. *Angew.Chem.Int.Ed.Engl.* **1996**, *35*, 1107-1110.

(57) Fritz, G.; Schneider, H.-W. *Z.Naturforsch.* **1988**, *43b*, 561-566.

(58) Baudler, M.; Heumüller, R.; Düster, D.; Germeshausen, J.; Hahn, J. *Z.Anorg.Allg.Chem.* **1984**, *518*, 7-13.

(59) Tebbe, K.-F.; Fehér, M.; Baudler, M. *Z.Kristallogr.* **1985**, *170*, 180-181.

(60) Cowley, A. H.; Kemp, R. A. *Chem.Rev.* **1985**, *85*, 367-382.

(61) Burford, N.; Cameron, T. S.; Ragogna, P. J.; Ocando-Mavarez, E.; Gee, M.; McDonald, R.; Wasylishen, R. E. *J.Am.Chem.Soc.* **2001**, *123*, 7947-7948.

(62) Burford, N.; Ragogna, P. J.; McDonald, R.; Ferguson, M. *J.Am.Chem.Soc.* **2003**, *125*, 14404-14410.

(63) Hoffmann, D.; Gruenewald, R. *Chem.Ber.* **1961**, *94*, 186-193.

(64) Schultz, C. W.; Parry, R. W. *Inorg.Chem.* **1976**, *15*, 3046-3050.

(65) Kopp, R. W.; Bond, A. C.; Parry, R. W. *Inorg.Chem.* **1976**, *15*, 3042-3046.

(66) Thomas, M. G.; Schultz, C. W.; Parry, R. W. *Inorg.Chem.* **1977**, *16*, 994-1001.

(67) Shagvaleev, F. Sh.; Zykova, T. V.; Tarasova, R. I.; Sitdikova, T. Sh.; Moskva, V. V. *Zh.Obshch.Khim.* **1990**, *60*, 1775-1779.

(68) Burford, N.; Cameron, T. S.; LeBlanc, D. J.; Losier, P.; Sereda, S.; Wu, G. *Organometallics* **1997**, *16*, 4712-4717.

(69) Krossing, I. *Dalton Trans.* **2002**, 500-512.

(70) Lynam, J. M.; Copsey, M. C.; Green, M.; Jeffrey, J. C.; McGrady, J. E.; Russell, C. A.; Slattery, J. M.; Swain, A. C. *Angew.Chem.Int.Ed.* **2003**, *42*, 2782.

(71) Gonsior, M.; Krossing, I.; Mueller, L.; Raabe, I.; Jansen, M.; van Wuellen; L. *Chem.Eur.J.* **2002**, *8*, 4475-4492.

(72) Krossing, I.; Raabe, I. *Angew.Chem.Int.Ed.* **2001**, *40*, 4406-4409.

(73) Schmidpeter, A.; Lochschmidt, S. *Angew.Chem.Int.Ed.Engl.* **1986**, *25*, 253-254.

(74) Lochschmidt, S.; Schmidpeter, A. *Z.Naturforsch.* **1985**, *40b*, 765-773.

(75) Ellis, B. D.; Carlesimo, M.; Macdonald, C. *Chem.Commun.* **2003**, 1946-1947.

(76) Schmidpeter, A.; Lochschmidt, S.; Sheldrick, W. S. *Angew.Chem.Int.Ed.Engl.* **1985**, *24*, 226-227.

(77) Barnham, R. J.; Deng, R. M. K.; Dillon, K. B.; Goeta, A. E.; Howard, J. A. K.; Puschmann, H. *Heteroat.Chem.* **2001**, *12*, 501-510.

(78) Ellis, B. D.; Macdonald, C. L. B. *Inorg.Chem.* **2006**, *45*, 6864-6874.

(79) Schmidpeter, A.; Lochschmidt, S. *Inorg.Synth.* **1990**, *27*, 253-258.

(80) Loss, S.; Widauer, C.; Grützmacher, H. *Angew.Chem.Int.Ed.* **1999**, *38*, 3329-3331.

(81) Romanenko, V. D.; Rudzevich, V. L.; Rusanov, E. B.; Chernega, A. N.; Senio, A.; Sotiropoulos, J. M.; Pfister-Guillouzo, G.; Sanchez, M. *Chem.Commun.* **1995**, 1383-1385.

(82) Romanenko, V. D.; Rudzevich, V. L.; Rusanov, E. B.; Chernega, A. N.; Senio, A.; Sotiropoulos, J.-M.; Pfister-Guillouzo, G.; Sanchez, M. *Phosphor.Sulfur Silicon* **1996**, *111*, 200.

(83) Heuer, L.; Ernst, L.; Schmutzler, R.; Schomburg, D. *Angew.Chem.Int.Ed.Engl.* **1989**, *28*, 1507-1509.

(84) Schomburg, D.; Bettermann, G.; Ernst, L.; Schmutzler, R. *Angew.Chem.Int.Ed.Engl.* **1985**, *24*, 975-976.

(85) Nikitin, E. V.; Romakhin, A. S.; Zagumennov, V. A.; Babkin, Yu. A. *Electrochim.Acta* **1997**, *42*, 2217-2224.

(86) Romakhin, A. S.; Palyutin, F. M.; Ignat'ev, Yu. A.; Nikitin, E. V.; Kargin, Yu. M.; Litvinov, I. A.; Naumov, V. A. *Izv.Akad.Nauk.SSSR, Ser.Khim.* **1990**, *3*, 664-669.

(87) Alder, R. W.; Ganter, C.; Harris, C. J.; Orpen, A. G. *J.Chem.Soc., Chem.Commun.* **1992**, 1172-1174.

(88) Alder, R. W.; Ganter, C.; Harris, C. J.; Orpen, A. G. *J.Chem.Soc., Chem.Commun.* **1992**, 1170-1172.

(89) Alder, R. W.; Ellis, D. D.; Gleiter, R.; Harris, C. J.; Lange, H.; Orpen, A. G.; Read, D.; Taylor, P. N. *Perkin.Trans.1* **1998**, 1657-1668.

(90) Schmidpeter, A.; Lochschmidt, S.; Karaghiosoff, K.; Sheldrick, W. S. *Chem.Commun.* **1985**, 1447-1448.

(91) Lochschmidt, S.; Muller, G.; Huber, B.; Schmidpeter, A. *Z.Naturforsch.* **1986**, *41b*, 444-454.

(92) Kilian, P.; Slawin, A. M. Z.; Woollins, J. D. *Dalton Trans.* **2006**, 2175-2183.

(93) Karsch, H. H.; Witt, E. *J.Organomet.Chem.* **1997**, *529*, 151-169.

(94) Luo, H.; McDonald, R.; Cavell, R. G. *Angew.Chem.Int.Ed.* **1998**, *37*, 1098-1099.

(95) Burford, N.; Phillips, A. D.; Spinney, H. A.; Lumsden, M. D.; Werner-Zwanziger, U.; Ferguson, M. J.; McDonald, R. *J.Am.Chem.Soc.* **2005**, *127*, 3921-3927.

(96) Huynh, K.; Lough, A. J.; Manners, I. *J.Am.Chem.Soc.* **2006**, *128*, 14002-14003.

(97) Bouhadir, G.; Reed, R. W.; Réau, R.; Bertrand, G. *Heteroat.Chem.* **1995**, *6*, 371-375.

(98) Weiss, R.; Engel, S. *Synthesis* **1991**, 1077-1079.

(99) Reed, R.; Réau, R.; Dahan, F.; Bertrand, G. *Angew.Chem.Int.Ed.Engl.* **1993**, *32*, 399-401.

(100) Burford, N.; Dyker, C. A.; Lumsden, M. D.; Decken, A. *Angew.Chem.Int.Ed.* **2005**, *44*, 6196-6199.

(101) Hahn, J.; Baudler, M.; Kruger, C.; Tsay, Y.-H. *Z.Naturforsch.* **1982**, *37b*, 797-805.

(102) Issleib, K.; Rockstroh, C.; Duchek, I.; Fluck, E. *Z.Anorg.Allg.Chem.* **1968**, *360*, 77-87.

(103) Appel, R.; Milker, R. *Z.Anorg.Allg.Chem.* **1975**, *417*, 161-170.

(104) Laali, K. K.; Geissler, B.; Regitz, M. *J.Org.Chem.* **1995**, *60*, 3149-3154.

(105) Riegel, B.; Pfitzner, A.; Heckmann, G.; Binder, H.; Fluck, E. *Z.Anorg.Allg.Chem.* **1995**, *621*, 1365-1372.

(106) Weigand, W.; Cordes, A. W.; Swepston, P. N. *Acta Crystallogr., Sect.B* **1981**, *37*, 1631.

(107) Bart, J. C. J. *Acta Crystallogr., Sect.B* **1969**, *25*, 762.

(108) Gil, V. M. S.; Philipsborn, W. V. *Magn.Reson.Chem.* **1989**, *27*, 409-430.

(109) Burford, N.; Dyker, C. A.; Decken, A. *Angew.Chem.Int.Ed.* **2005**, *44*, 2364-2367.

(110) Kilpatrick, J. E.; Pitzer, K.; Spitzer, R. *J.Am.Chem.Soc.* **1947**, *69*, 2483-2488.

(111) Strauss, H. L. *Ann.Rev.Phys.Chem.* **1983**, *34*, 301-328.

(112) Experimental work done by Susanne D. Riegel.

(113) Albrand, J. P.; Robert, J. B. *C.R.Acad.Sci.Paris* **1978**, *C287*, 89-91.

(114) Albrand, J. P.; Robert, J. B. *J.Chem.Soc., Chem.Commun.* **1974**, 644-645.

(115) Baudler, M.; Koch, P.; Hasenbach, J.; Hahn, J. *Z.Anorg.Allg.Chem.* **1989**, *576*, 17-24.

(116) Spek, A. L. *J.Appl.Crystallogr.* **2003**, *36*, 7-13.

(117) Spencer, C. J.; Simpson, P. G.; Lipscomb, W. N. *Acta Cryst.* **1962**, *15*, 509.

(118) Spencer, C. J.; Lipscomb, W. N. *Acta Cryst.* **1961**, *14*, 250-256.

(119) Lex, J.; Baudler, M. *Z.Anorg.Allg.Chem.* **1977**, *431*, 49-60.

(120) Wolf, R.; Hey-Hawkins, E. *Chem.Commun.* **2004**, 2626-2627.

(121) Baudler, M.; Vesper, J.; Kloth, B.; Koch, D.; Sandmann, H. *Z.Anorg.Allg.Chem.* **1977**, *431*, 39-48.

(122) Lambert, J. B.; Jackson III, G. F.; Mueller, D. C. *J.Am.Chem.Soc.* **1970**, *92*, 3093-3097.

(123) Bashall, A.; García, F.; Hopkins, A. A.; Wood, J. A.; McPartlin, M.; Woods, A. D.; Wright, D. S. *Dalton Trans.* **2003**, 1143-1147.

(124) Bashall, A.; Beswick, M. A.; Choi, N.; Hopkins, A. D.; Kidd, S. J.; Lawson, Y. G.; Mosquera, M. E. G.; McPartlin, M.; Raithby, P. R.; Wheatley, A. A. E. H.; Wood, J. A.; Wright, D. S. *J.Chem.Soc., Dalton Trans.* **2000**, 479-486.

(125) Baudler, M.; Vesper, J.; Junkes, P.; Sandmann, H. *Angew.Chem.Int.Ed.* **1971**, *10*, 940.

(126) Dunitz, J. D. *X-ray Analysis and the Structure of Organic Molecules*; Cornell University Press: Ithaca, 1979; pp 301-390.

(127) Altona, C.; Sundaralingam, M. *J.Am.Chem.Soc.* **1972**, *94*, 8205-8212.

(128) Scheschkewitz, D.; Amii, H.; Gornitzka, H.; Schoeller, W. W.; Bourissou, D.; Bertrand, G. *Angew.Chem.Int.Ed.* **2004**, *43*, 585-587.

(129) Muetterties, E. L.; Guggenberger, L. J. *J.Am.Chem.Soc.* **1974**, *96*, 1748-1756.

(130) Cremer, D.; Pople, J. A. *J.Am.Chem.Soc.* **1975**, *97*, 1354-1358.

(131) Baudler, M.; Reuschenbach, G.; Hahn, J. *Z.Anorg.Allg.Chem.* **1981**, *482*, 27-39.

(132) Parshall, G. W. *J.Inorg.Nucl.Chem.* **1960**, *12*, 372-373.

(133) Grim, S. O.; Yankowsky, A. W.; Bruno, S. A.; Bailey, W. J.; Davidoff, E. F.; Marks, T. J. *J.Chem.Eng.Data* **1970**, *15*, 497-499.

(134) Weigand, J. J.; Riegel, S. D.; Burford, N.; unpublished.

(135) Dyker, C. A.; Burford, N.; Lumsden, M. D.; Decken, A. *J.Am.Chem.Soc.* **2006**, *128*, 9632-9633.

(136) Weigand, J. J.; Burford, N.; Lumsden, M. D. *Angew.Chem.Int.Ed.* **2006**, *45*, 6733-6737.

(137) Krossing, I.; Raabe, I. *Angew.Chem.Int.Ed.* **2004**, *43*, 2066-2090.

(138) Shriver, D. F.; Drezdzon, M. A. *The Manipulation of Air-Sensitive Compounds*; John Wiley and Sons: Toronto, 1986.

(139) Budzelaar, P. H. M. gNMR for Windows. (4.0). 1997. The Magdalen Centre, Oxford Science Park, Oxford OX4 4GA, UK, Cherwell Scientific Publishing Limited.

(140) Finer, E. G.; Harris, R. K. *Prog.Nucl.Magn.Reson.Spectrosc.* **1971**, *6*, 61-118.

(141) SAINT 6.02, 1997-1999, Bruker AXS, Inc., Madison, Wisconsin, USA.

(142) SADABS George Sheldrick, 1999, Bruker AXS, Inc., Madison, Wisconsin, USA.

(143) Sheldrick, G. M. *SHELXL-97, Program for crystal structure determination, University of Goettingen, Germany* **1997**.